modelling the propagation of high-energy particles

Rafael Alves Batista

University of Oxford

rafael.alvesbatista@physics.ox.ac.uk

www.8rafael.com

São Carlos
15/Dec/2016

cosmic rays

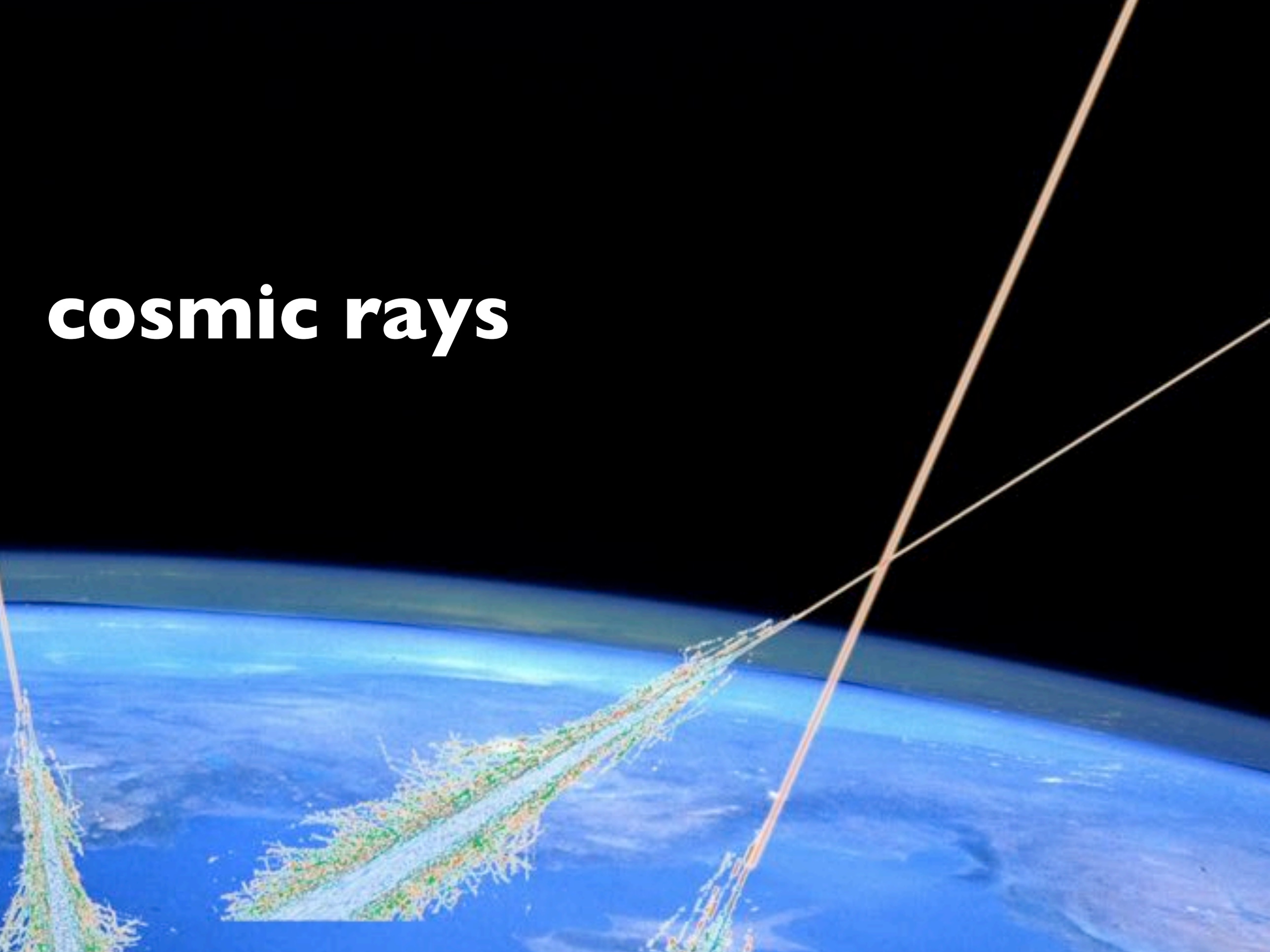

the cosmic ray spectrum at high energies

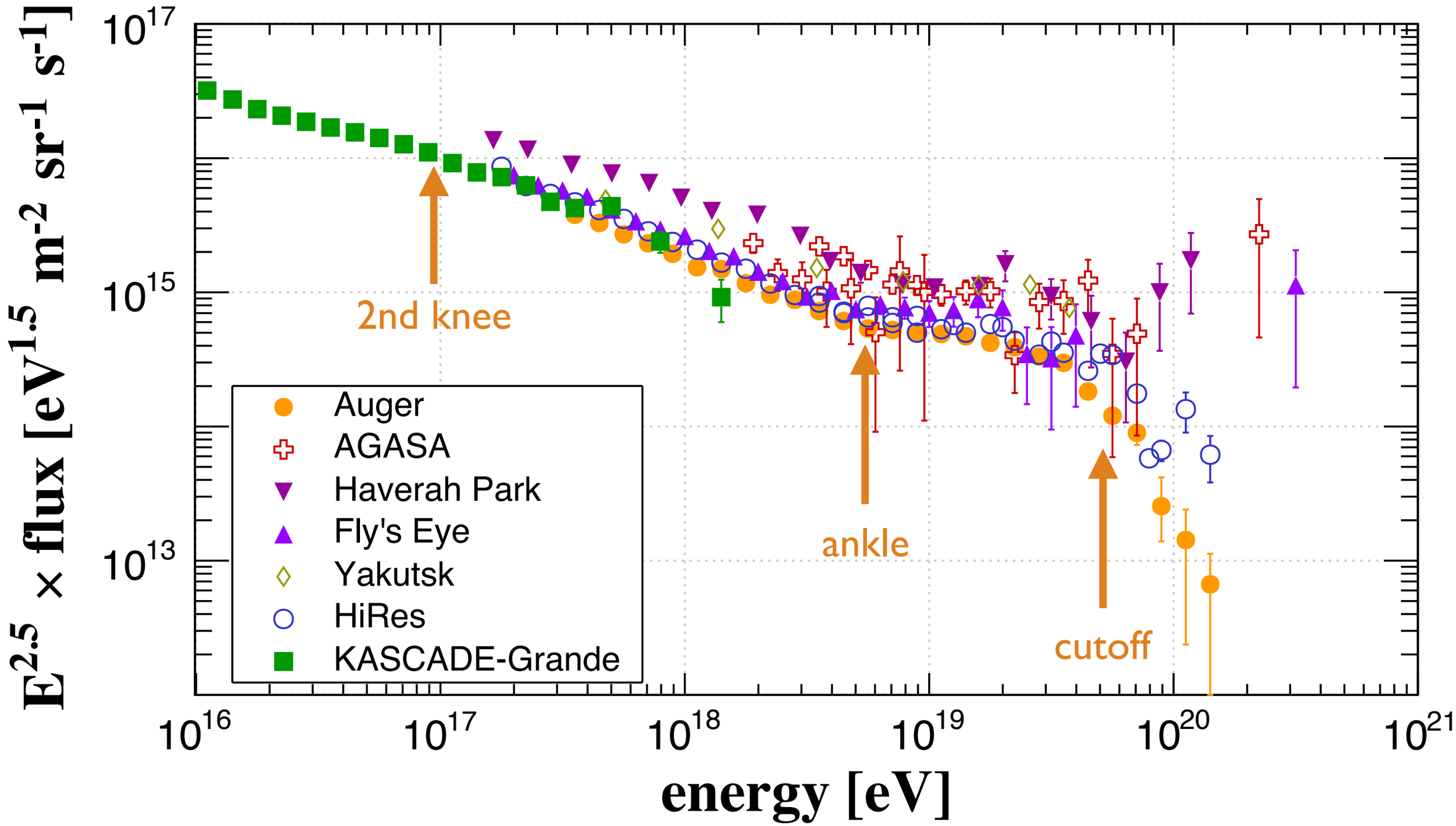

ultra-high energy cosmic rays

fundamental questions

- where do they come from?
- what are they made of?
- how are they accelerated?

some problems

- what is the maximum energy they can reach?
- do we see a GZK cutoff
- where does the transition between galactic and extragalactic cosmic rays take place?
- where does the transition between diffusive and ballistic regimes happen?

- observables from CR experiments: spectrum, composition, anisotropy
- cosmic magnetic fields (galactic and extragalactic) are important
- test new physics scenarios using UHECRs (?)

propagation picture

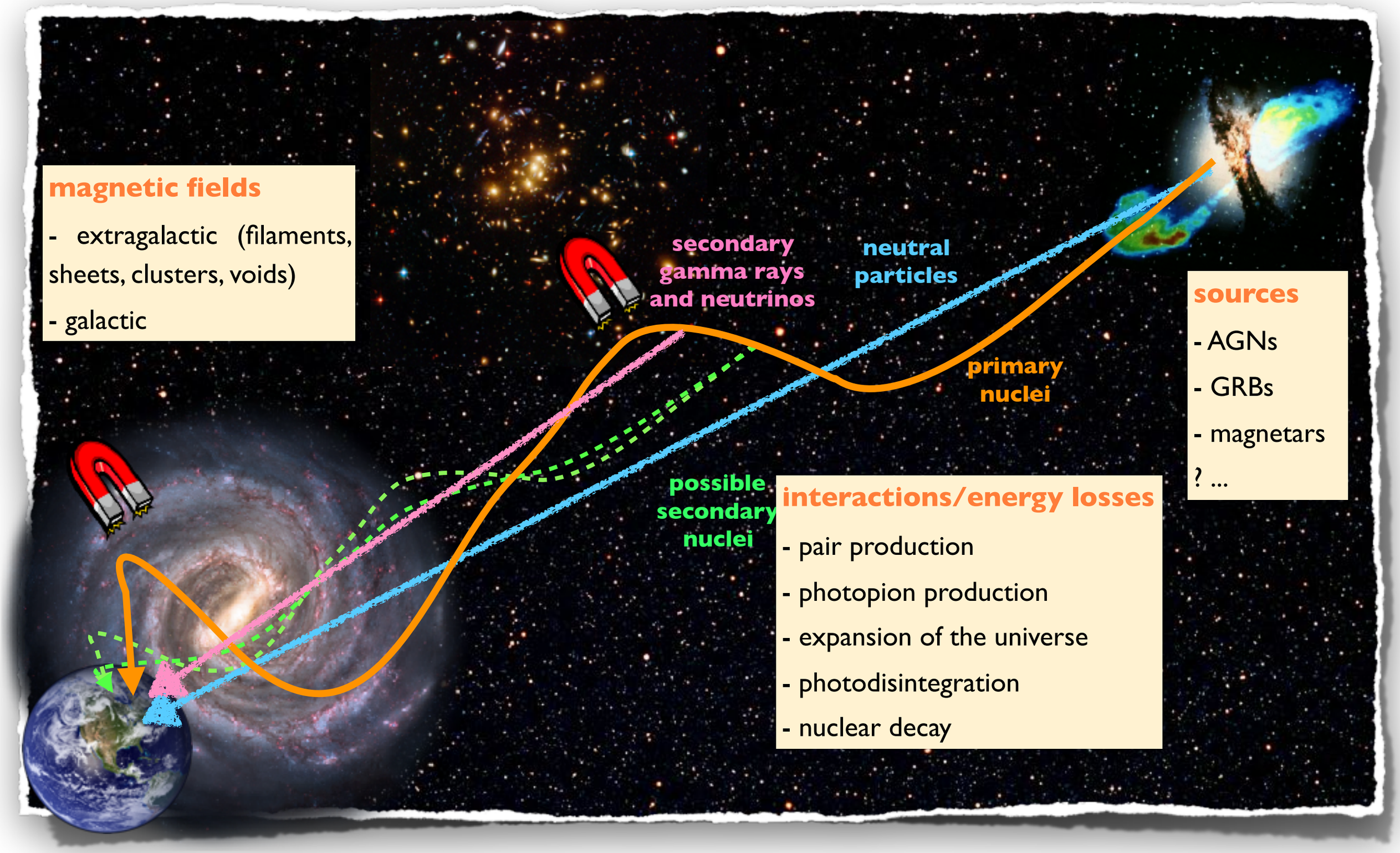

modelling the propagation of UHECRs: photon backgrounds

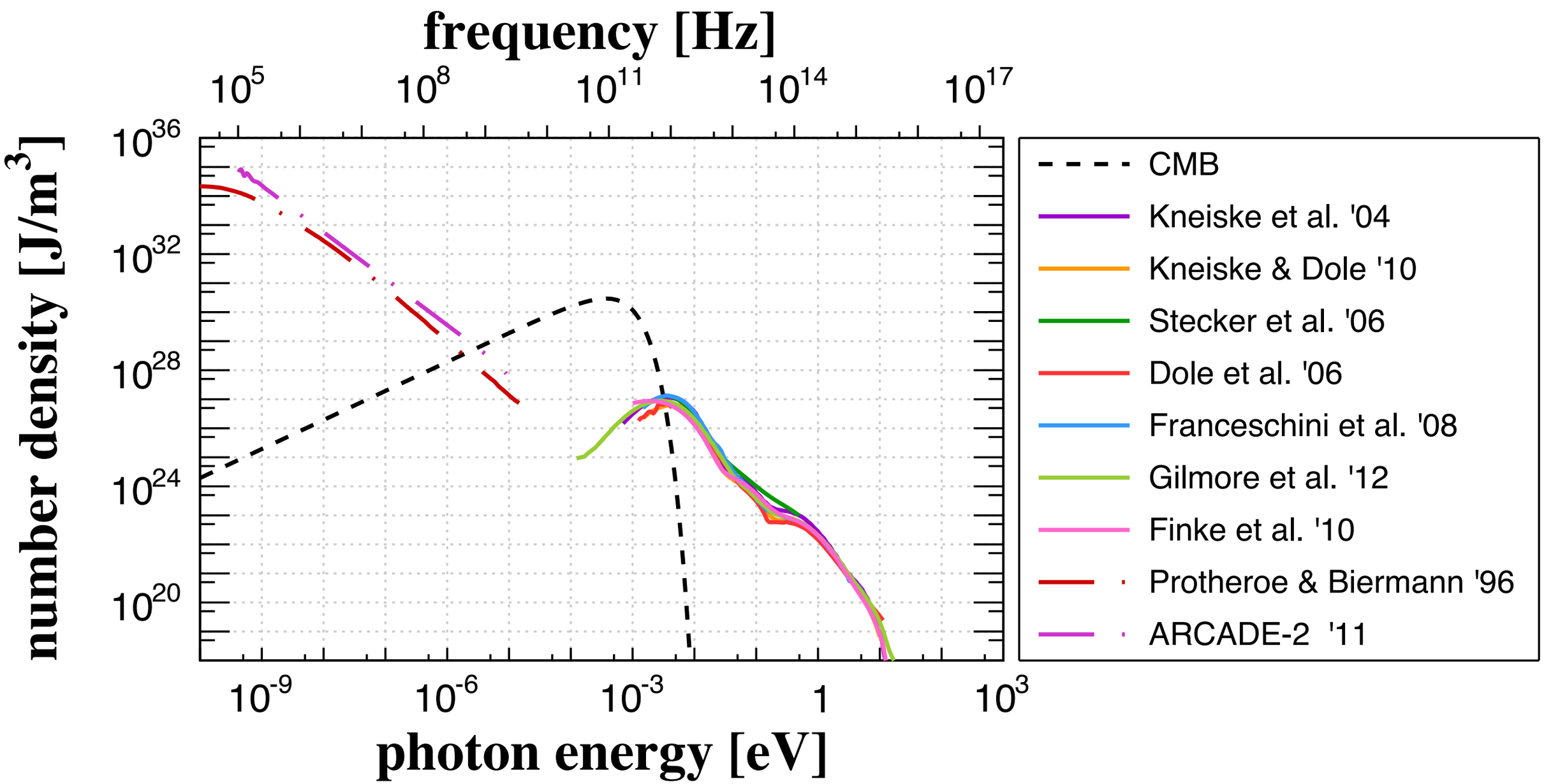

modelling the propagation of UHECRs: energy losses

photopion production

$$p + \gamma \rightarrow \Delta^+ \rightarrow \begin{cases} p + \pi^0 \\ n + \pi^+ \end{cases}$$

mean free path for nuclei written as a function of the mfp for protons and neutrons

expansion of the universe

$$\frac{dt}{dz} = \frac{1}{H_0} \frac{1}{1+z} \frac{1}{\sqrt{\Omega_m (1+z)^3 + \Omega_\Lambda}} \qquad E = \frac{E_0}{1+z}$$

ΛCDM cosmology

pair production

$$-\frac{dE_{A,Z}}{dt} = 3\alpha\sigma_T h^{-3} Z^2 m_e c^2 k_B T f(\Gamma)$$

photodisintegration

$$\frac{1}{\lambda(\Gamma)} = \int_{E_{min}}^{E_{max}} n(\epsilon, z)\bar{\sigma}(\epsilon'_{max} = 2\Gamma\epsilon) d\epsilon$$

nuclear decay

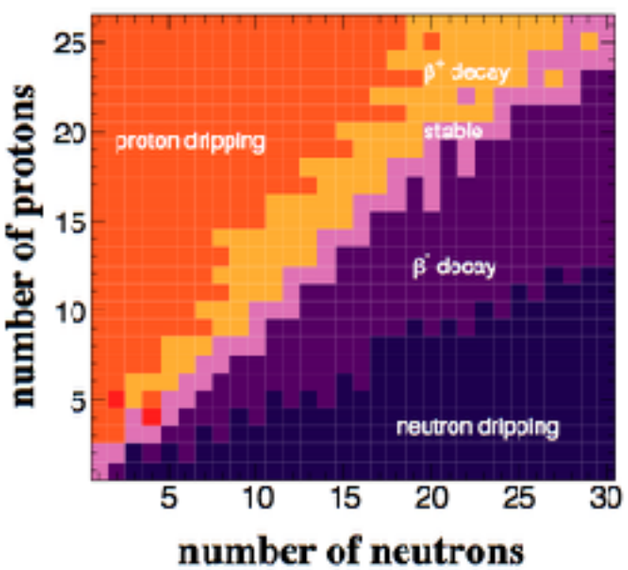

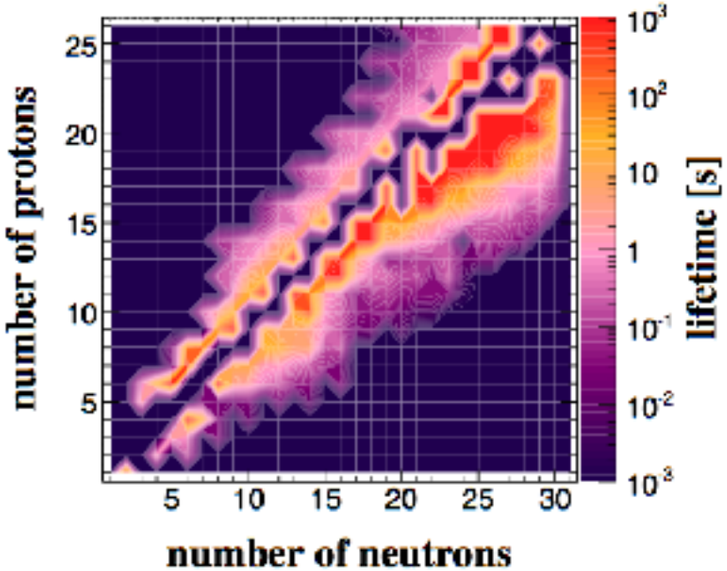

modelling the propagation of UHECRs: energy losses

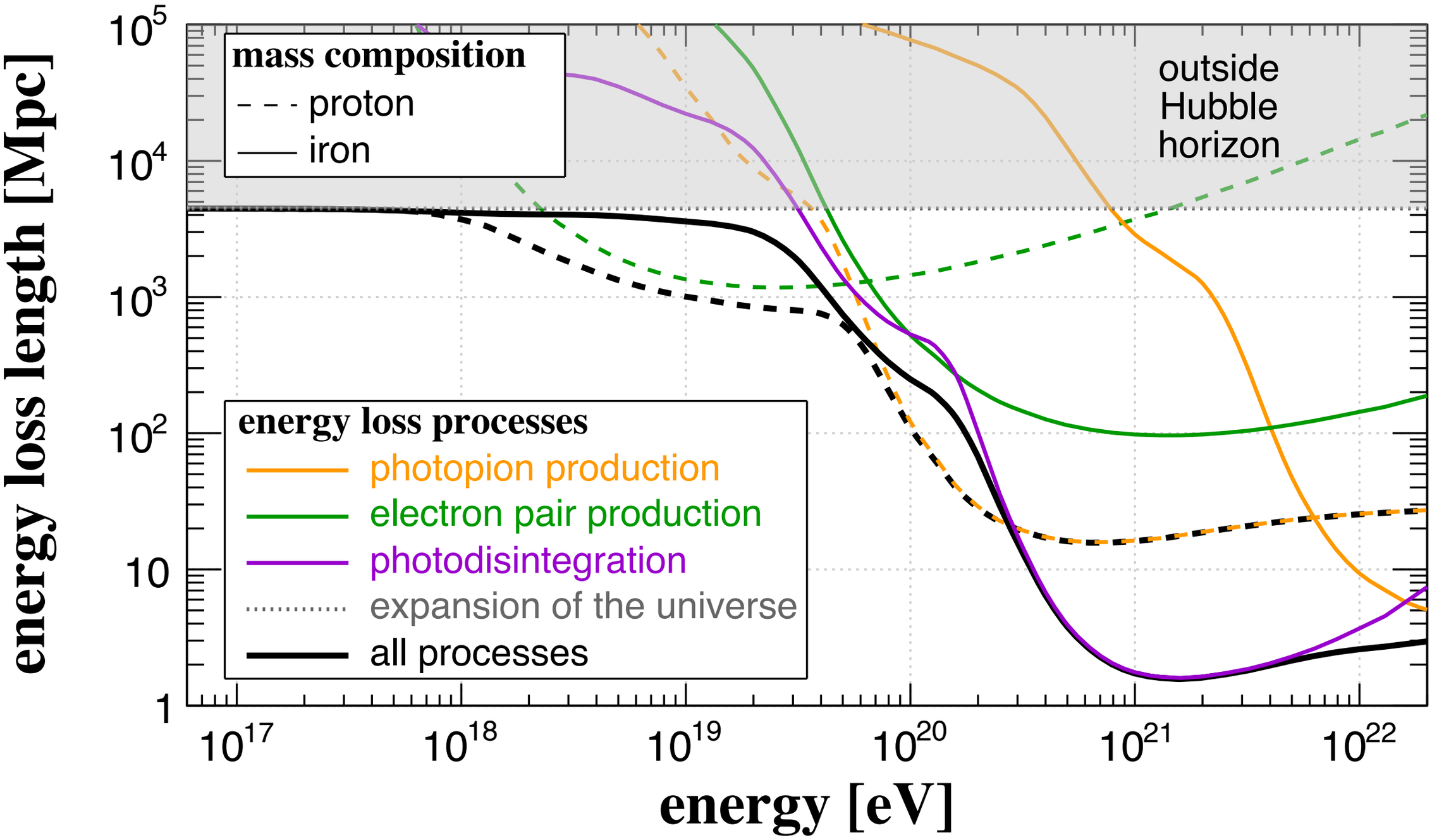

modelling the propagation of UHECRs

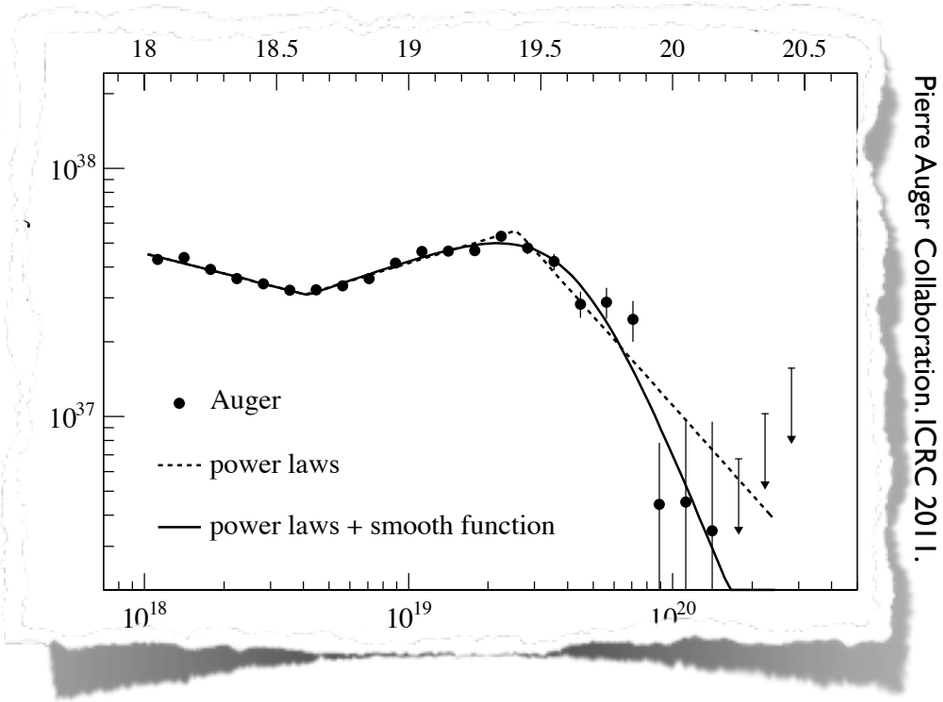

Pierre Auger Collaboration. ICRC 2011.

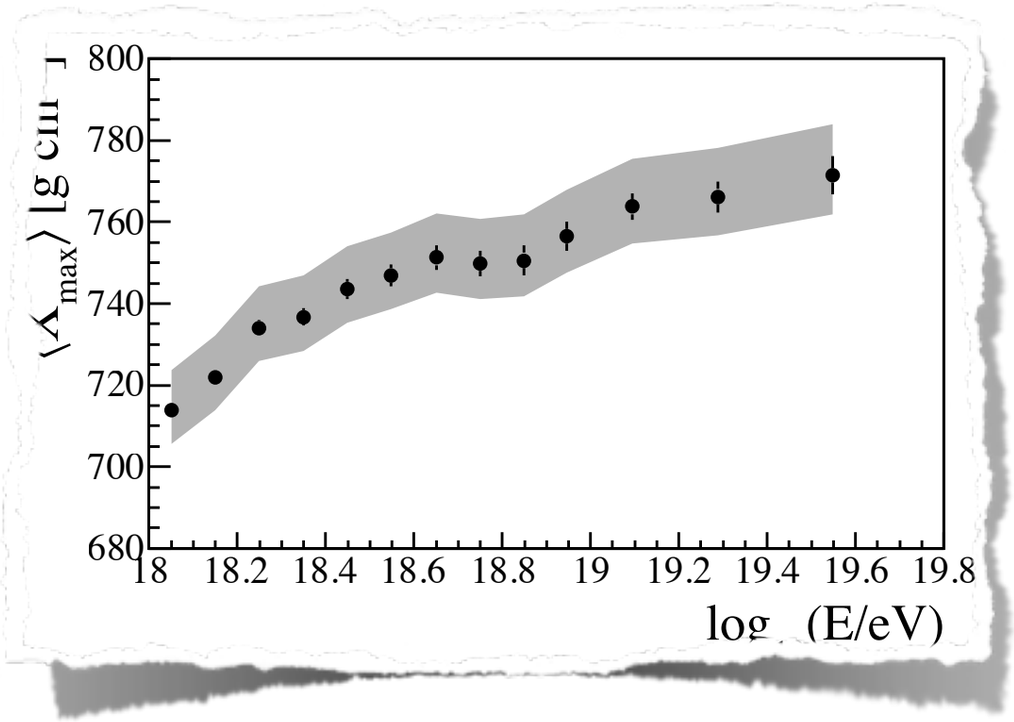

Pierre Auger Collaboration. JCAP 02 (2013) 026.

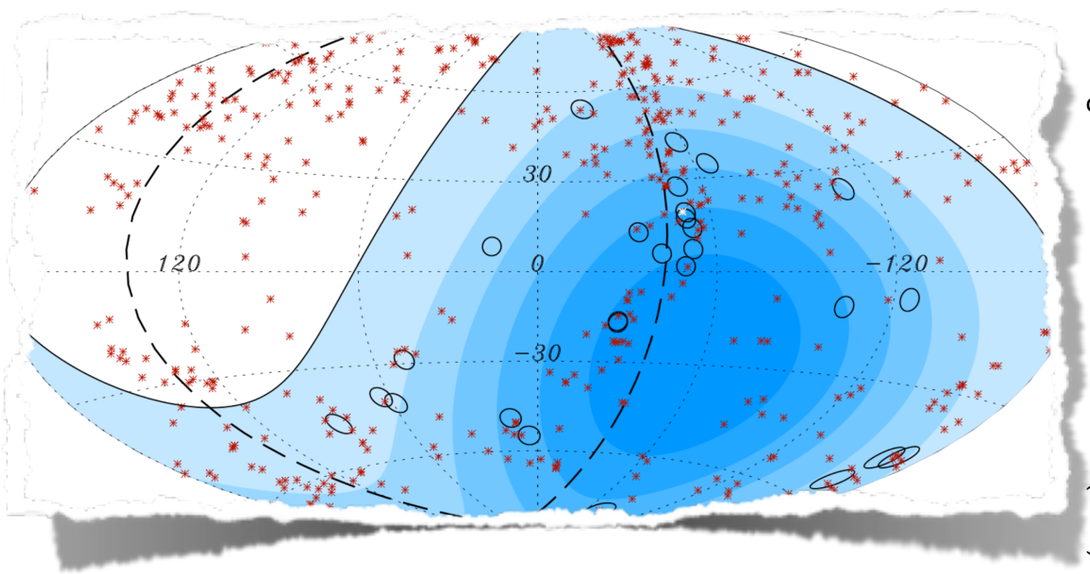

Pierre Auger Collaboration. Science 318 (2007) 938.

- explain these three observables
- explain also gamma ray and neutrino counterparts
- magnetic fields and source distribution may affect spectrum and composition, and certainly affect anisotropy
- 3D simulations are needed
- large parameter space → fast simulations

modelling the propagation of UHECRs: CRPropa

RAB et al. JCAP 05 (2016) 038. arXiv:1603.07142

- publicly available Monte Carlo code for propagating UHECRs and their secondaries in the intergalactic space
- modular structure
- parallelisation with OpenMP
- 1D, 3D and "4D" simulations
- relevant energy losses implemented
- variety of tools to handle custom magnetic field models
- predict spectrum, composition, and anisotropies simultaneously
- several models of EBL available
- possible to compute secondary gamma and neutrinos fluxes

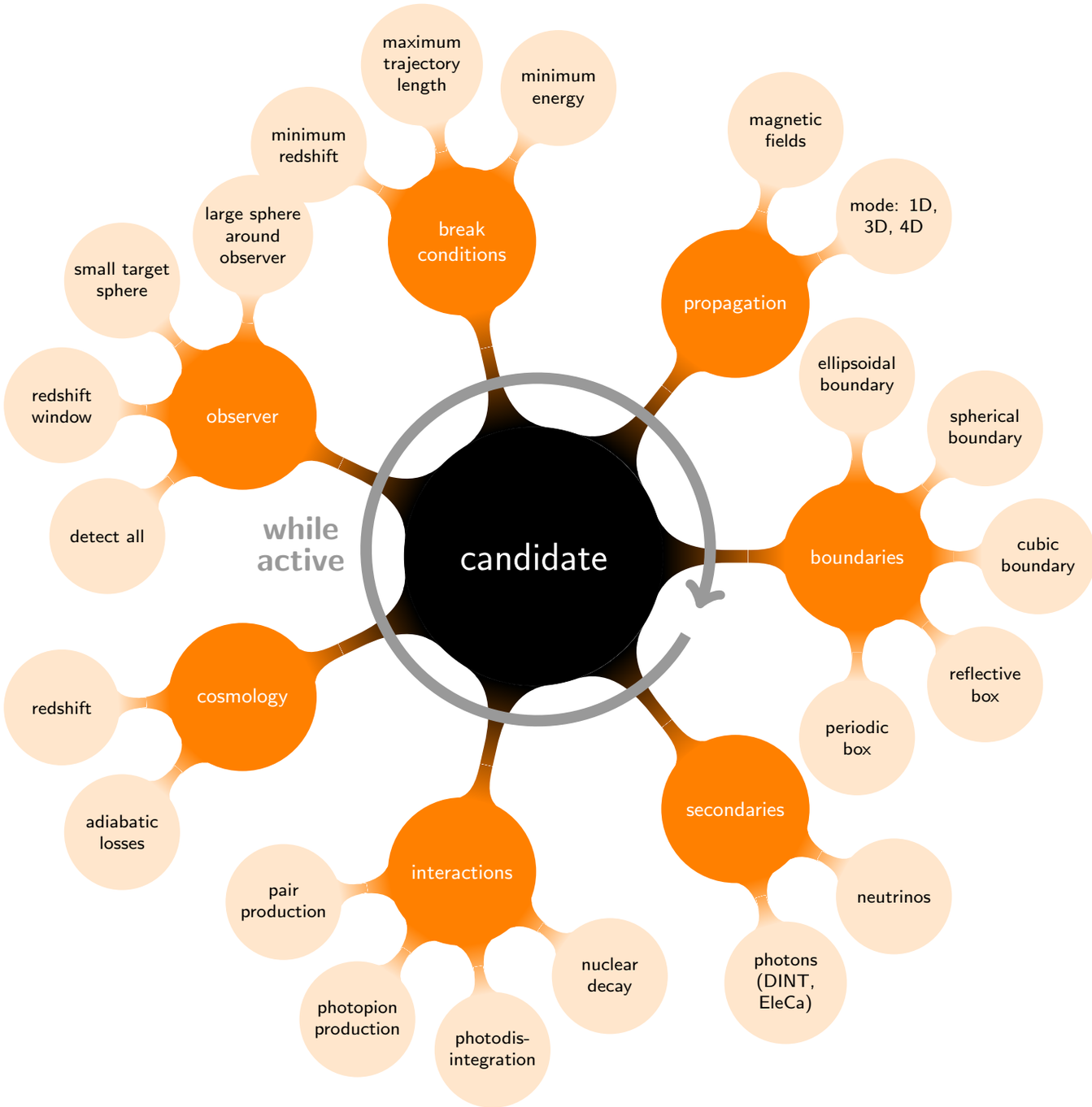

crpropa.desy.de

1D example: gamma rays and neutrinos

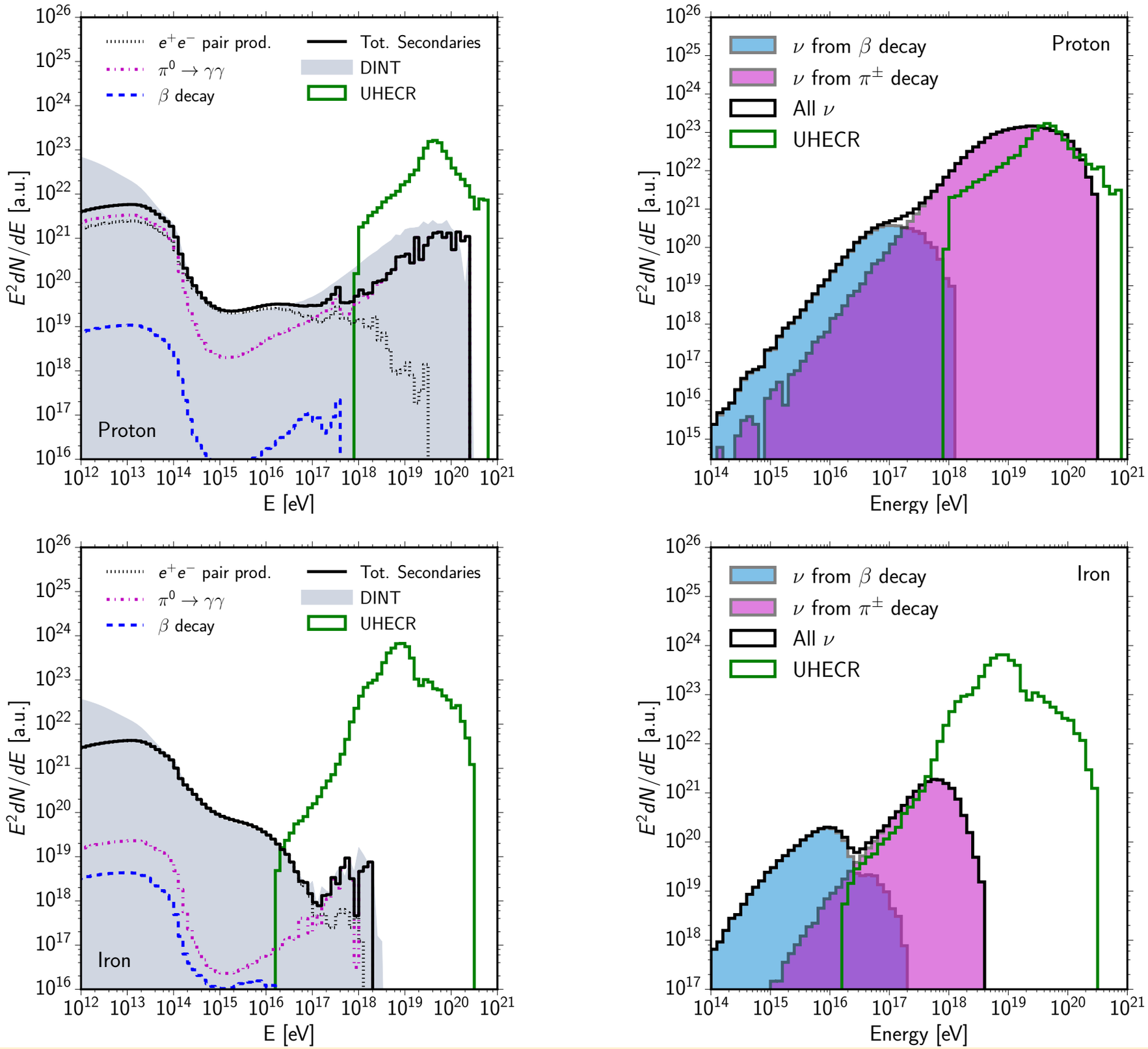

RAB et al. JCAP 05 (2016) 038.
arXiv:1603.07142

3D/4D examples: including galactic lensing

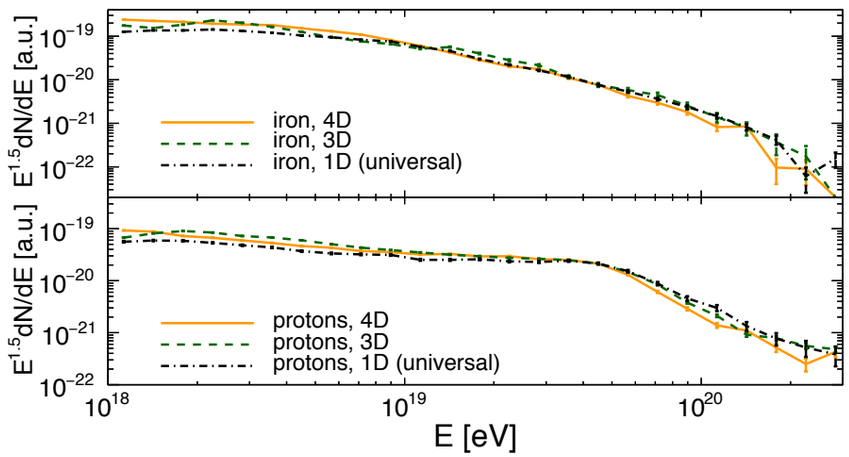

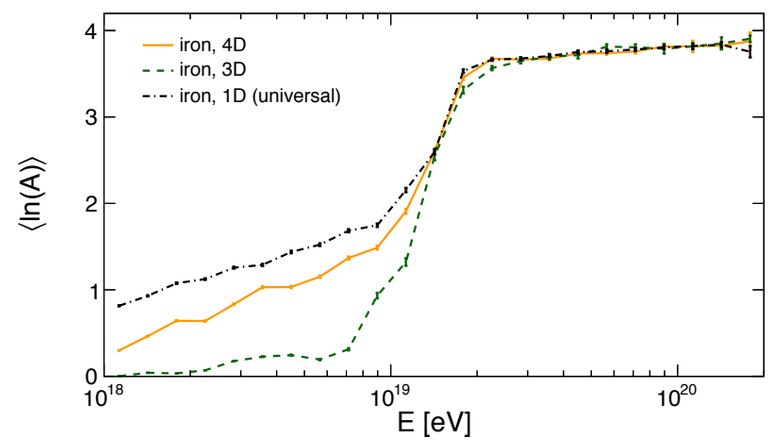

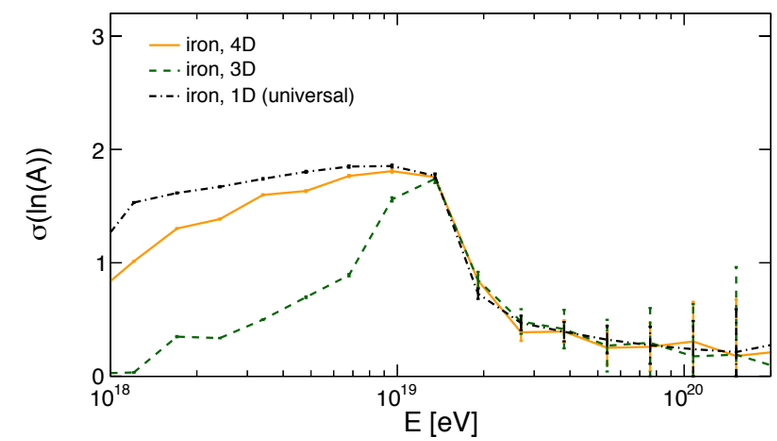

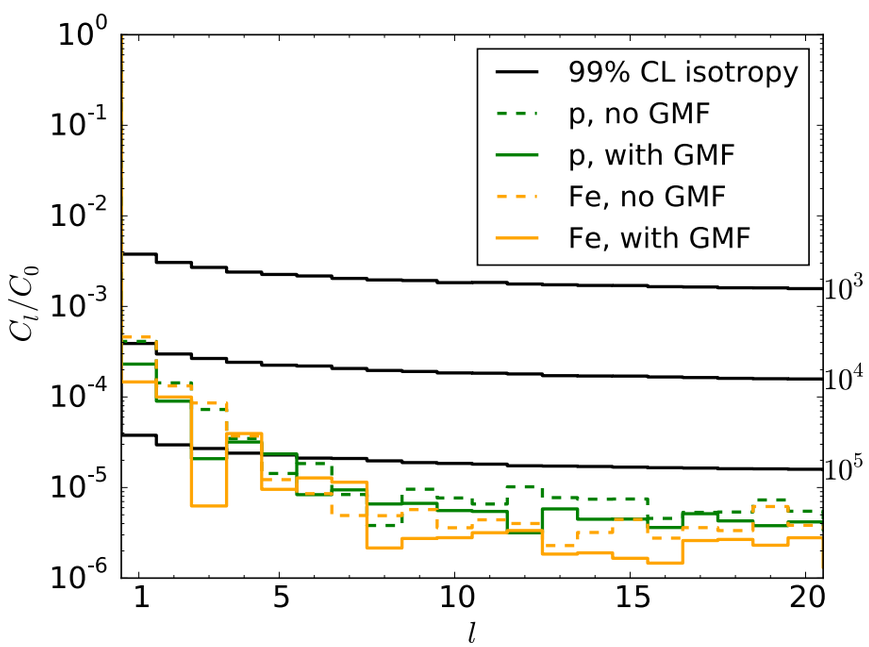

proton - only EGMF

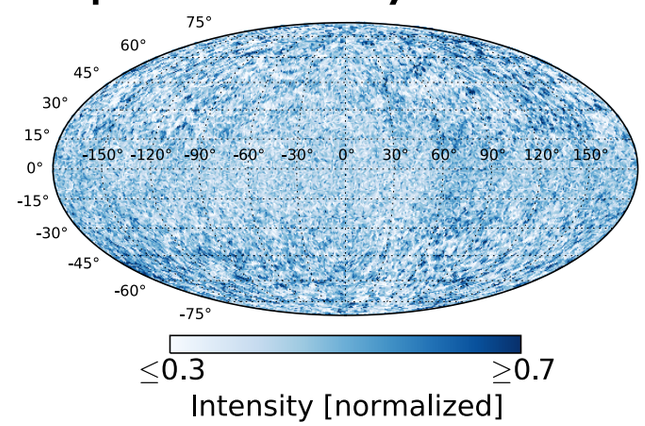

proton - EGMF+GMF

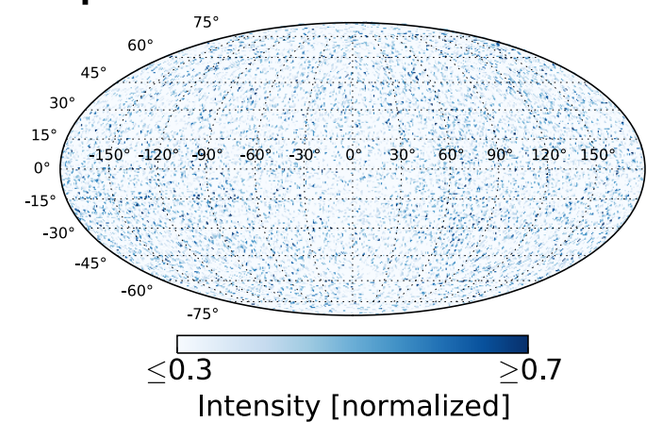

iron - only EGMF

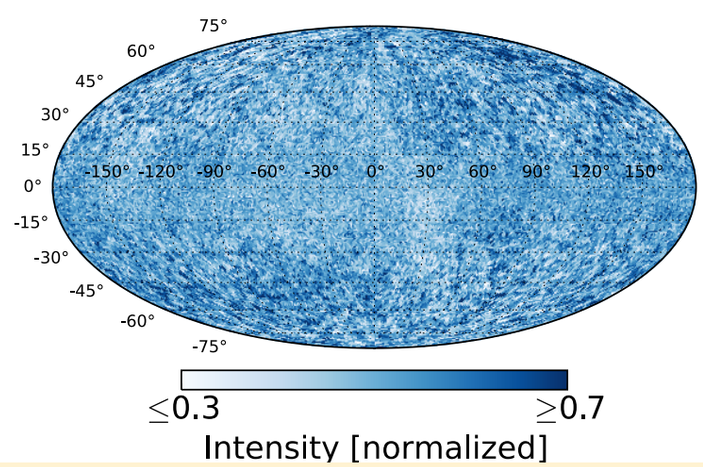

iron - EGMF+GMF

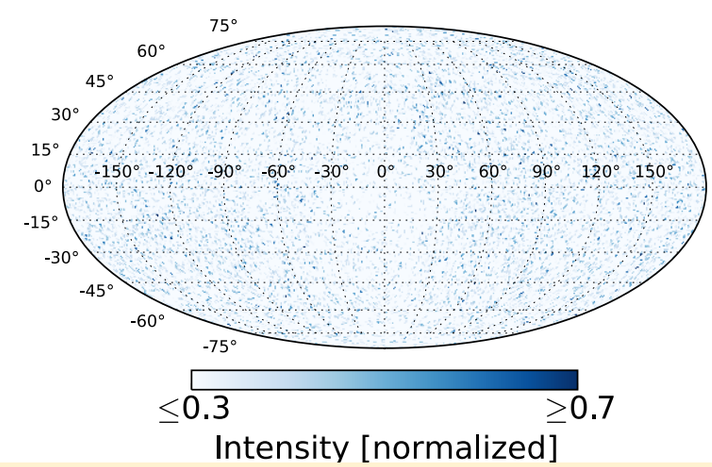

RAB et al. JCAP 05 (2016) 038. arXiv:1603.07142

theoretical uncertainties in the modelling

RAB, Boncioli, di Matteo, van Vliet, Walz. JCAP 1510 (2015) 063. arXiv:1508.01824

main sources of uncertainties

- photodisintegration cross sections
- EBL model
- propagation codes

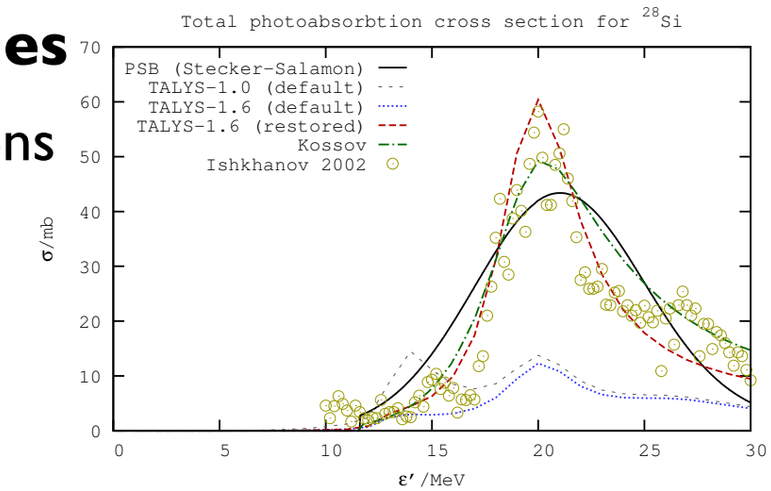

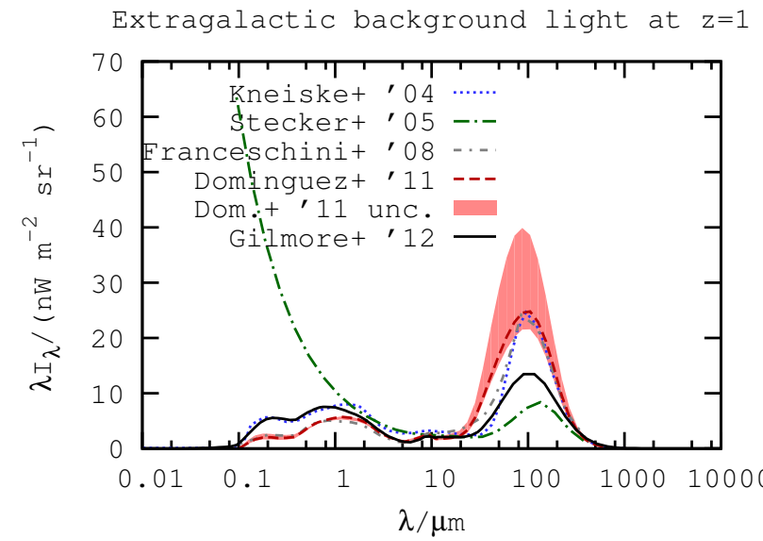

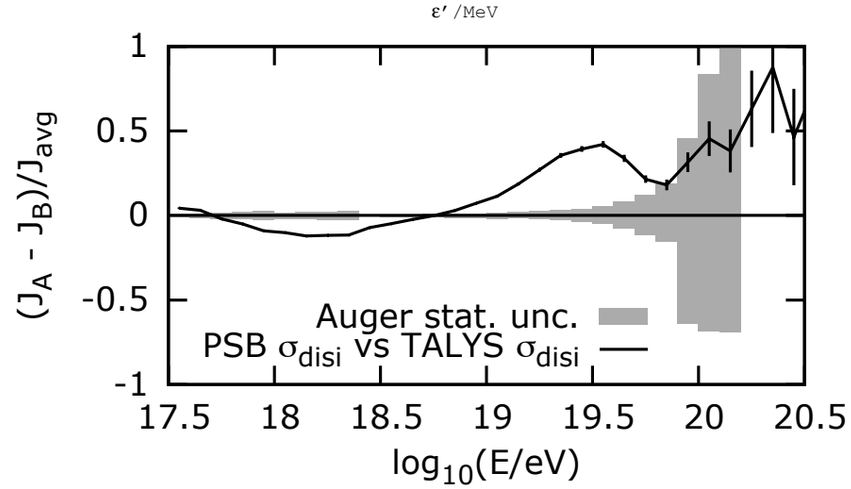

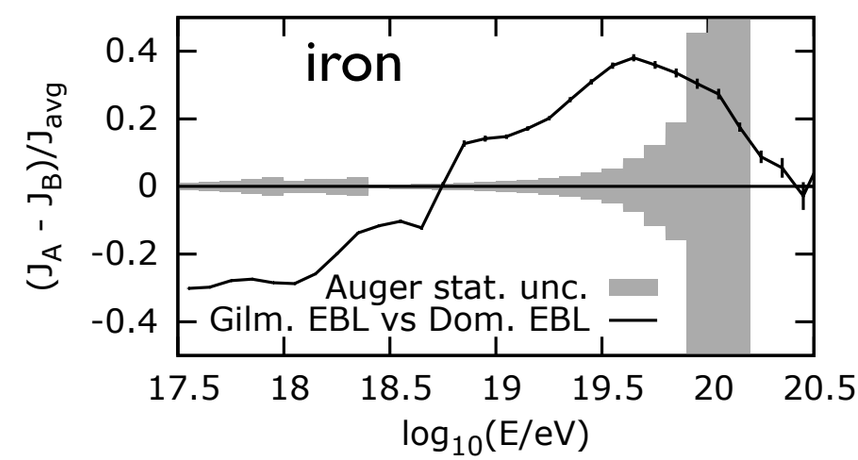

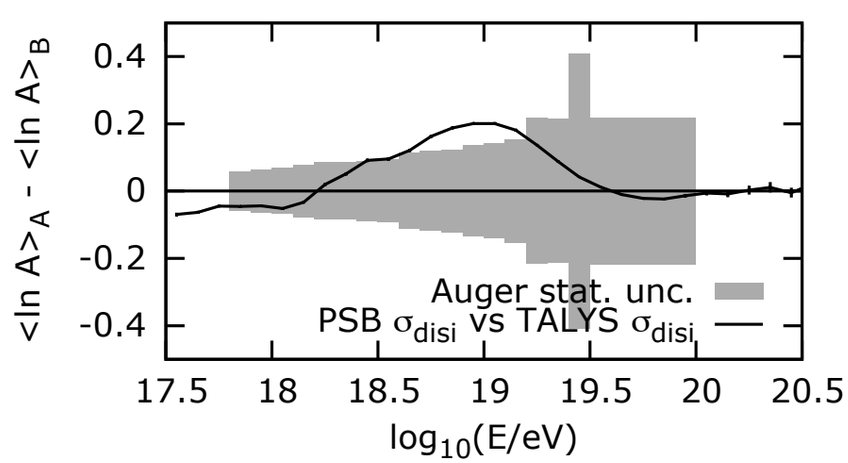

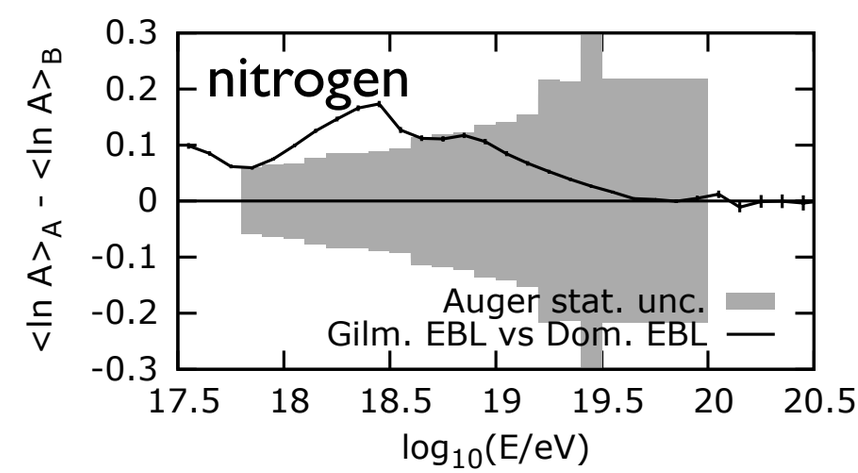

modelling the propagation of UHECRs: magnetic fields

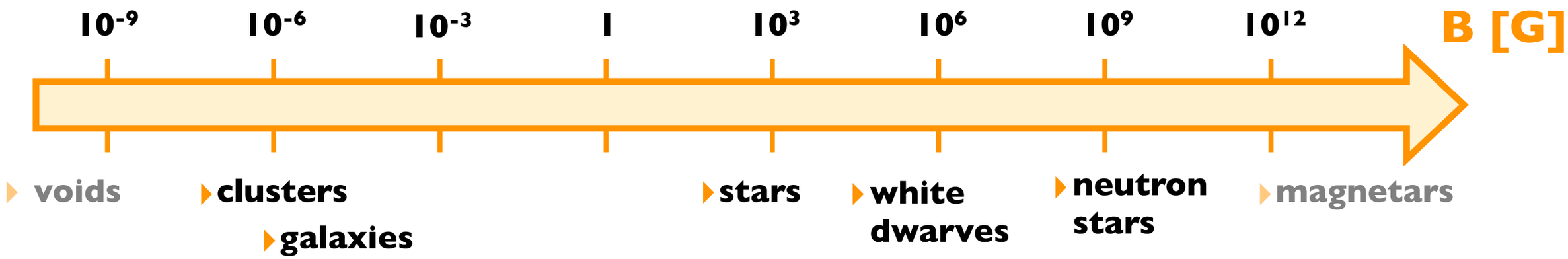

- are there cosmological magnetic fields?
- how did the magnetic fields in the universe come to be? astrophysical vs cosmological origin
- we have upper and lower bounds, but parameter space is still large

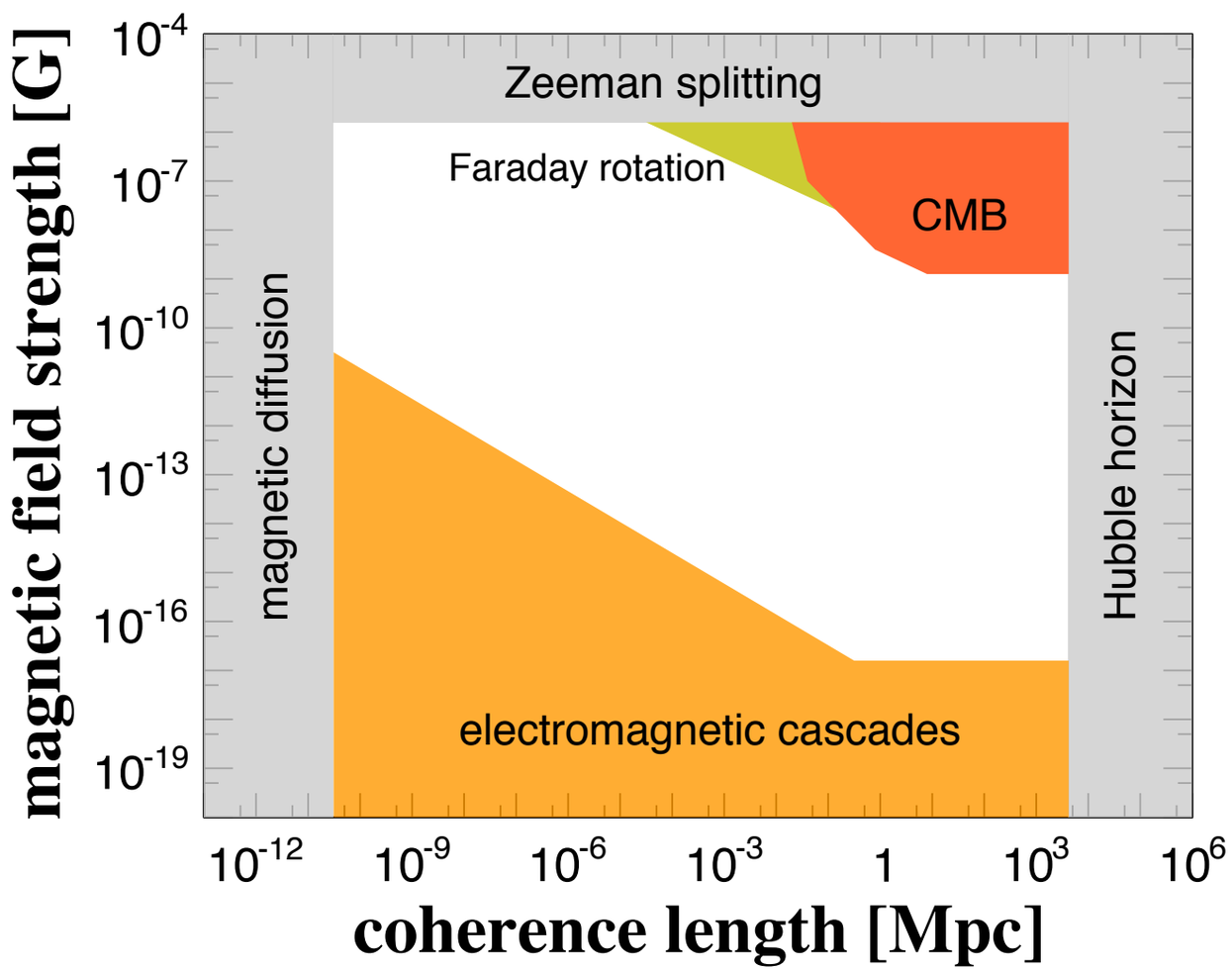

effects on the spectrum

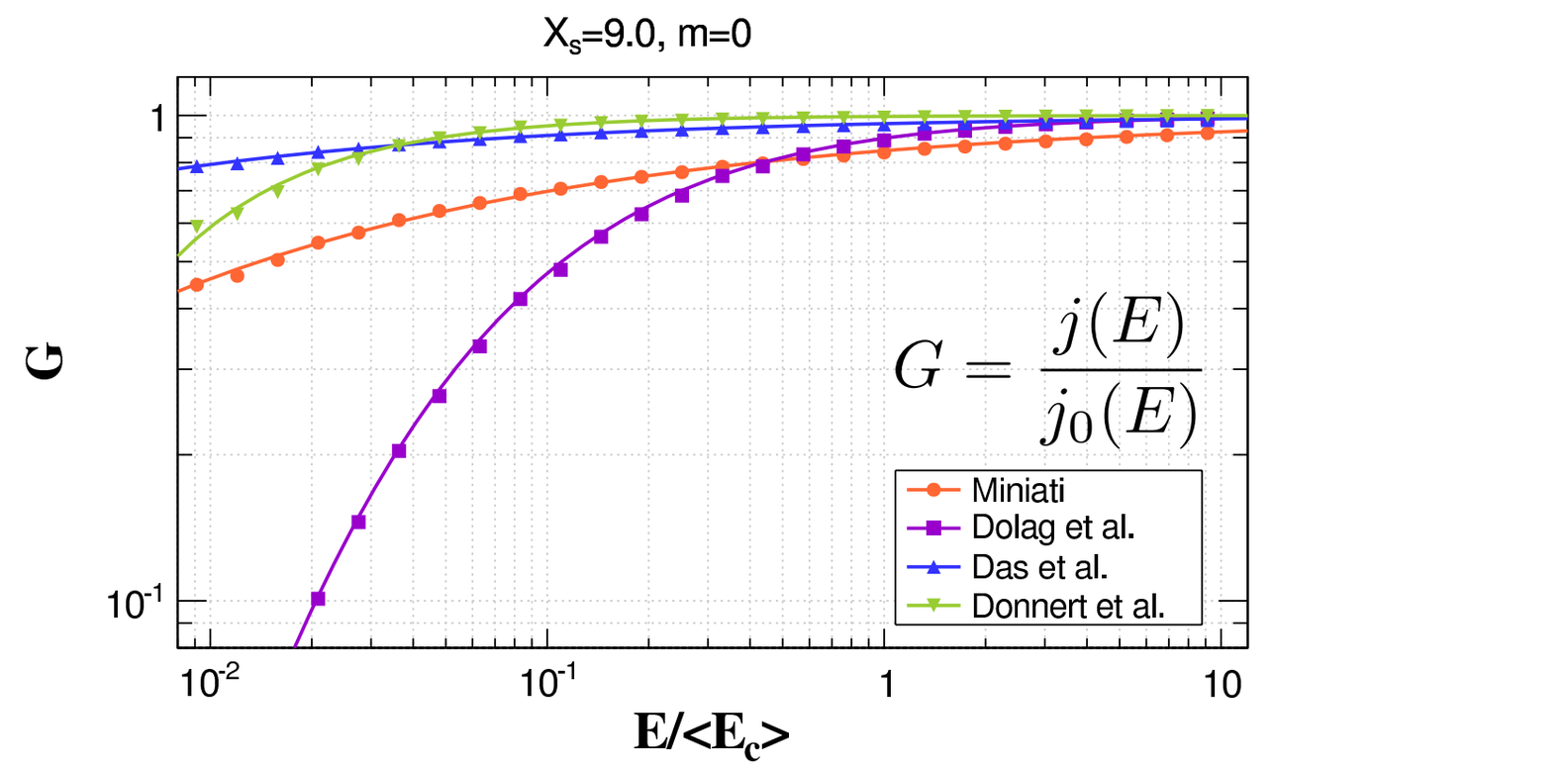

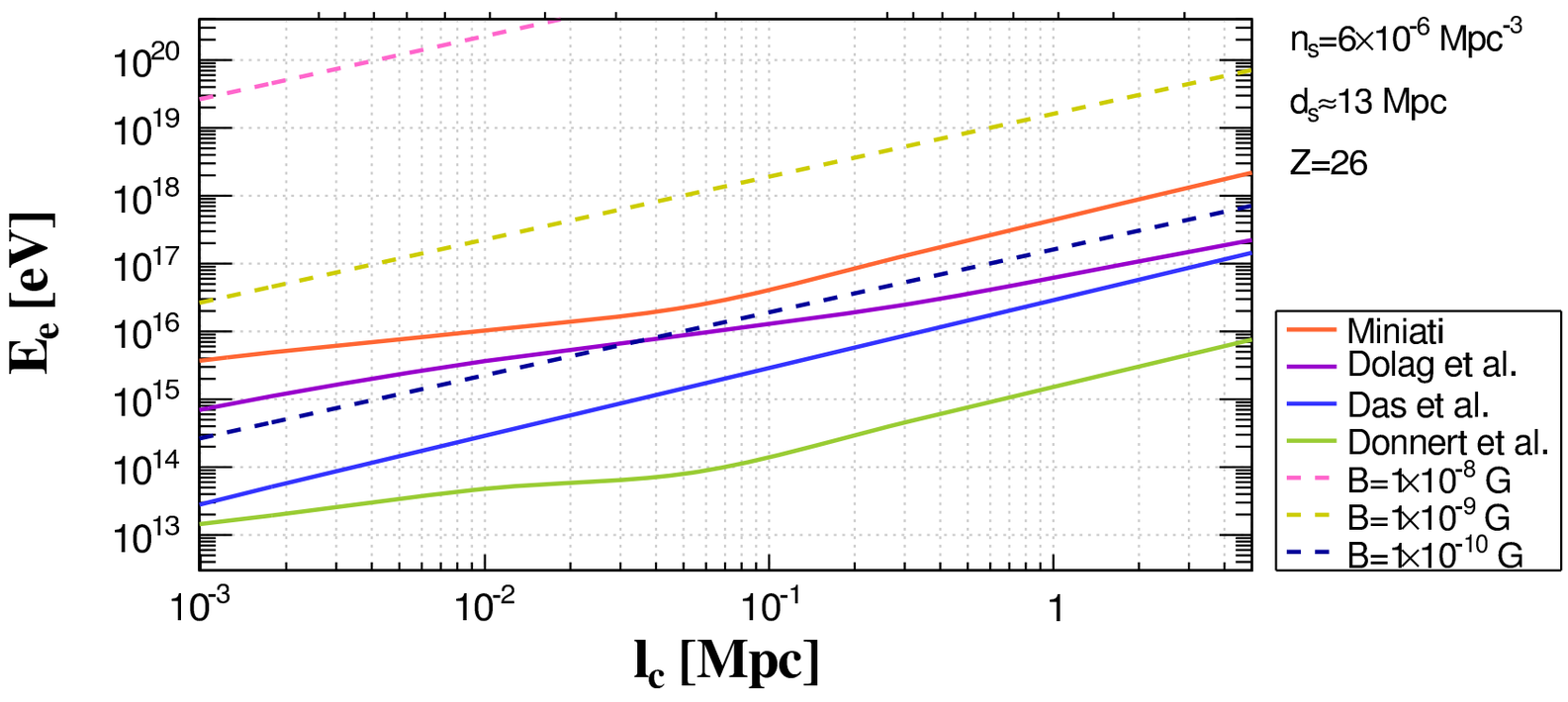

RAB & G. Sigl. JCAP 1411 (2014) 031. arXiv:1407.6150

- the shape of the spectrum is affected by diffusion in magnetic fields → magnetic horizons
- magnetic horizons were postulated by Mollerach & Roulet '13 to explain the "hard spectra" problem (combined spectrum-composition fits favoring sources with hard spectral indexes ~ 1-1.5)
- problem with this: simple turbulent field was assumed
- suppression is small at E ~ 1 EeV in "realistic" EGMF models

UHECR astronomy?

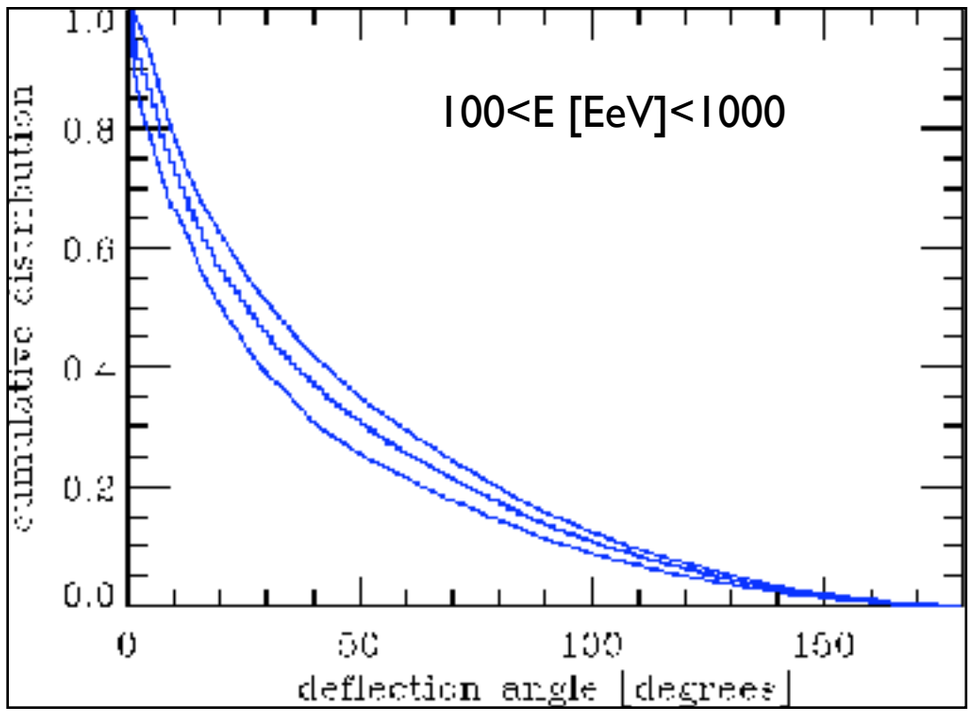

Sigl, Miniati, Ensslin. PRD 70 (2004) 043007

- cumulative deflections displayed are for protons
- Sigl+: deflections are high
- Dolag+: deflections are small
- for heavy nuclei deflections can be even higher
- UHECR astronomy may be possible in the later but not in the former scenario

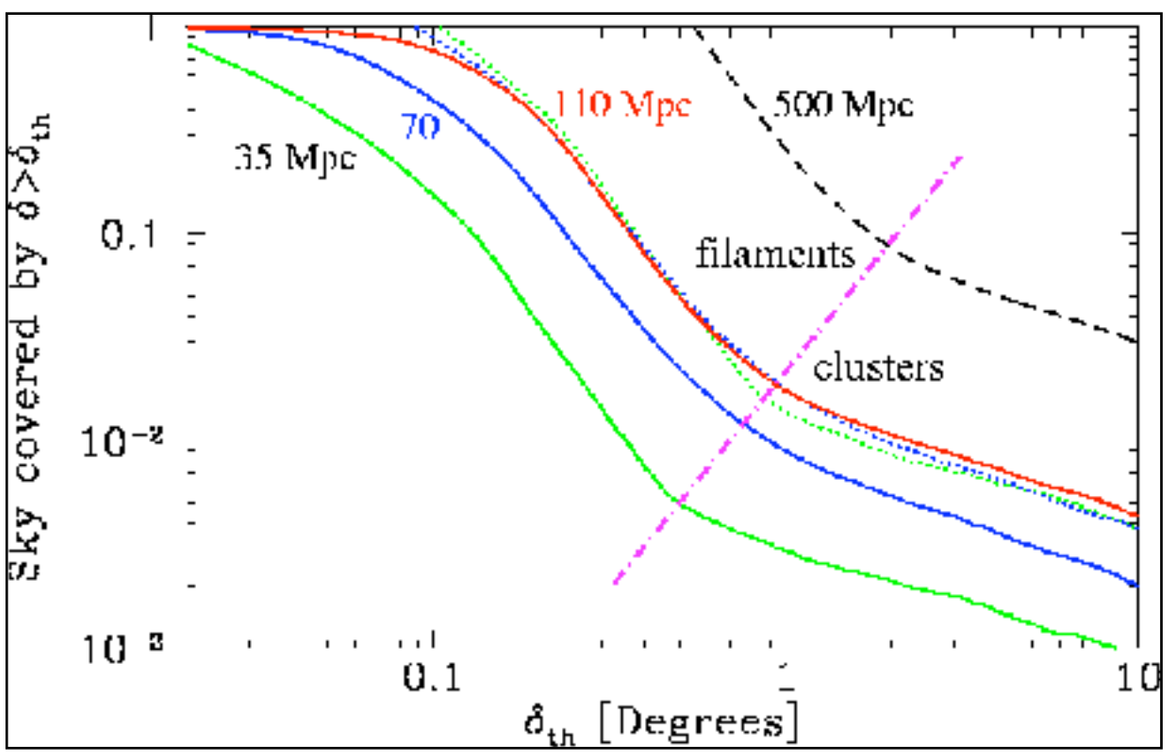

Dolag et al. JETP 79(2004) 583

power spectrum of seed fields

RAB, M.-S. Shin, J. Devriendt, D. Semikoz, G. Sigl. In preparation. arXiv:1612.XXXXX

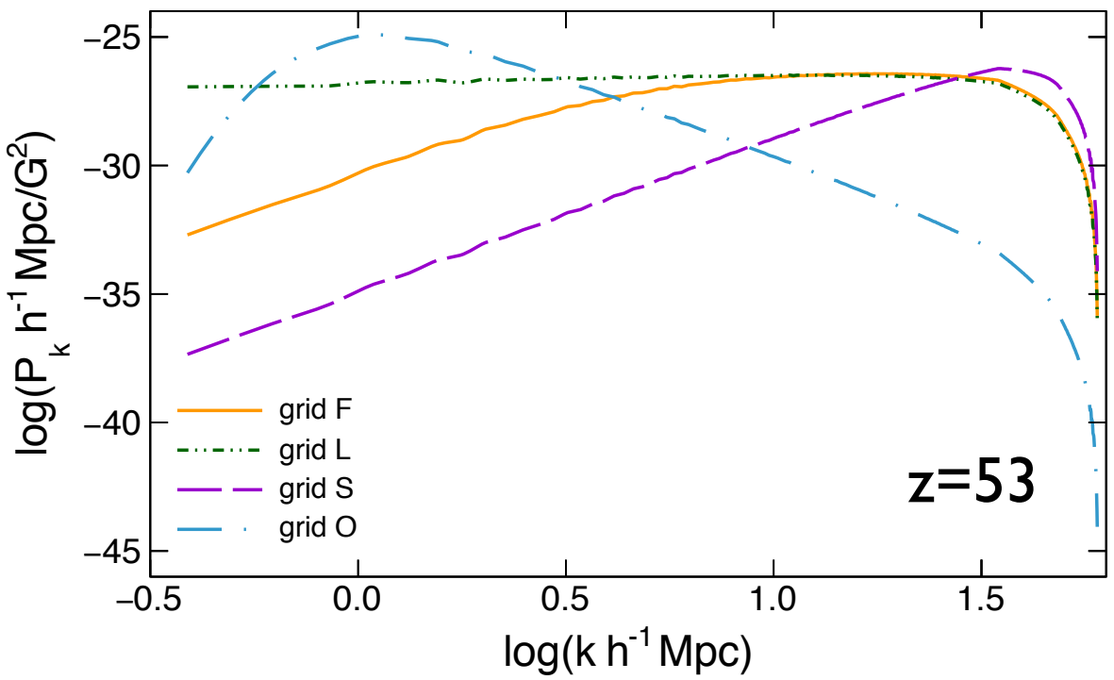

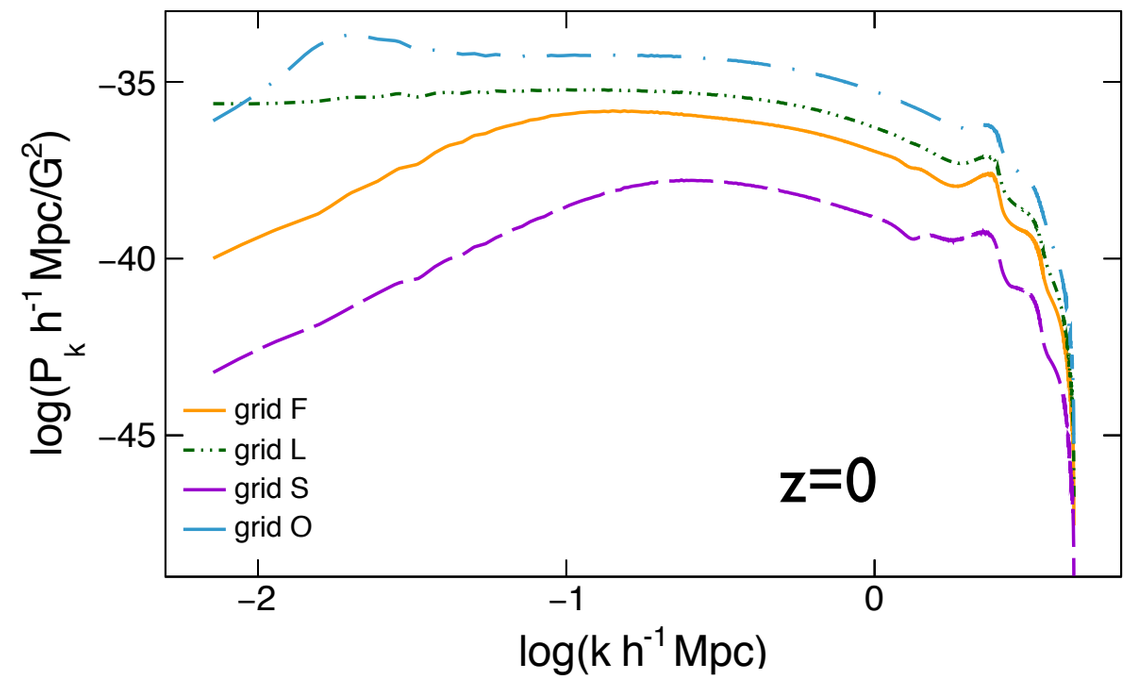

grid S

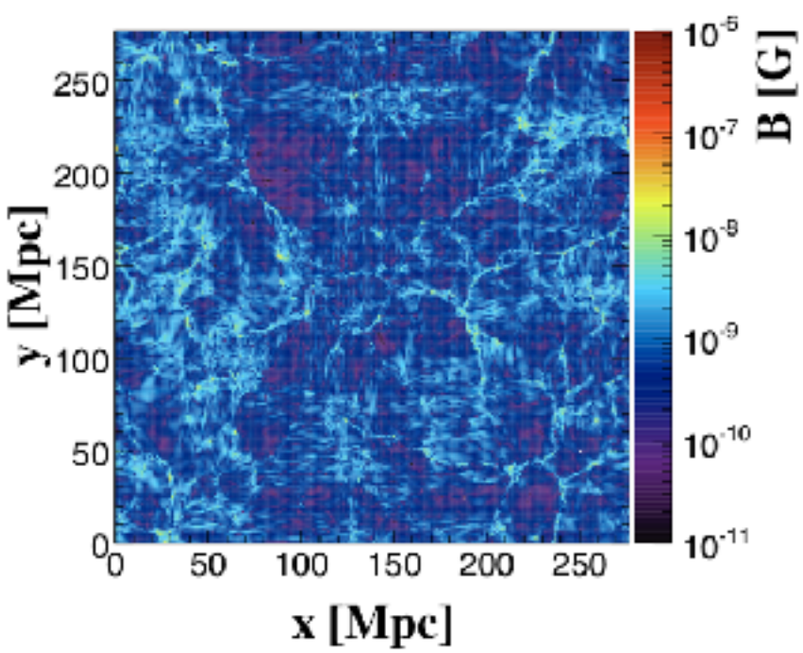

grid L

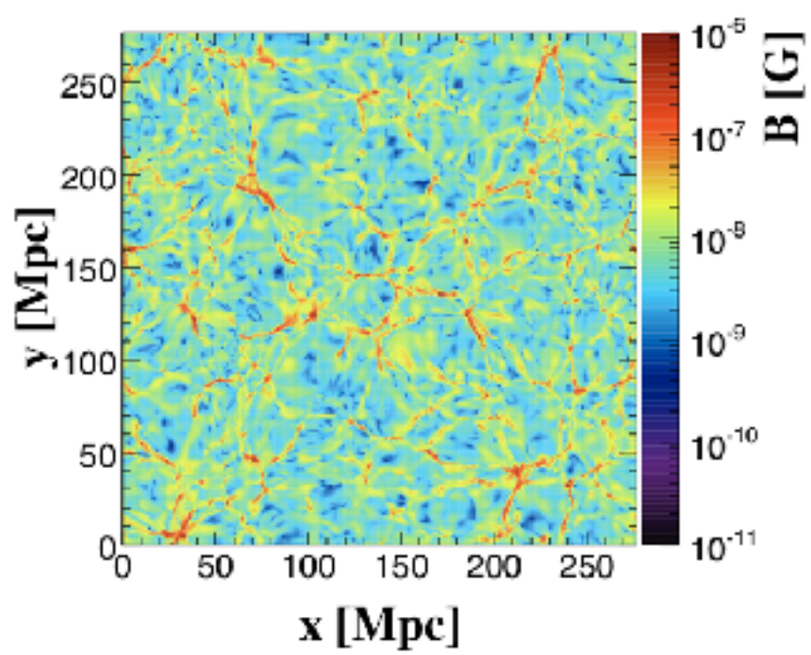

grid F

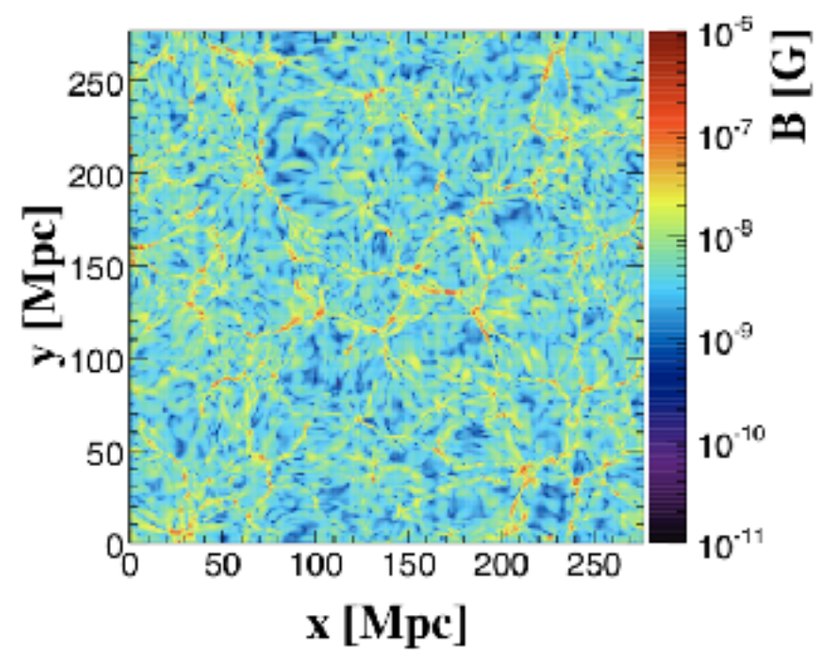

the magnetised cosmic web

- we use Planck's upper limit to normalise the magnetic field in voids
- upper limit on (extragalactic) UHECR deflection

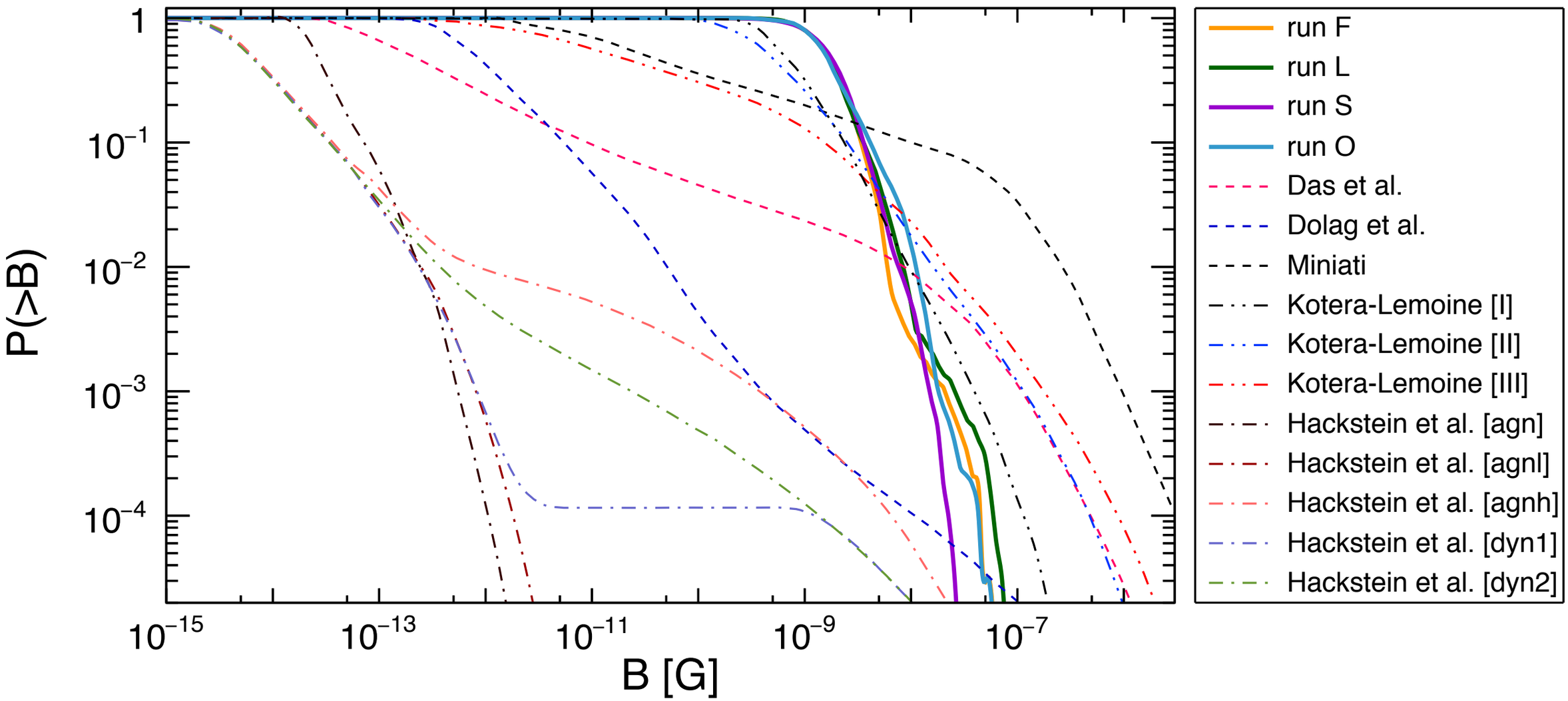

RAB, M.-S. Shin, J. Devriendt, D. Semikoz, G. Sigl. In preparation. arXiv:1612.XXXXX

UHECR spectrum: impact of the B power spectrum

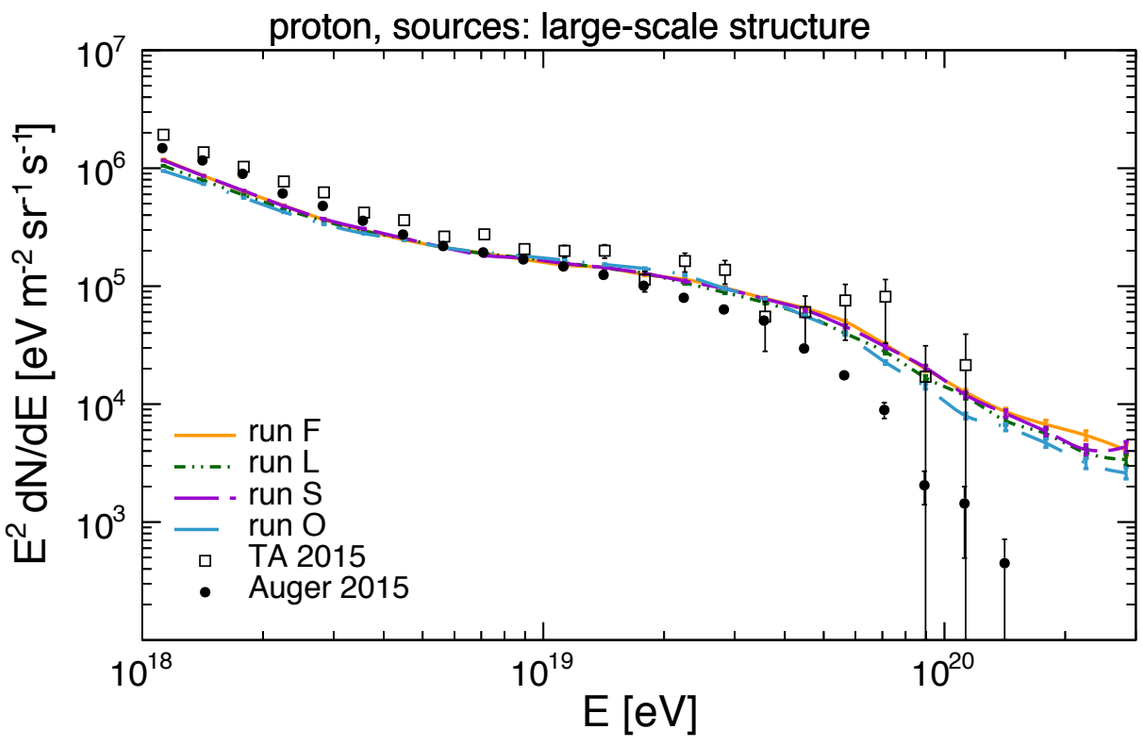

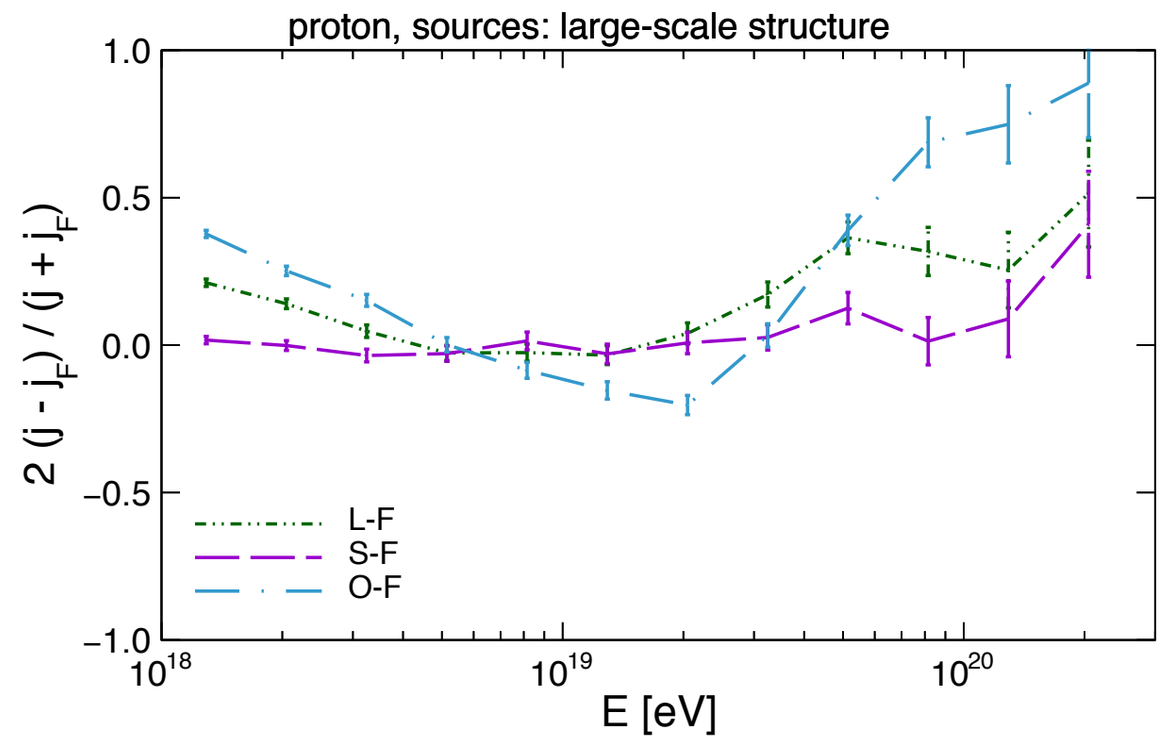

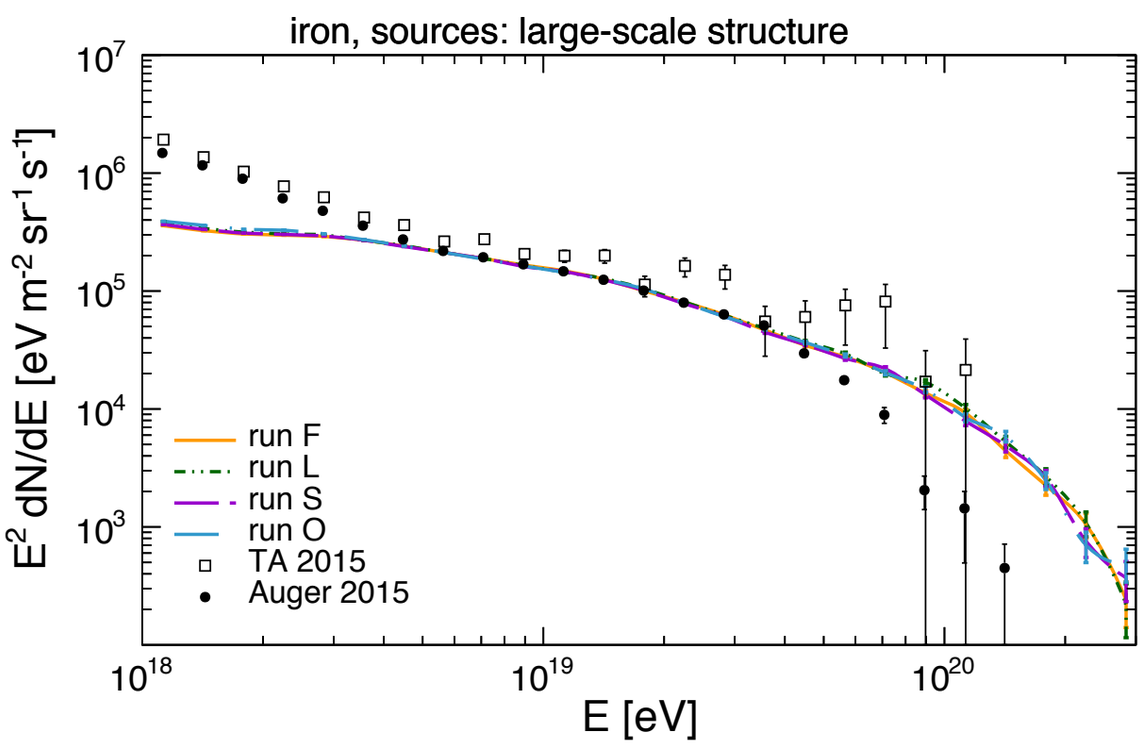

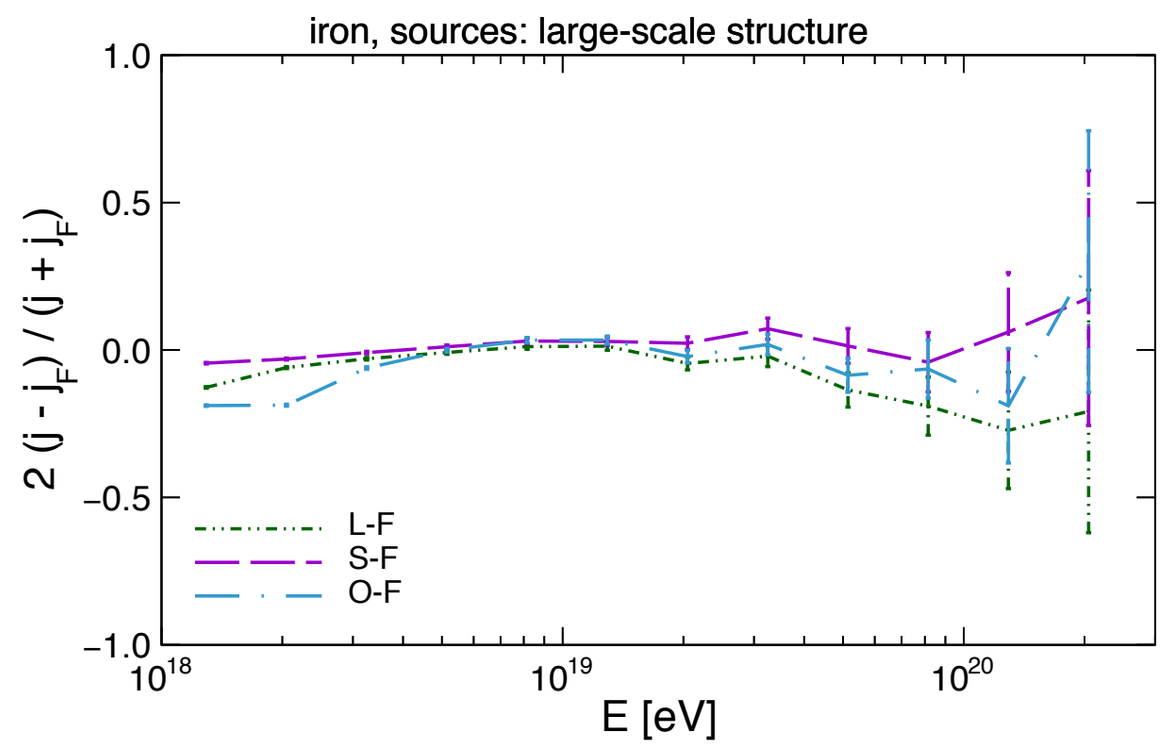

RAB, M.-S. Shin, J. Devriendt, D. Semikoz, G. Sigl. In preparation. arXiv:1610.XXXXX

UHECR deflections: impact of the B power spectrum

RAB, M.-S. Shin, J. Devriendt, D. Semikoz, G. Sigl. In preparation. arXiv:1612.XXXXX

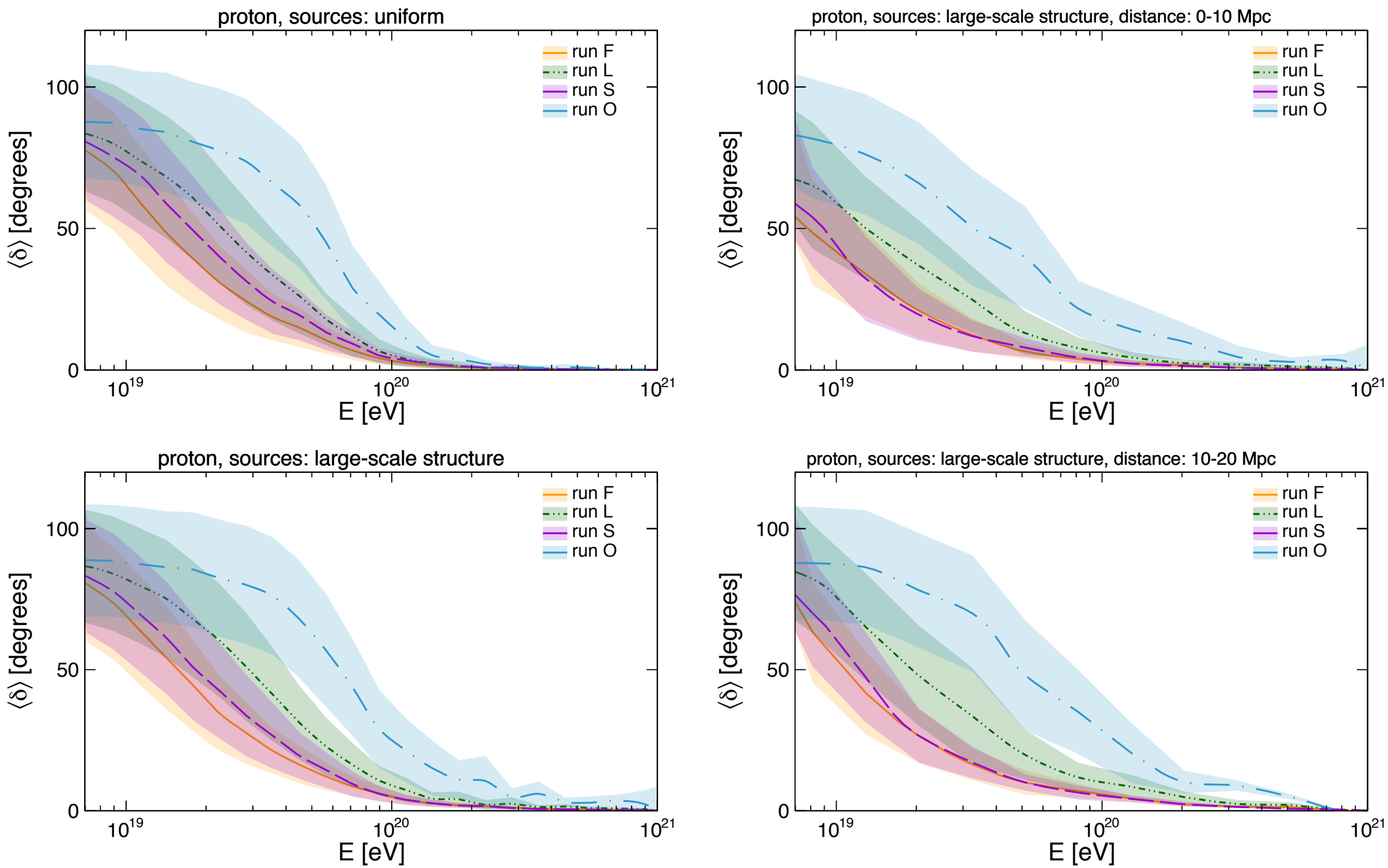

UHECRs and the galactic magnetic field

- state of the art GMF model: Jansson & Farrar '12 (JF12)
- this model is based on fits of synchrotron emission + Faraday rotation + polarisation measurements

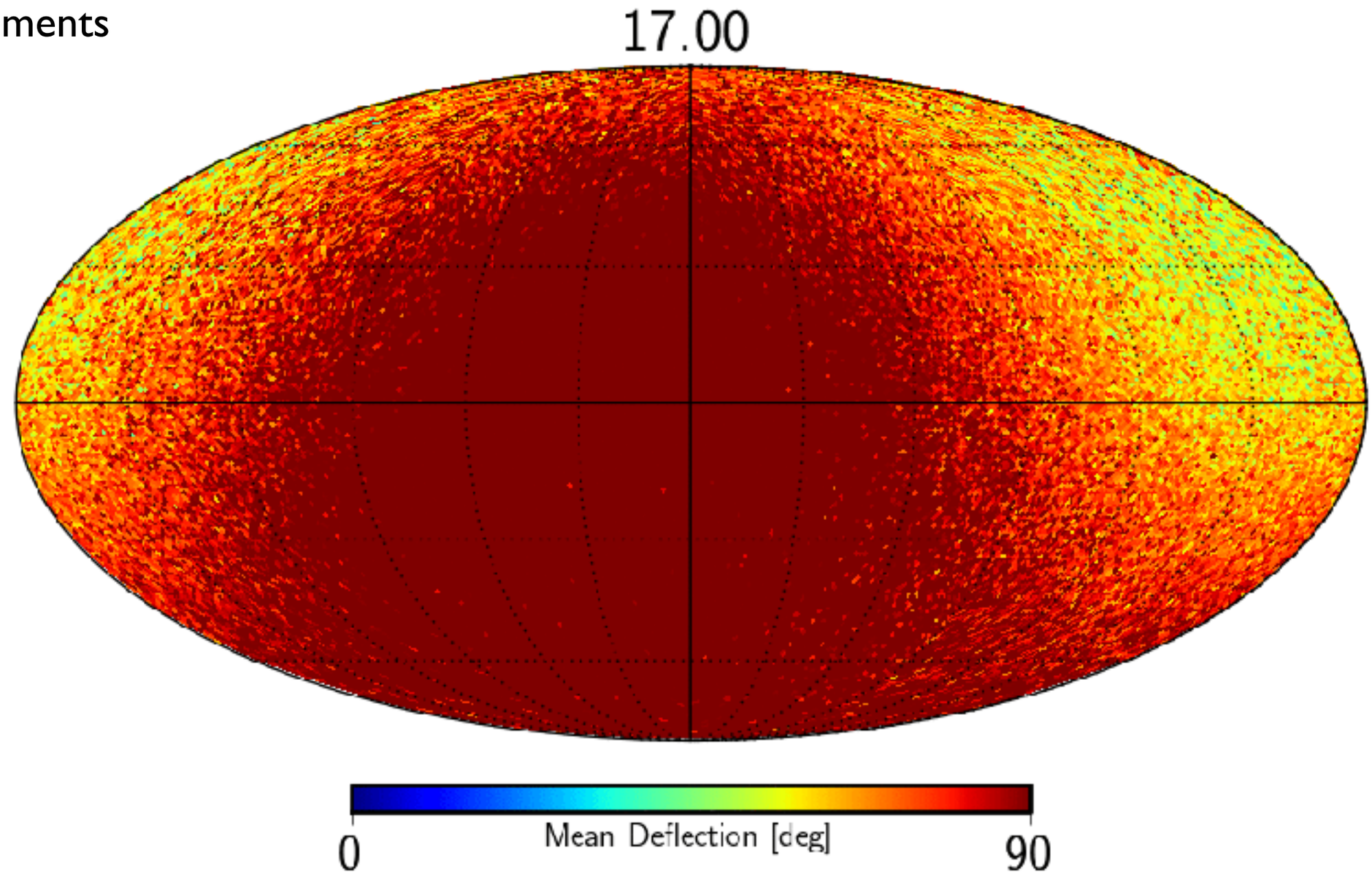

obtained with the PARSEC code:

http://web.physik.rwth-aachen.de/Auger_MagneticFields/PARSEC

UHECRs and the galactic magnetic field

- the case of Centaurus A, assuming only galactic deflections and the complete JF12 field

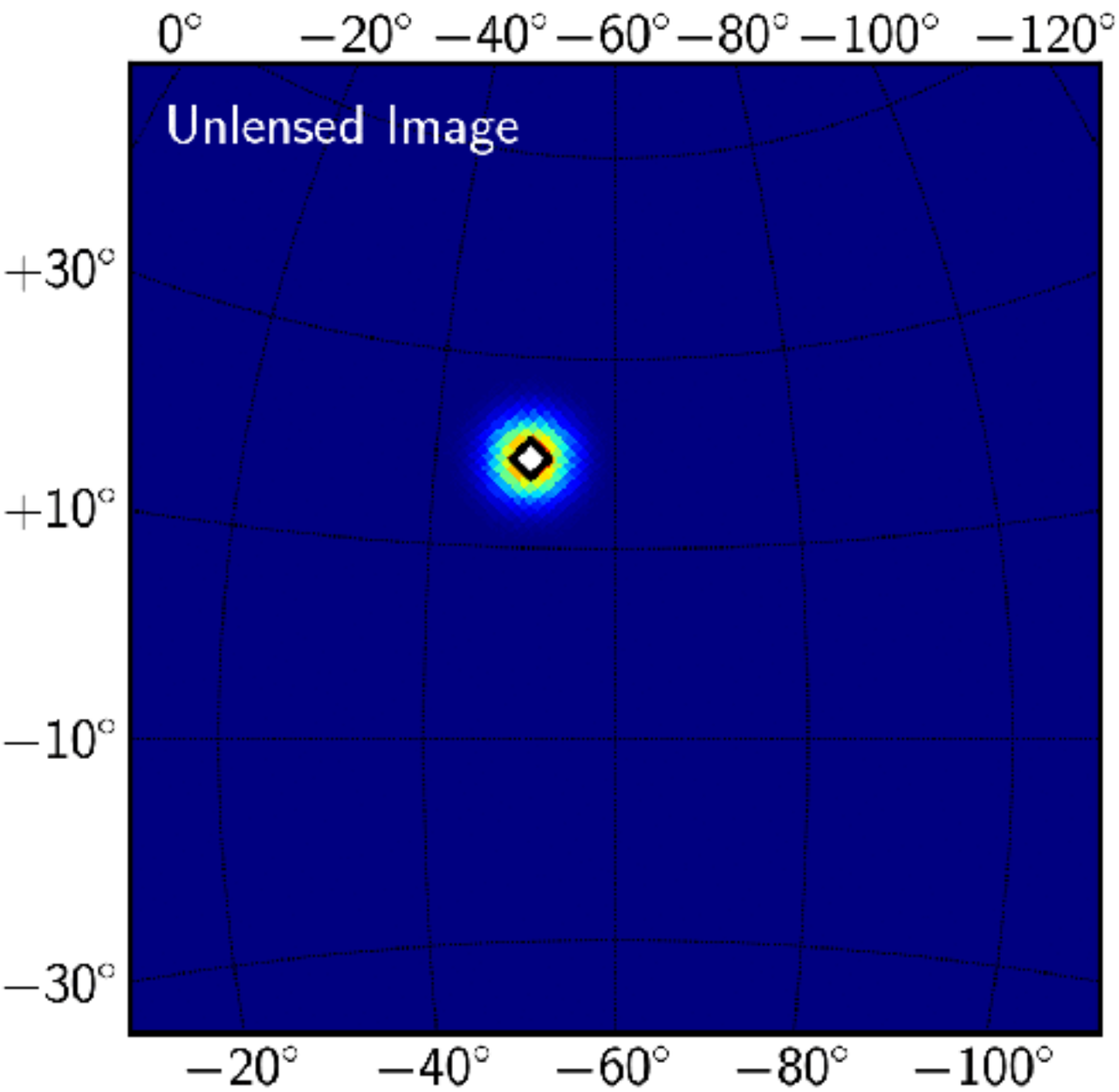

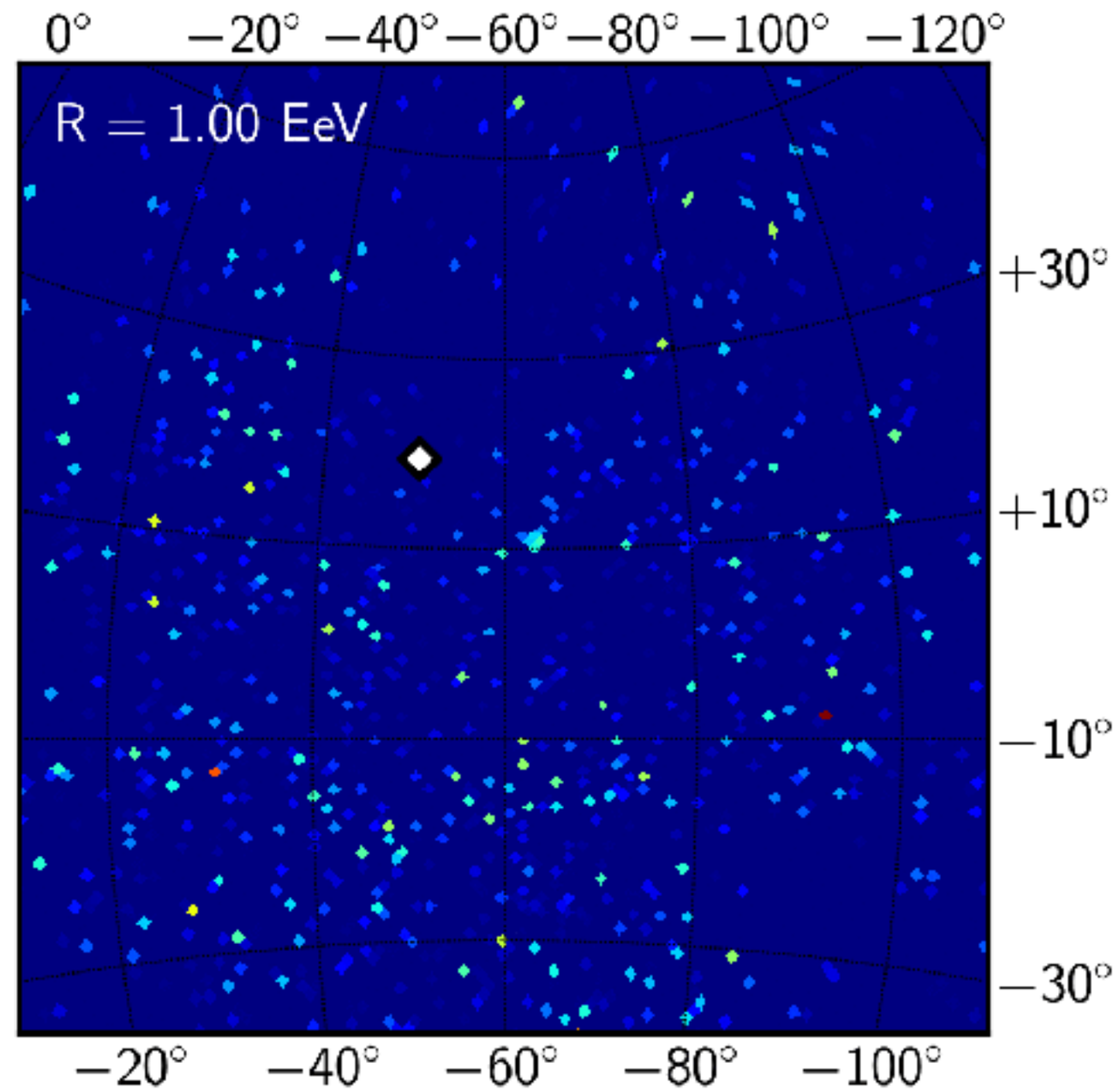

obtained with the PARSEC code

UHECRs and the galactic magnetic field

M. Zimbres, RAB, E. Kemp. Astropart. Phys. 54 (2014) 54. arXiv:1305.0523

- if galactic deflections dominate over extragalactic, can we reconstruct source position?

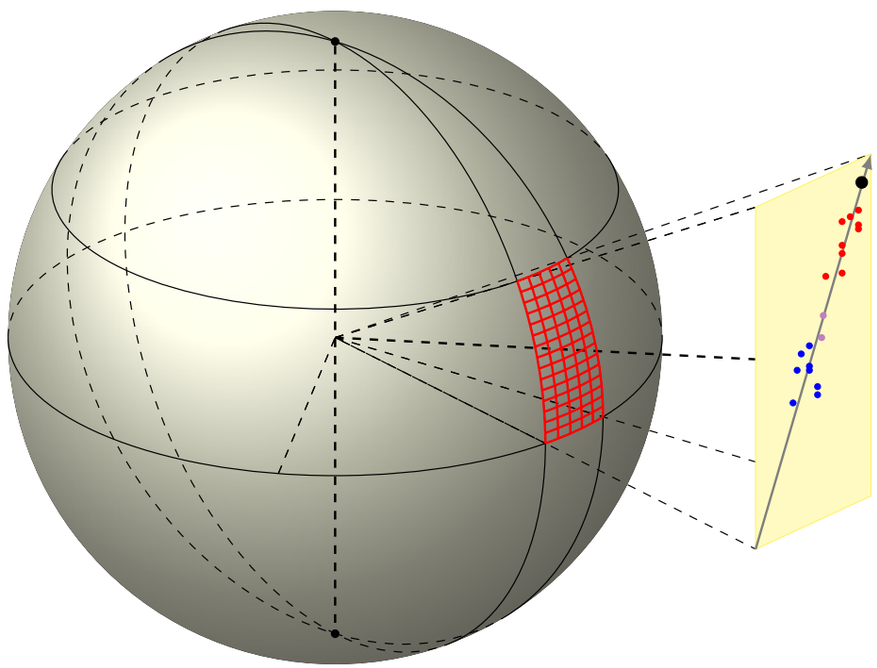

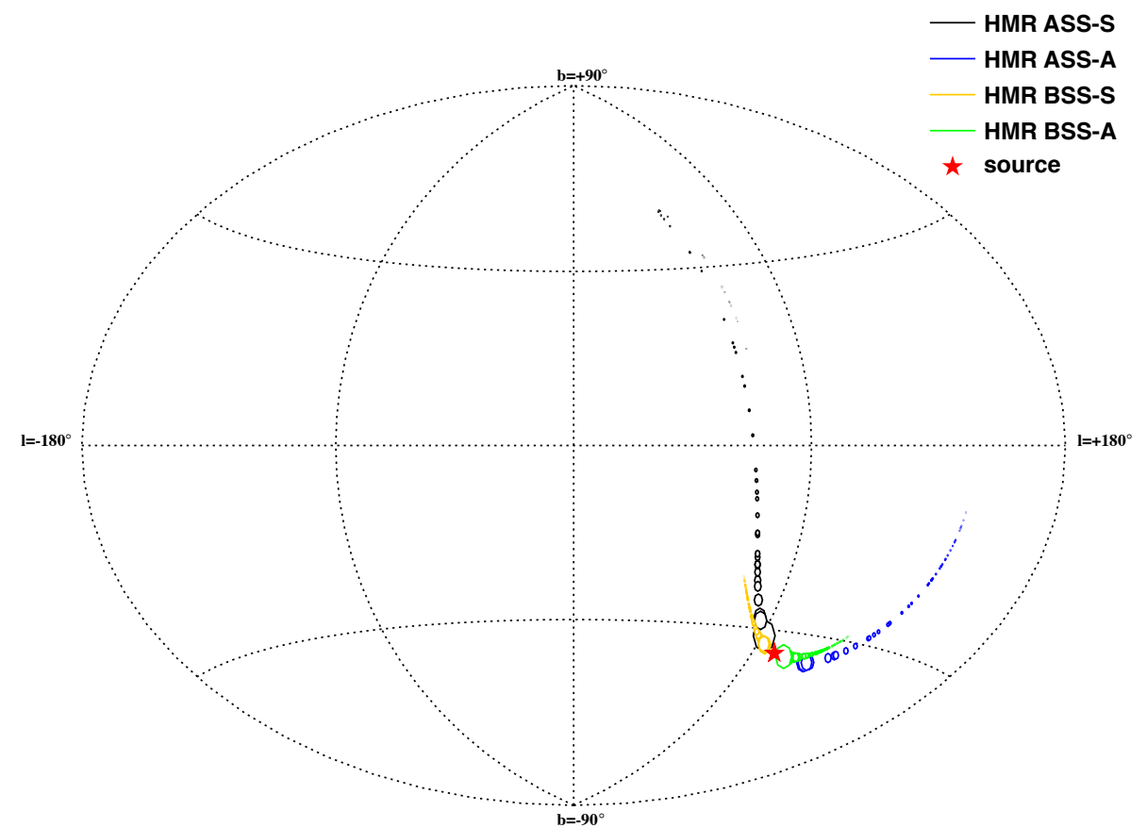

- no multiplets detected in Auger data *[Auger '12]*
- constrain models of GMF with multiplets?
- probably unlikely to be detected, unless source is really close and magnetic fields are "well-behaved"

constraining the composition of UHECR

A. van Vliet, RAB, J. Hörandel. In preparation.

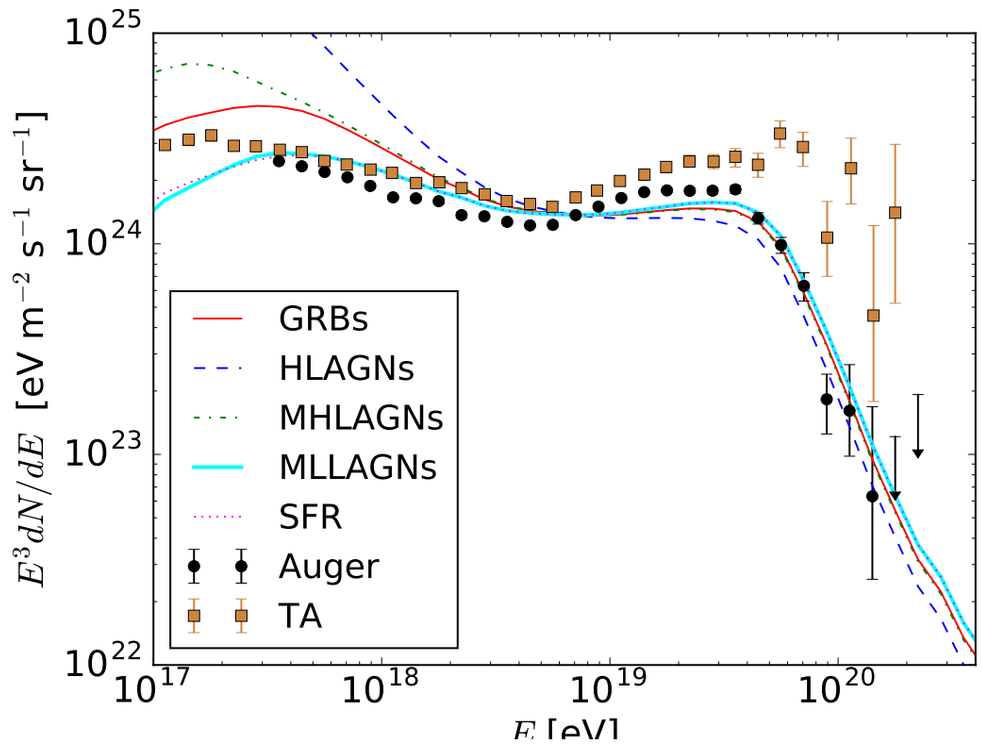

protons, $E^{-1.5}$,
Rmax=$10^{18.6}$ eV

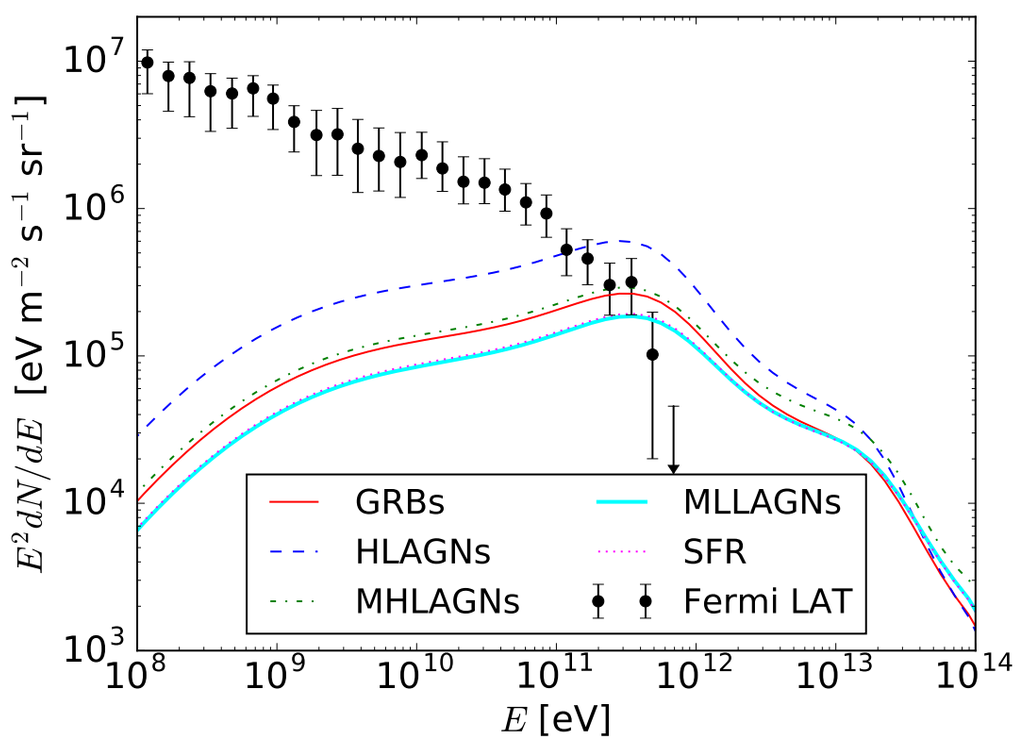

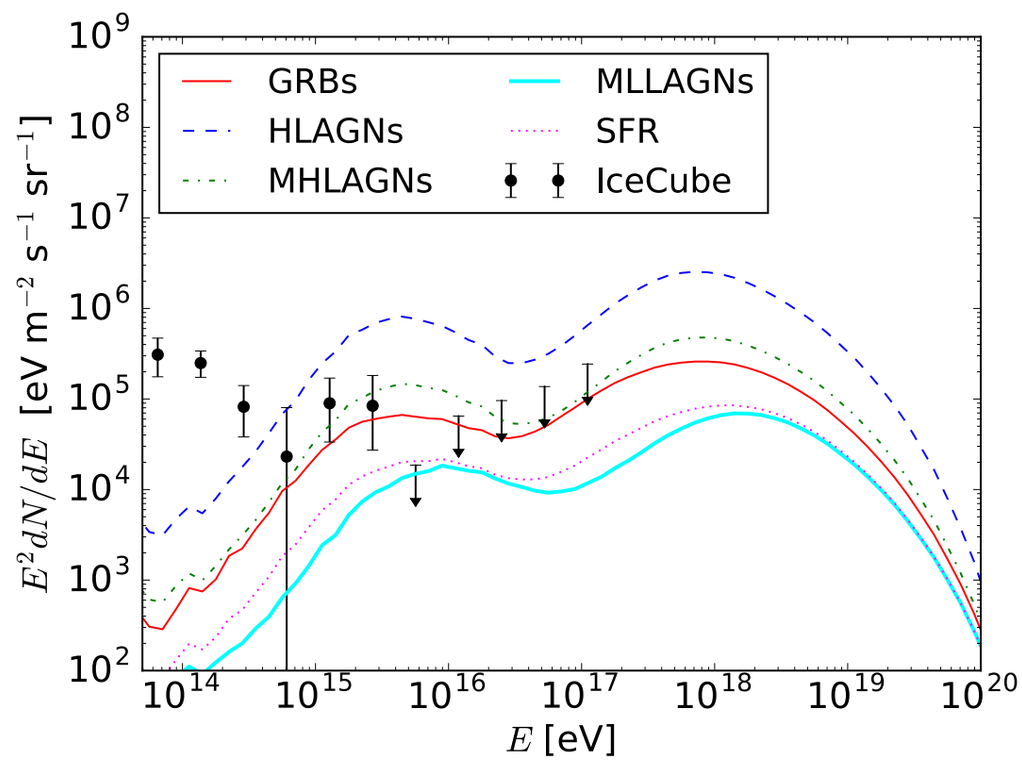

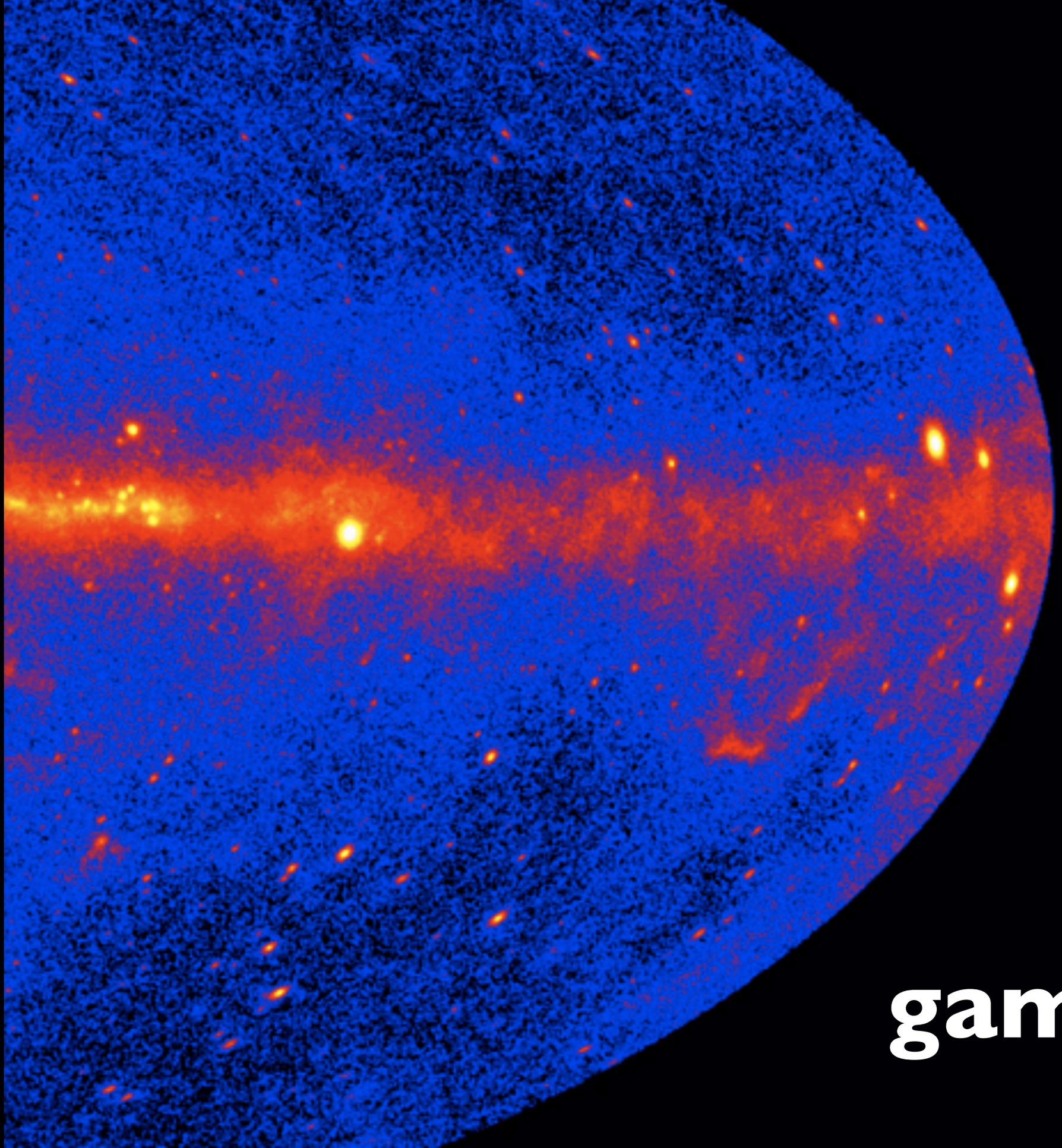

gamma rays

modelling the propagation of gamma rays

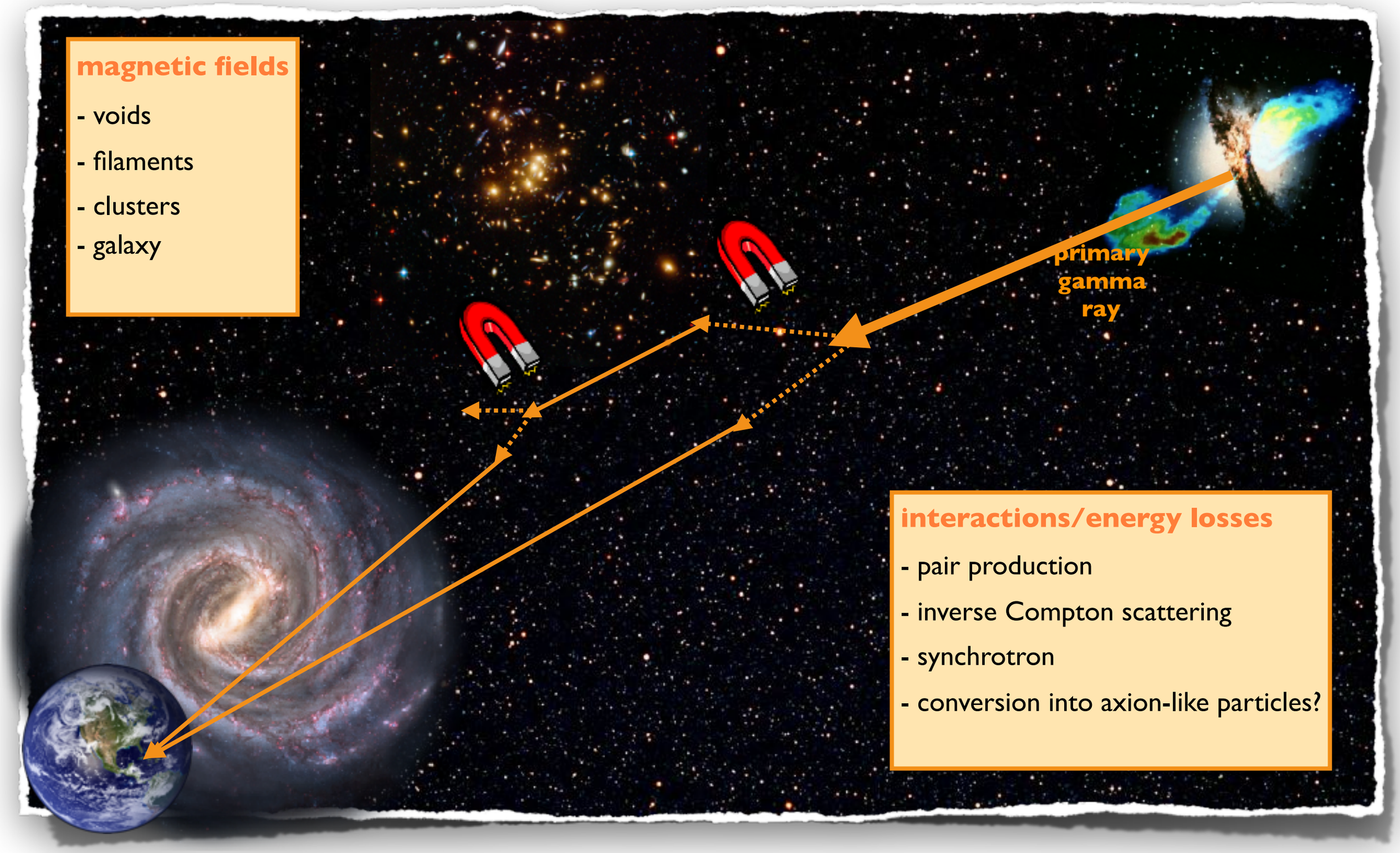

electromagnetic cascades

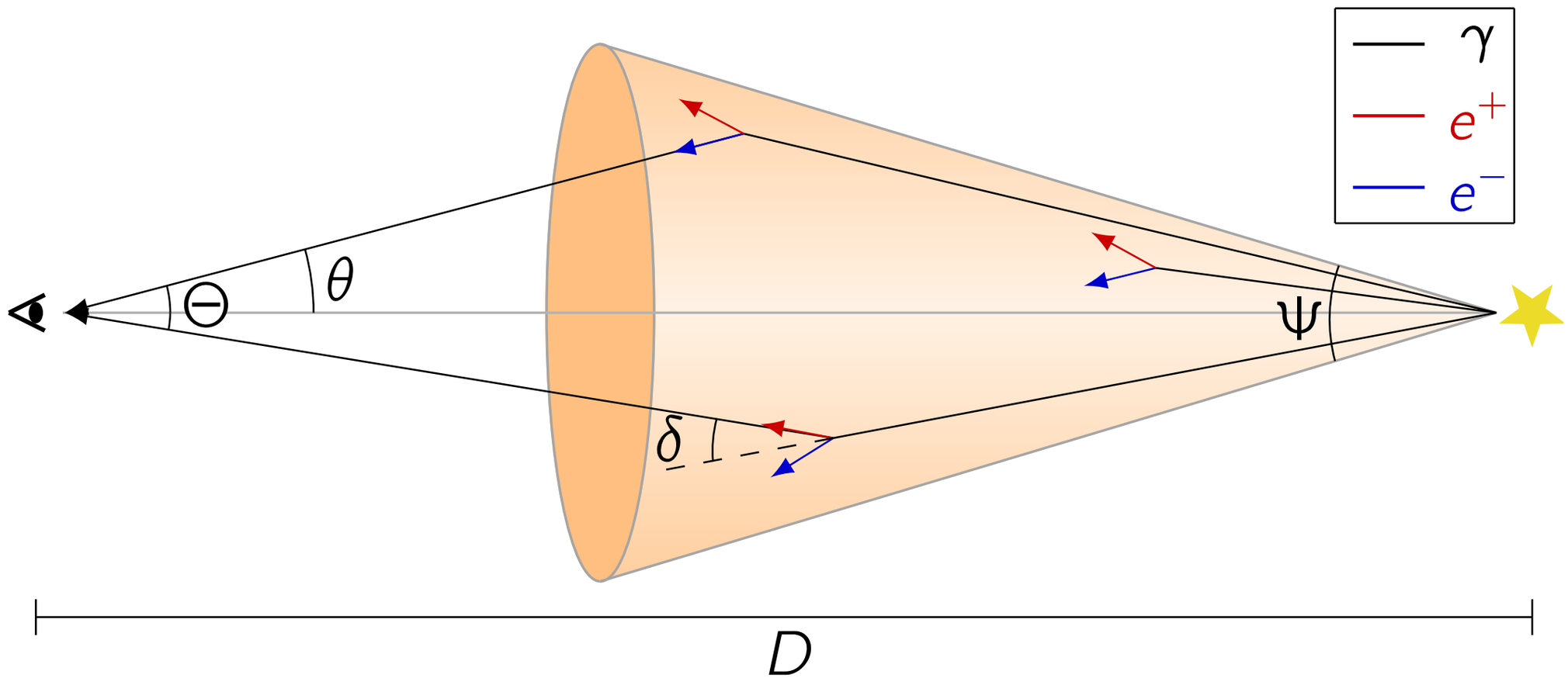

- point-like sources will appear extended
  [R. Plaga. Nature. 374 (1995) 430]
- the charged component of the cascade is sensitive to the **strength** and **structure** of intervening magnetic fields

effects of magnetic fields on the spectrum

Savelliev et al. arXiv:1311.6752

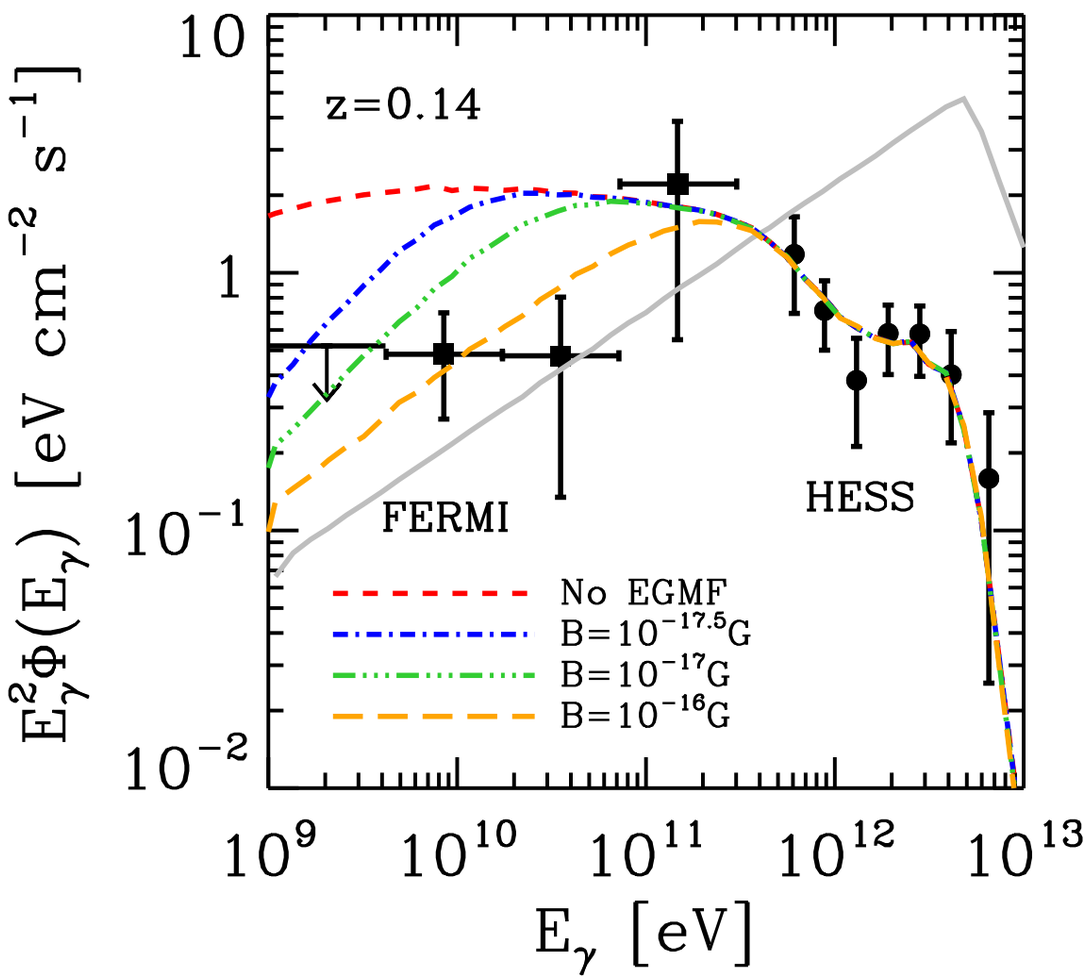

alternative explanations

- B>10^{-17} G disperses the GeV cascade
  [A. Neronov, I. Vovk. Science 328 (2010) 72; A. Taylor et al. A&A 529 (2011) A144]
- plasma instabilities suppresses the development of the cascades
  [A. Broderick et al. ApJ 752 (2012) 22; R. Schlickeiser et al. ApJ 777 (2013) 49]
- primary CRs continuously produces TeV gamma rays
  [W. Essey et al. ApJ 731 (2011) 51; W. Essey et al. PRL 104 (2010) 141102]
- gamma ray mixing with ALPs or hidden photons
  [D. Horns et al. PRD 86 (2011) 075024; M. Meyer et al. PRD 87 (2013) 035027; A. Dobrynina et al. PRD 91 (2015) 083003]
- Lorentz invariance violation
  [U. Jacob, T. Piran. PRD 78 (2008) 124010; F. Tavecchio, G. Bonnoli. A&A 585 (2016) A25]

GRPropa

RAB, A. Saveliev. In preparation.

- Based on the modular code structure of the CRPropa 3 code for cosmic-ray propagation
  CRPropa: github.com/CRPropa/CRPropa3 *[RAB et al. JCAP 05 (2016) 038. arXiv:1603.07142]*
- four-dimensional (3D + time) simulation of gamma-ray propagation
- other codes: Elmag (1D + time; small-angle approximation)
  [M. Kachelriess et al. Comp. Phys. Comm. 183 (2011) 1036]
- energy range: 0.1 GeV - 1 PeV (will be extended)
- "thinning" to optimise performance
- arbitrary magnetic field configurations and a few default options
- code already used in arXiv:1607.00320
  [RAB et al. Phys. Rev. D 94 (2016) 083005]

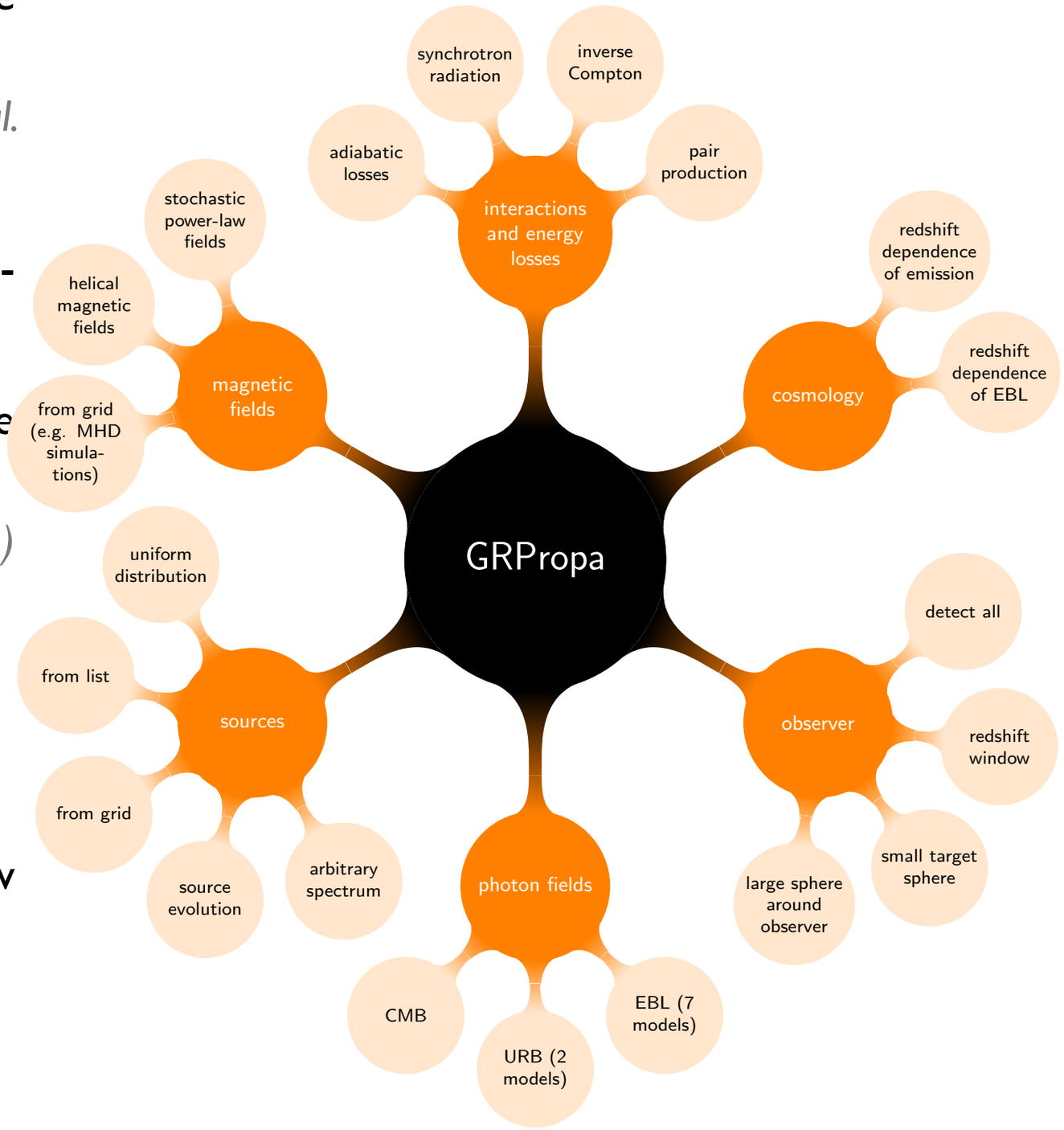

GRPropa: interactions

RAB, A. Saveliev. In preparation.

inverse Compton

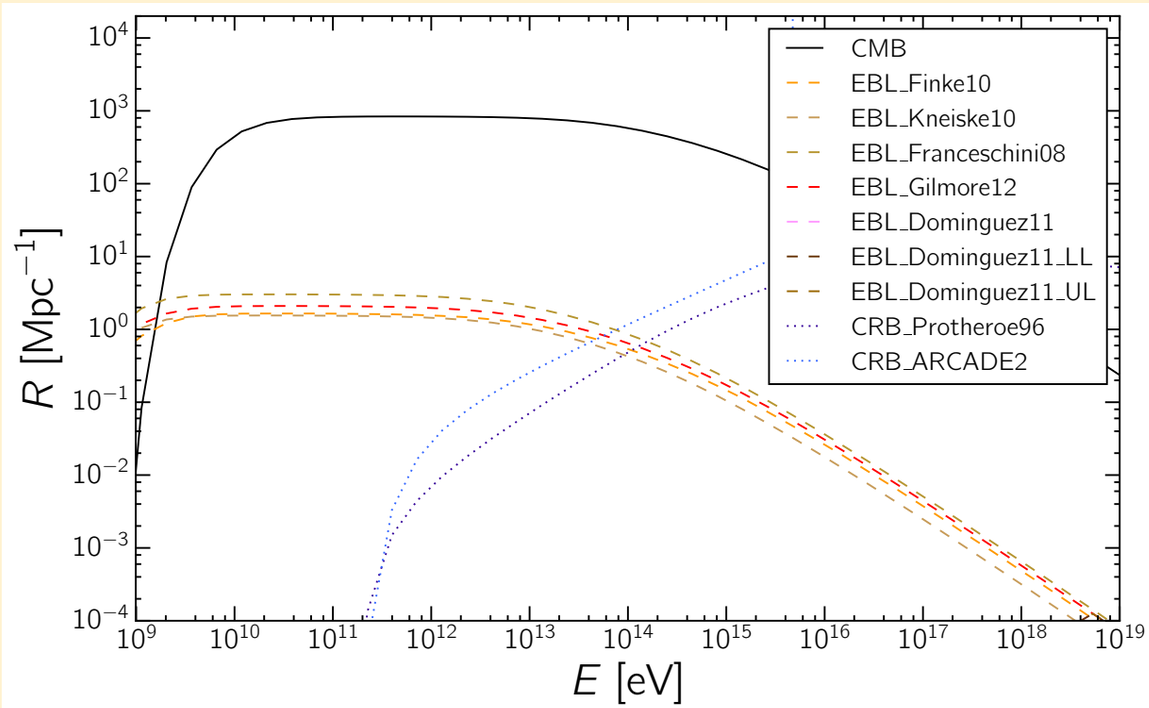

pair production

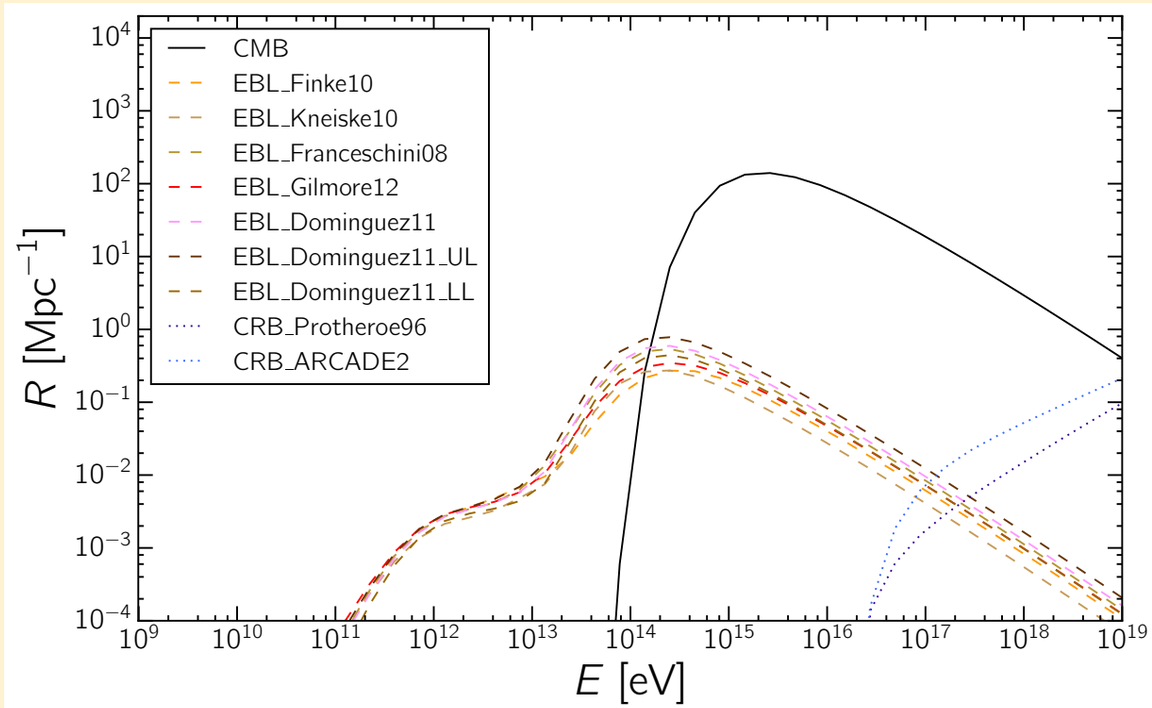

synchrotron

$$\frac{dE}{dx} \approx \frac{m_e^2 c^4 \chi^2}{\hbar c \left(1 + 4.8(1+\chi)\ln(1+1.7\chi) + 3.44\chi^2\right)^{\frac{2}{3}}} \qquad \chi = \frac{\left|\vec{p} \times \vec{B}\right|}{m_e c\, 4.4 \times 10^{13}\ \mathrm{G}}$$

redshift losses

$$\frac{dt}{dz} = \frac{1}{H_0(1+z)} \frac{1}{\sqrt{\Omega_m (1+z)^3 + \Omega_\Lambda}}$$

GRPropa: simulation of blazar pair halo

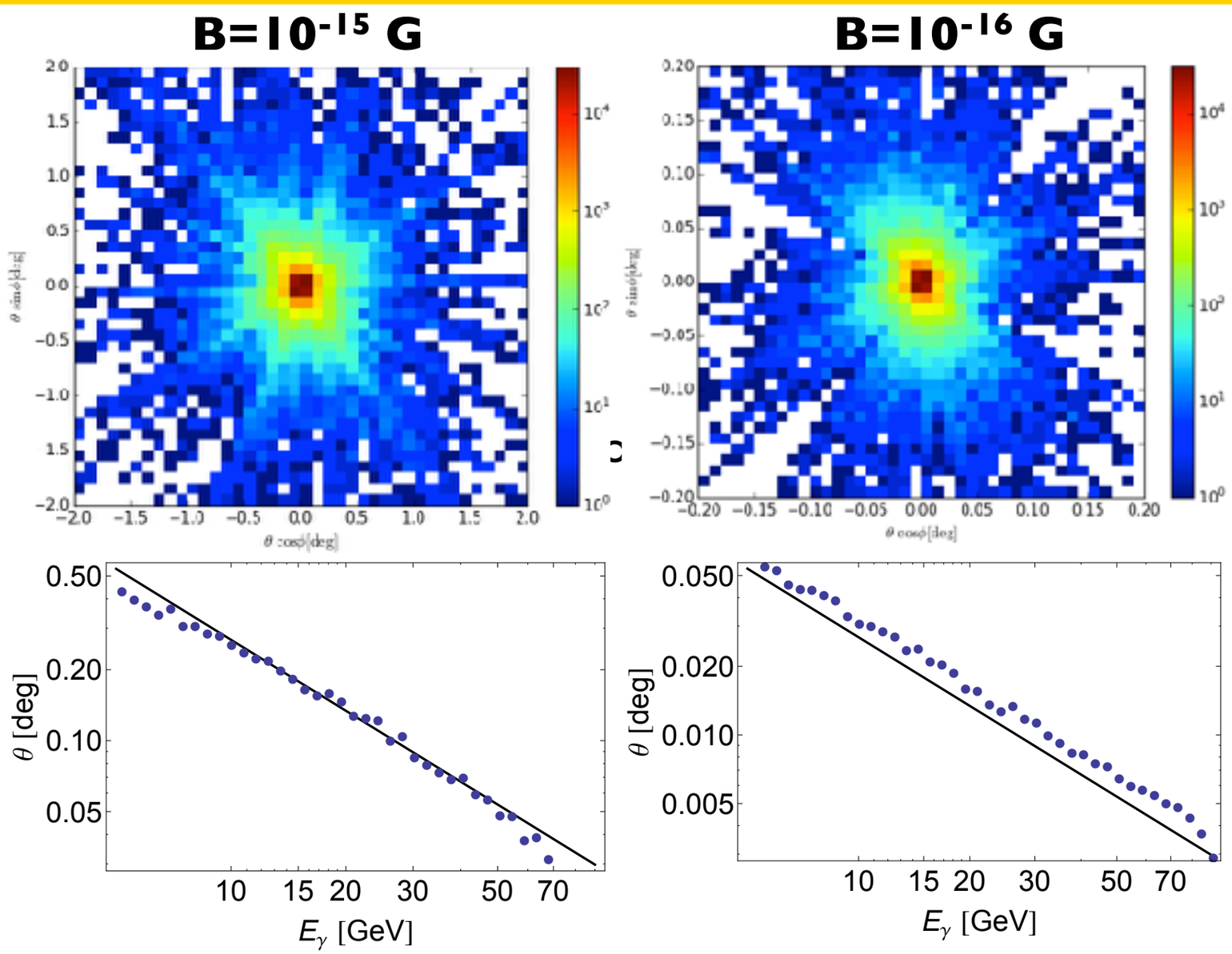

RAB, A. Saveliev, G. Sigl, T. Vachaspati. PRD 94 (2016) 083005. arXiv:1607.00320

- stochastic magnetic field with Batcherlor spectrum
- blazar located at D=1 Gpc
- performance: 10^5 initial photons , without thinning, take about 8 hours on 64 cores at 2.3 GHz

theoretical prediction

Neronov & Semikoz. PRD 80 (2009) 123012.

$$\theta(E_\gamma) \simeq 0.05^\circ \kappa (1+z_s)^{-4} \left(\frac{B}{\mathrm{fG}}\right) \left(\frac{E_\gamma}{0.1\,\mathrm{TeV}}\right)^{-1} \left(\frac{D_s}{\mathrm{Gpc}}\right)^{-1} \left(\frac{E_{\mathrm{TeV}}}{10\,\mathrm{TeV}}\right)^{-1}$$

helical intergalactic magnetic fields

- helicity $\mathcal{H} = \frac{1}{V}\int_V d^3r\, \vec{A}\cdot\vec{B}$
- helical magnetic fields may be related to baryogenesis via bubble collisions and linked Z-string creation [J. M. Cornwall PRD 56 (1996) 6146; T. Vachaspati PRL 87 (2001) 251302]
- advantage of helical magnetic fields: from MHD, we know they are less likely to dissipate
- helicity is odd under CP transformation
- parity-odd correlators give B~10 fG *[H. Tashiro & T. Vachaspati. MNRAS 448 (2015) 299]*
- morphology of arrival directions of gamma-rays can be used to infer the helicity of IGMFs

[A. Long & T. Vachaspati. JCAP 09 (2015) 065]

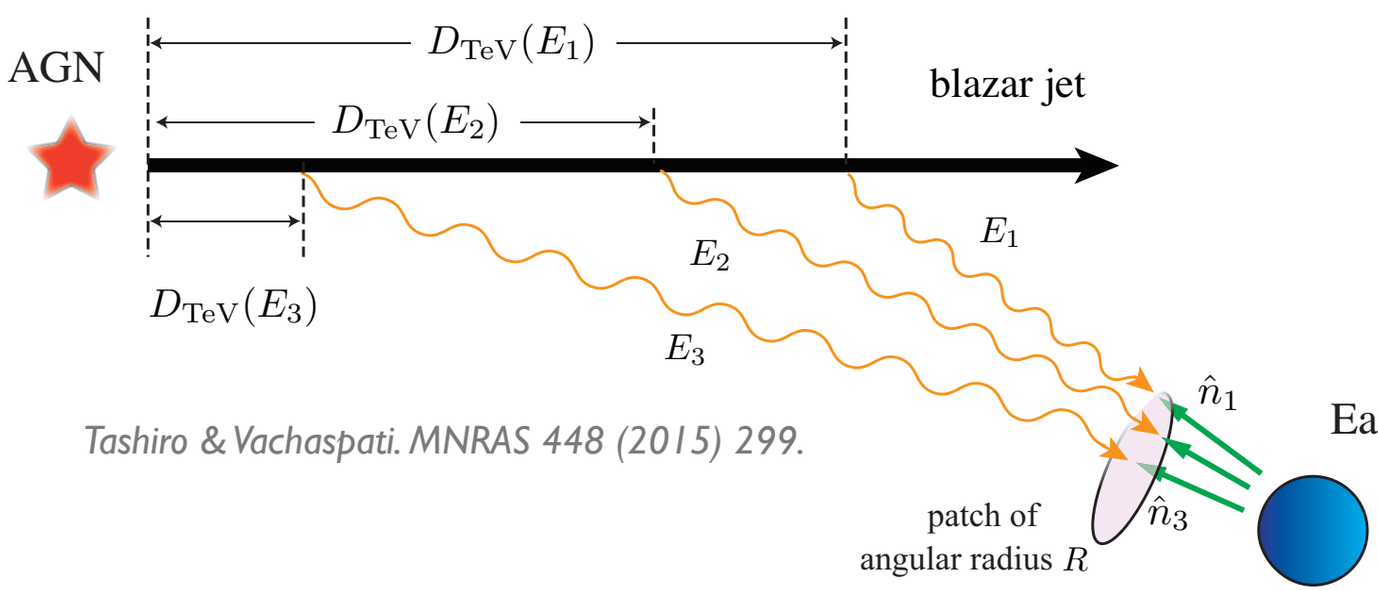

Tashiro & Vachaspati. MNRAS 448 (2015) 299.

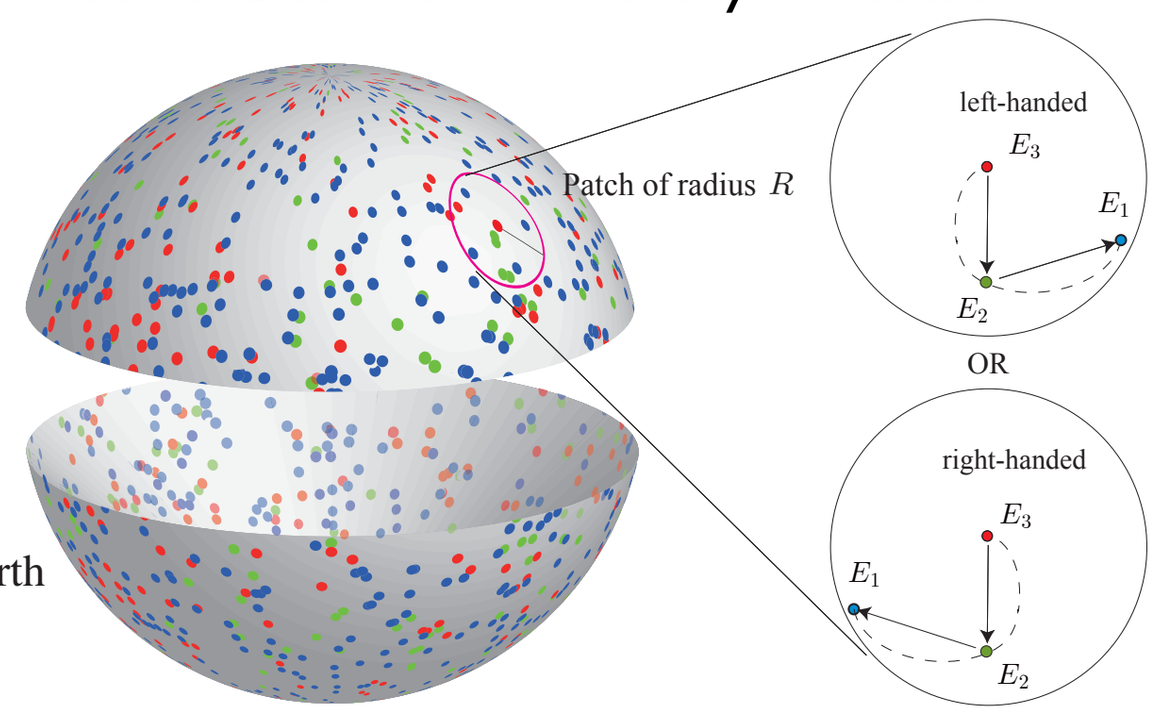

Chen et al. MNRAS Lett. 445 (2014) L41.

the S-statistics

RAB, A. Saveliev, G. Sigl, T. Vachaspati. PRD 94 (2016) 083005. arXiv:1607.00320

1. calculate average deflection per energy bin

$$\overline{\theta}(\phi^{(j)}, E_\gamma) = \frac{1}{N_j} \sum_{\{i|\phi^{(j)} \leq \phi_i < \phi^{(j+1)}\}} \theta_i$$

2. estimate Φ_+ and Φ_-

$$\Phi_- = \sum_{j=j_{\max}-\delta_{\rm bin}}^{j_{\max}-1} \overline{\theta}(\phi^{(j)}, E_\gamma) \quad \Phi_+ = \sum_{j=j_{\max}+1}^{j_{\max}+\delta_{\rm bin}} \overline{\theta}(\phi^{(j)}, E_\gamma)$$

3. compute S

$$S = \frac{\Phi_- - \Phi_+}{\Phi_- + \Phi_+}$$

$\delta_{\rm bin}$: number of bins necessary to fully encompass the peak

(φ_i, θ_i): coordinates of the i-th event in the bin

- S<0 for a left-handed spiral, and S>0 if the spiral is right-handed
- alternative method: Q-statistics

  [H. Tashiro et al. MNRAS Lett. 445 (2014) L41; H. Tashiro & T. Vachaspati. MNRAS 448 (2015) 299;]

S-statistics: application

RAB, A. Saveliev, G. Sigl, T. Vachaspati. PRD 94 (2016) 083005. arXiv:1607.00320

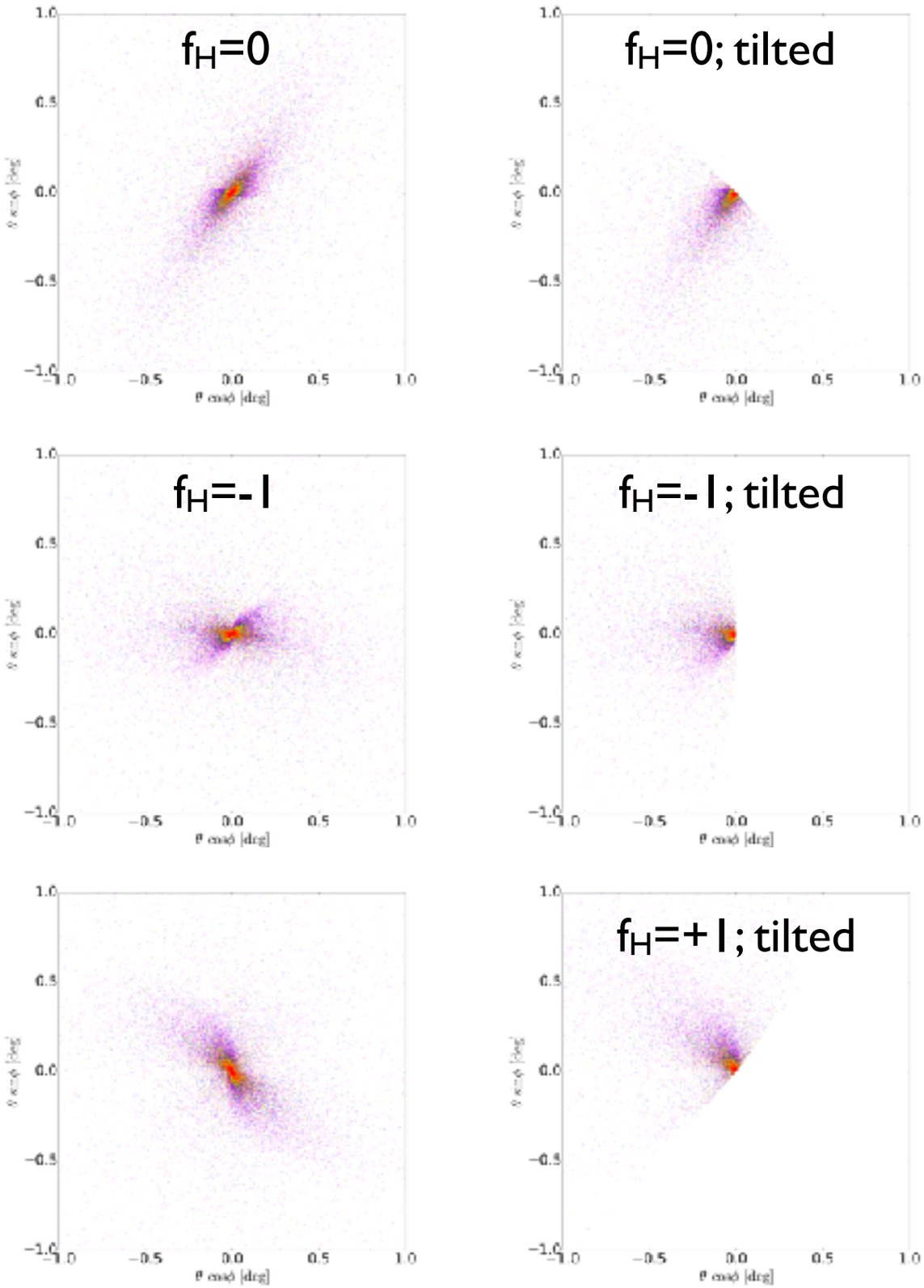

magenta: E=5-10 GeV
blue: E=10-15 GeV
green: E=15-20 GeV
yellow: E=20-30 GeV
orange: E=30-50 GeV
red: E=50-100 GeV

Batchelor spectrum
tilt angle: 5°
D=1 Gpc
B=1 fG
Ψ=5°

E_γ/GeV	j_{max}	ϕ_{max}/deg	Φ_-	Φ_+	S
5–10	6	108.0	0.768	1.67	-0.37
	16	288.0	0.649	1.60	-0.42
10–15	7	126.0	0.813	0.904	-0.05
	17	306.0	0.709	0.882	-0.11
15–20	7	126.0	0.472	0.818	-0.27
	18	324.0	0.637	0.473	0.15
20–30	6	108.0	0.222	0.625	-0.48
	17	306.0	0.370	0.428	-0.07
30–50	6	108.0	0.163	0.507	-0.51
	16	288.0	0.170	0.385	-0.39
50–100	7	126.0	0.151	0.200	-0.13
	17	306.0	0.145	0.172	-0.09

E_γ/GeV	j_{max}	ϕ_{max}/deg	Φ_-	Φ_+	S
5–10	19	342.0	1.23	1.01	+0.10
	9	162.0	1.15	1.32	-0.07
10–15	19	342.0	0.888	0.713	+0.11
	9	162.0	0.785	0.822	-0.02
15–20	0	0.0	0.722	0.284	+0.44
	9	162.0	0.594	0.542	+0.05
20–30	19	342.0	0.428	0.309	+0.16
	10	180.0	0.655	0.405	+0.24
30–50	19	342.0	0.296	0.203	+0.19
	9	162.0	0.285	0.338	-0.08
50–100	19	342.0	0.157	0.131	+0.09
	10	180.0	0.120	0.138	+0.18

helical intergalactic magnetic fields

RAB, A. Saveliev, G. Sigl, T. Vachaspati. PRD 94 (2016) 083005.
arXiv:1607.00320

the effect of the coherence length

for maximally positive helicity

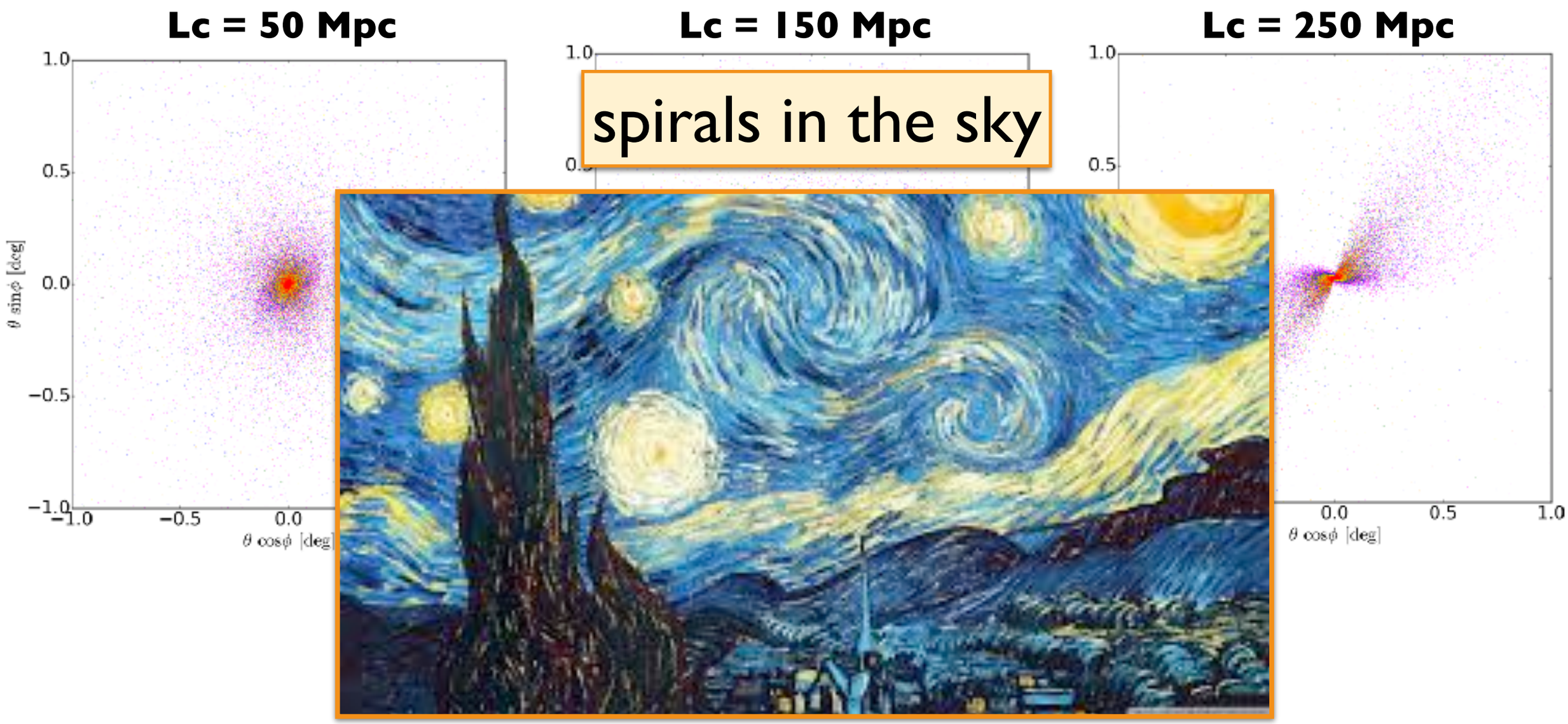

summary and outlook

- main uncertainties in propagation: photonuclear cross sections (photodisintegration), EBL model, magnetic fields
- magnetogenesis process related to UHECR deflections
- MHD simulations suggest that UHECR may not be possible in the whole sky if sources are distant more than 20 Mpc
- Even in an extreme scenario (B_{voids} ~ 1 nG, Planck upper limit), it would be possible to identify nearby sources of UHE protons provided that galactic deflections are small
- prospects for UHECR astronomy don't look so good; too many uncertainties: EBL, cross sections, magnetic fields, …
- new code for 4D simulations of electromagnetic cascacades
- new method to infer the helicity of IGMFs based on gamma-ray observations

Thank you!

backup slides

combined spectrum-composition fits

A. di Matteo+ (Pierre Auger Collaboration). ICRC 2015 Proceedings. arXiv:1509.03732

- attempt to fit the Auger spectrum and composition
- assumption: identical sources uniformly distributed in comoving volume
- nuclear species: ^{1}H, ^{4}He, ^{14}N and ^{56}Fe
- magnetic fields are neglected in this 1st order approximation → 1D propagation
- we fit with the function (above $10^{18.7}$ eV)

$$\frac{dN}{dE} = \sum_i J_0 p_i \left(\frac{E}{E_0}\right)^{-\gamma} \begin{cases} 1 & \text{if } E < Z_i R_{cut} \\ \exp\left(1 - \frac{E}{Z_i R_{cut}}\right) & \text{if } E > Z_i R_{cut} \end{cases}$$

- interactions with the atmosphere modelled with: EPOS-LHC, QGSJET II-04, Sybill 2.1
- sources of uncertainties: EBL model, photodisintegration cross sections [RAB+' 15]
- two codes used for cross-checking: CRPropa, SimProp
- EBL models studied: Kneiske '04, Domínguez+ '11, Gilmore+ '12
- photodisintegration cross sections: TALYS, Geant 4, Puget-Stecker-Bredekamp
- upcoming paper by Auger Collaboration

UHECR deflections: impact of the B power spectrum

TABLE I. Average deflections and corresponding 1σ standard deviations of UHECRs from nearby sources in runs F, L, S, and O. Results are presented for the case of sources uniformly distributed ('uni'), and following the large scale structure ('lss'), both for proton (p) and iron (Fe) primaries.

nucleus	E [EeV]	D [Mpc]	sources	run F	run L	run S	run O
p	10	0-10	uni	$21.4^\circ \pm 11.5^\circ$	$31.7^\circ \pm 19.6^\circ$	$30.5^\circ \pm 16.5^\circ$	$67.6^\circ \pm 24.6^\circ$
p	10	0-10	lss	$41.3^\circ \pm 16.2^\circ$	$60.0^\circ \pm 21.1^\circ$	$42.9^\circ \pm 17.4^\circ$	$81.6^\circ \pm 21.0^\circ$
p	60	0-5	uni	$1.5^\circ \pm 1.1^\circ$	$1.7^\circ \pm 1.5^\circ$	$2.3^\circ \pm 1.3^\circ$	$4.0^\circ \pm 2.8^\circ$
p	60	0-5	lss	$4.3^\circ \pm 2.0^\circ$	$8.8^\circ \pm 6.1^\circ$	$4.7^\circ \pm 2.4^\circ$	$27.1^\circ \pm 16.0^\circ$
p	60	0-10	uni	$2.5^\circ \pm 1.4^\circ$	$3.0^\circ \pm 3.2^\circ$	$3.1^\circ \pm 1.6^\circ$	$6.9^\circ \pm 4.0^\circ$
p	60	0-10	lss	$4.9^\circ \pm 2.4^\circ$	$9.8^\circ \pm 6.3^\circ$	$5.5^\circ \pm 2.7^\circ$	$27.3^\circ \pm 15.6^\circ$
p	60	0-10	uni	$2.5^\circ \pm 1.4^\circ$	$3.0^\circ \pm 3.2^\circ$	$3.1^\circ \pm 1.6^\circ$	$6.9^\circ \pm 4.0^\circ$
p	60	0-10	lss	$4.9^\circ \pm 2.4^\circ$	$9.8^\circ \pm 6.3^\circ$	$5.5^\circ \pm 2.7^\circ$	$27.3^\circ \pm 15.6^\circ$
p	60	10-20	uni	$5.1^\circ \pm 2.3^\circ$	$7.4^\circ \pm 3.1^\circ$	$6.4^\circ \pm 3.3^\circ$	$21.7^\circ \pm 13.0^\circ$
p	60	10-20	lss	$7.4^\circ \pm 2.8^\circ$	$13.8^\circ \pm 7.9^\circ$	$7.2^\circ \pm 2.8^\circ$	$35.7^\circ \pm 15.3^\circ$
p	60	20-30	uni	$6.8^\circ \pm 2.2^\circ$	$10.8^\circ \pm 4.2^\circ$	$8.5^\circ \pm 3.7^\circ$	$34.7^\circ \pm 16.6^\circ$
p	60	20-30	lss	$8.4^\circ \pm 3.3^\circ$	$15.3^\circ \pm 7.0^\circ$	$9.0^\circ \pm 3.5^\circ$	$44.0^\circ \pm 16.8^\circ$
p	100	0-5	uni	$0.9^\circ \pm 0.5^\circ$	$1.0^\circ \pm 1.1^\circ$	$1.3^\circ \pm 0.8^\circ$	$2.1^\circ \pm 2.7^\circ$
p	100	0-5	lss	$2.3^\circ \pm 1.1^\circ$	$5.0^\circ \pm 3.2^\circ$	$2.7^\circ \pm 1.4^\circ$	$14.7^\circ \pm 11.5^\circ$
p	100	0-10	uni	$1.3^\circ \pm 0.8^\circ$	$1.8^\circ \pm 1.5^\circ$	$2.0^\circ \pm 1.3^\circ$	$3.9^\circ \pm 4.8^\circ$
p	100	0-10	lss	$2.8^\circ \pm 1.3^\circ$	$5.6^\circ \pm 3.4^\circ$	$2.9^\circ \pm 1.5^\circ$	$16.0^\circ \pm 10.9^\circ$
p	100	10-20	uni	$2.9^\circ \pm 1.2^\circ$	$4.5^\circ \pm 2.0^\circ$	$3.8^\circ \pm 1.7^\circ$	$10.6^\circ \pm 7.5^\circ$
p	100	10-20	lss	$4.1^\circ \pm 1.7^\circ$	$8.5^\circ \pm 4.9^\circ$	$4.3^\circ \pm 1.8^\circ$	$23.9^\circ \pm 12.3^\circ$
p	100	20-30	uni	$4.0^\circ \pm 1.4^\circ$	$6.0^\circ \pm 3.0^\circ$	$5.2^\circ \pm 2.1^\circ$	$19.3^\circ \pm 11.3^\circ$
p	100	20-30	lss	$4.8^\circ \pm 1.7^\circ$	$8.9^\circ \pm 3.2^\circ$	$5.0^\circ \pm 1.6^\circ$	$26.6^\circ \pm 12.4^\circ$
Fe	60	0-5	uni	$44.3^\circ \pm 20.9^\circ$	$43.6^\circ \pm 20.0^\circ$	$60.9^\circ \pm 22.5^\circ$	$64.6^\circ \pm 23.1^\circ$
Fe	60	0-5	lss	$76.6^\circ \pm 23.5^\circ$	$82.0^\circ \pm 20.6^\circ$	$70.0^\circ \pm 21.8^\circ$	$77.0^\circ \pm 19.5^\circ$
Fe	60	0-10	uni	$58.4^\circ \pm 22.4^\circ$	$67.3^\circ \pm 23.3^\circ$	$73.2^\circ \pm 21.7^\circ$	$77.6^\circ \pm 22.6^\circ$
Fe	60	0-10	lss	$78.6^\circ \pm 22.4^\circ$	$83.0^\circ \pm 20.2^\circ$	$78.9^\circ \pm 21.5^\circ$	$81.2^\circ \pm 19.4^\circ$
Fe	60	20-30	uni	$84.4^\circ \pm 18.6^\circ$	$87.7^\circ \pm 19.5^\circ$	$84.3^\circ \pm 19.5^\circ$	$90.2^\circ \pm 20.3^\circ$
Fe	60	20-30	lss	$84.0^\circ \pm 19.7^\circ$	$89.7^\circ \pm 21.2^\circ$	$90.7^\circ \pm 19.6^\circ$	$89.9^\circ \pm 19.0^\circ$
Fe	100	0-5	uni	$16.4^\circ \pm 9.5^\circ$	$32.0^\circ \pm 21.2^\circ$	$45.9^\circ \pm 23.5^\circ$	$51.8^\circ \pm 23.7^\circ$
Fe	100	0-5	lss	$56.0^\circ \pm 20.6^\circ$	$68.1^\circ \pm 21.1^\circ$	$60.9^\circ \pm 21.5^\circ$	$75.5^\circ \pm 24.1^\circ$
Fe	100	0-10	uni	$36.3^\circ \pm 19.8^\circ$	$48.2^\circ \pm 23.1^\circ$	$54.4^\circ \pm 22.9^\circ$	$69.7^\circ \pm 24.0^\circ$
Fe	100	0-10	lss	$64.0^\circ \pm 20.3^\circ$	$71.2^\circ \pm 21.4^\circ$	$64.8^\circ \pm 21.6^\circ$	$73.6^\circ \pm 22.1^\circ$
Fe	100	20-30	uni	$72.5^\circ \pm 17.5^\circ$	$84.3^\circ \pm 20.0^\circ$	$80.3^\circ \pm 23.4^\circ$	$77.4^\circ \pm 17.1^\circ$
Fe	100	20-30	lss	$92.4^\circ \pm 17.7^\circ$	$76.5^\circ \pm 19.0^\circ$	$75.7^\circ \pm 16.5^\circ$	$78.6^\circ \pm 19.3^\circ$

RAB, M.-S. Shin, J. Devriendt, D. Semikoz, G. Sigl. In preparation. arXiv:1612.XXXXX

UHECRs and the galactic magnetic field

- the case of Centaurus A, assuming only galactic deflections and only the regular component of the field

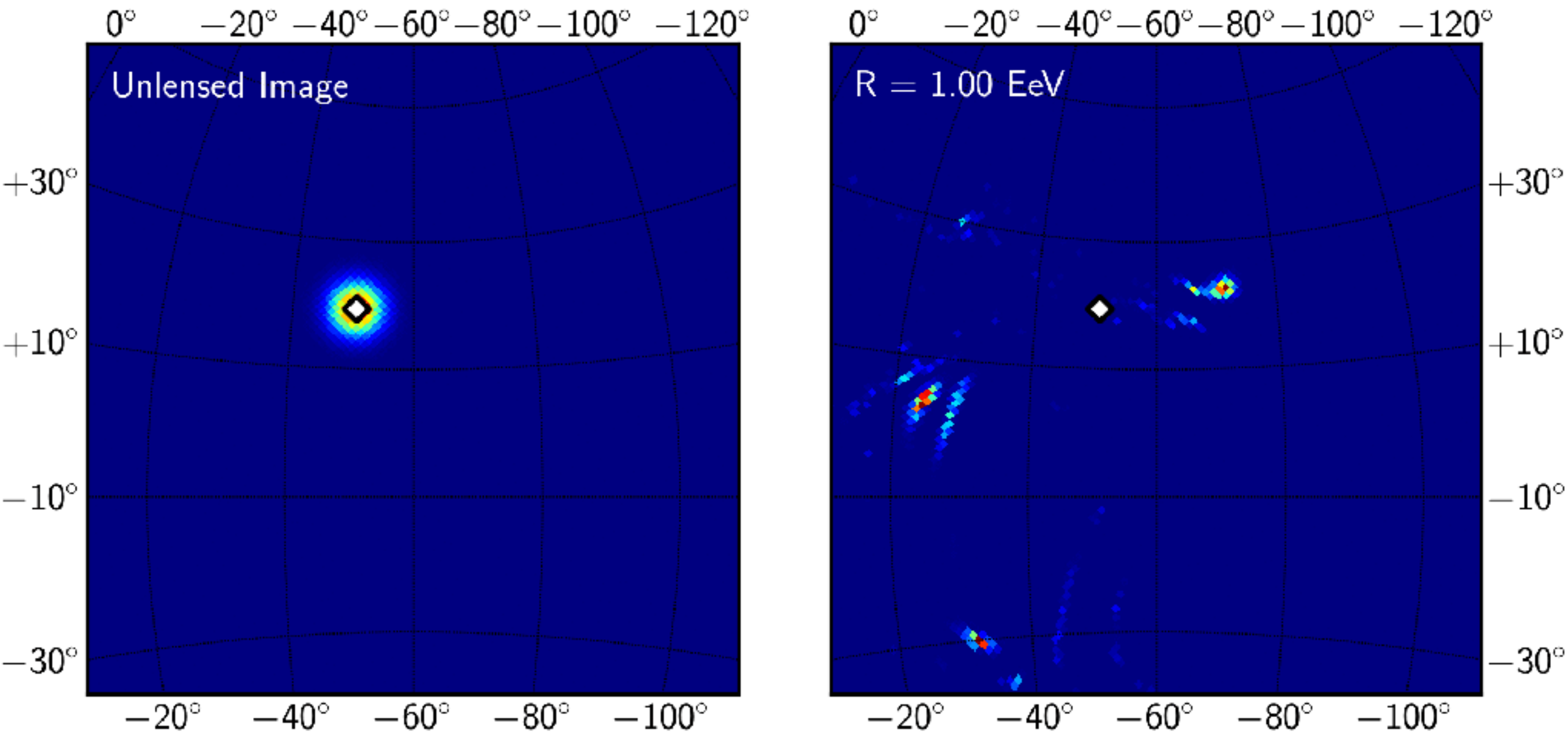

obtained with the PARSEC code

combined spectrum-composition fits

A. di Matteo+ (Pierre Auger Collaboration). ICRC 2015 Proceedings. arXiv:1509.03732

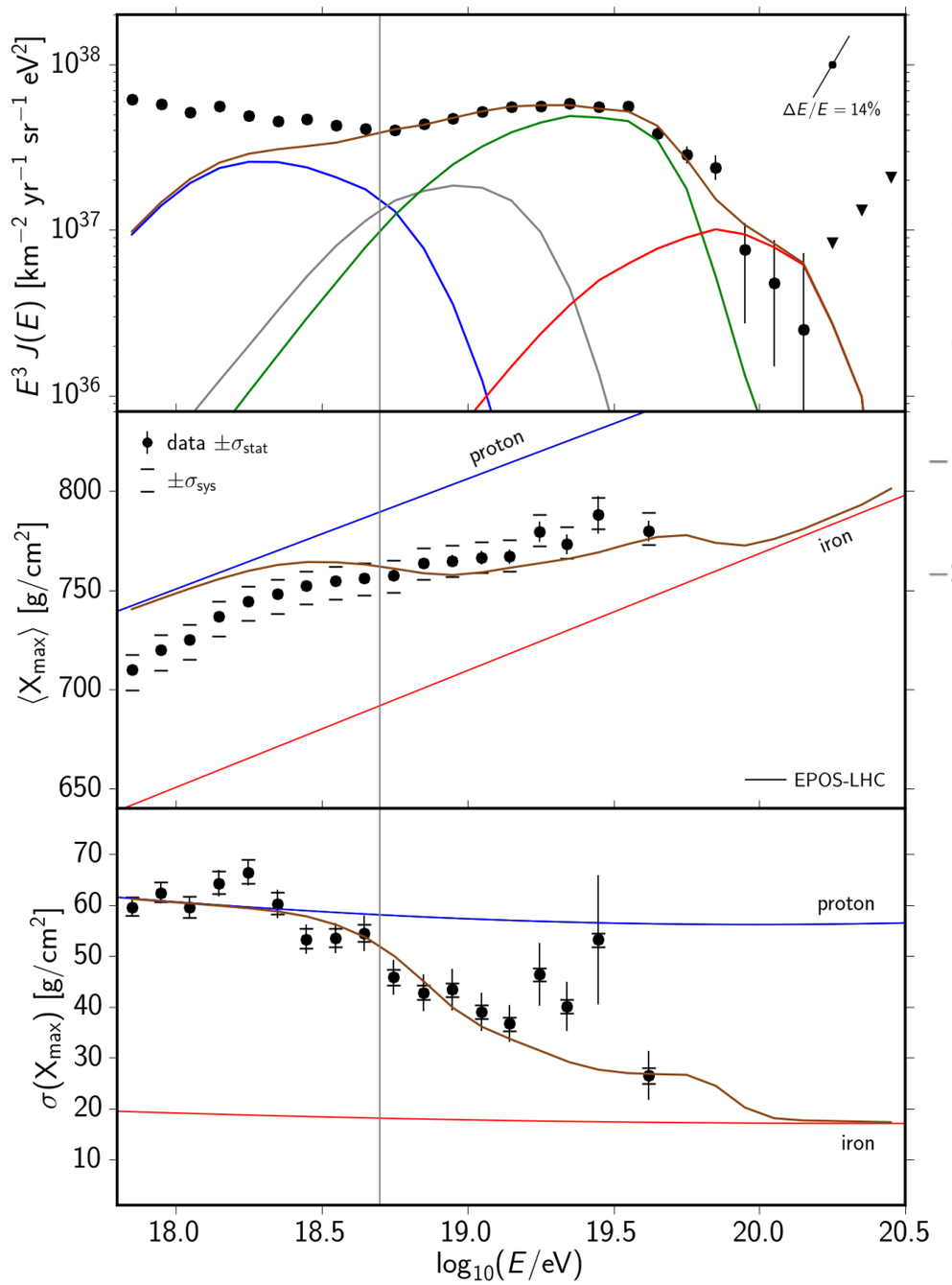

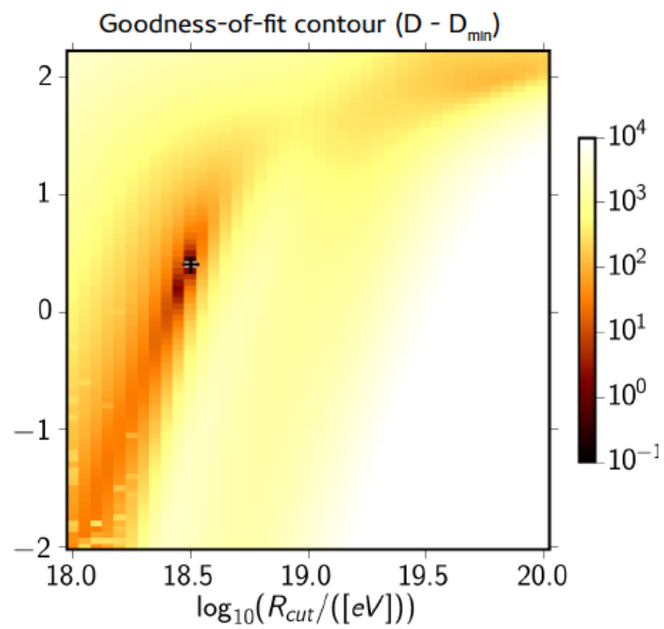

- log(Rcut / V) = 18.48
- γ = 0.29 (+0.08 | -0.07)
- fraction of H: 14.3% (+4.2 | -14.2)
- fraction of He: 10.0% (+2.2 | -10.0)
- fraction of N: 75.3% (+15.5 | -9.4)
- fraction of Fe: 0.5% (+0.1 | -0.1)

	γ (1st min)	$\log_{10}(R_{\mathrm{cut}}/\mathrm{V})$	$D^{D(J)}_{D(X_{\max})}$
SPG	$+0.94^{+0.09}_{-0.10}$	18.67 ± 0.03	$178.5^{18.8}_{159.8}$
SPD	-0.45 ± 0.41	$18.27^{+0.07}_{-0.06}$	$193.4^{21.1}_{172.3}$
STG	$+0.69^{+0.07}_{-0.06}$	18.60 ± 0.01	$176.9^{19.5}_{157.4}$
CTG	$+0.73^{+0.07}_{-0.06}$	18.58 ± 0.01	$195.3^{33.6}_{161.7}$
CTD	$-1.06^{+0.29}_{-0.22}$	$18.19^{+0.04}_{-0.02}$	$192.3^{21.2}_{171.1}$
CGD	$-1.29^{+0.38}_{*}$	$18.18^{+0.06}_{-0.04}$	$192.5^{19.2}_{173.3}$

CRPropa

Kneiske '04 EBL model

TALYS cross sections for PD

galactic lensing

- assumes no energy losses
- each "lens" corresponds to a different energy bin
- lenses generated by backtracking protons to the galactic border
- nuclei have deflection of Z times the deflection for protons
- technique based on the PARSEC code *[Bretz '14]*
- these lenses are applied to simulated data a posteriori

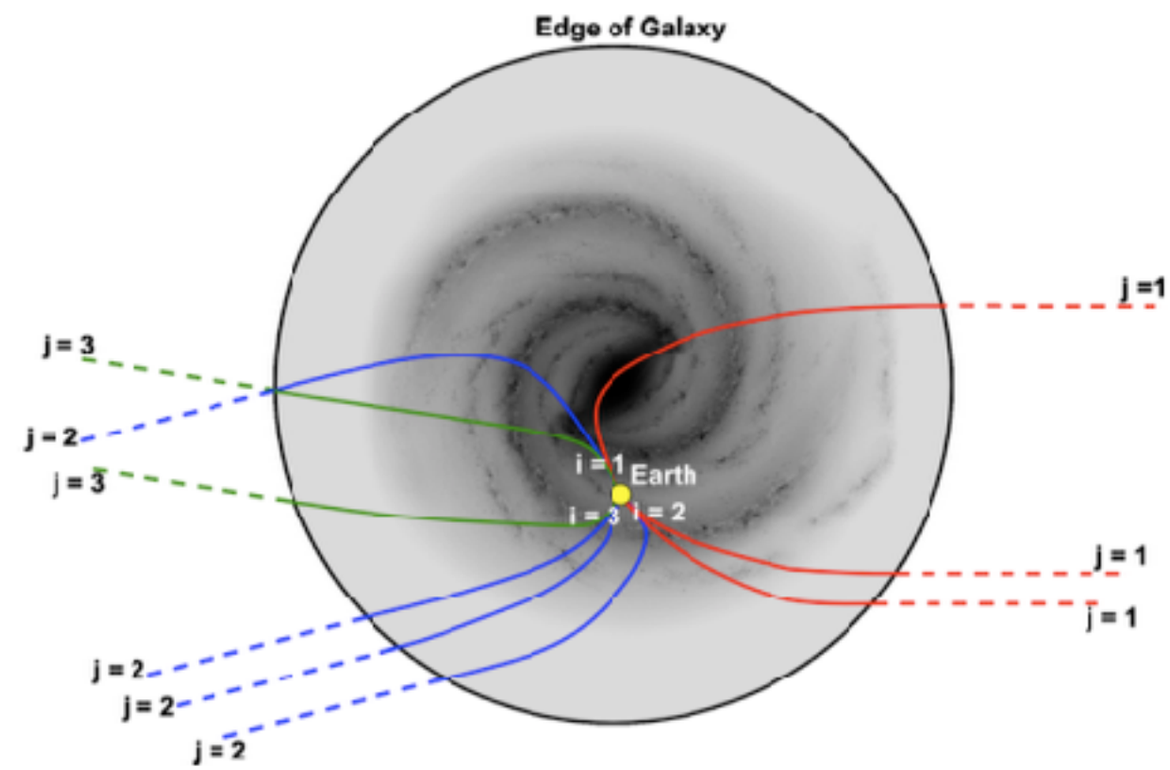

the “benchmark” scenario

- sources randomly distributed according to LSS (down to 3 Mpc)
- “galactic composition” *[DuVernois+ ’96]*
- source density: 10^{-4} Mpc^{-3}
- field strength obtained from B-ρ profile from the Miniati simulation *[Miniati ’02]*
- simulation volume: $(132\ Mpc)^3$ with a spacing of ~300 kpc from Dolag simulation *[Dolag+ ’02]*
- turbulent subgrid with 256^3 cells covering a volume of $(13.2\ Mpc)^3$ periodically repeated to cover the simulation volume

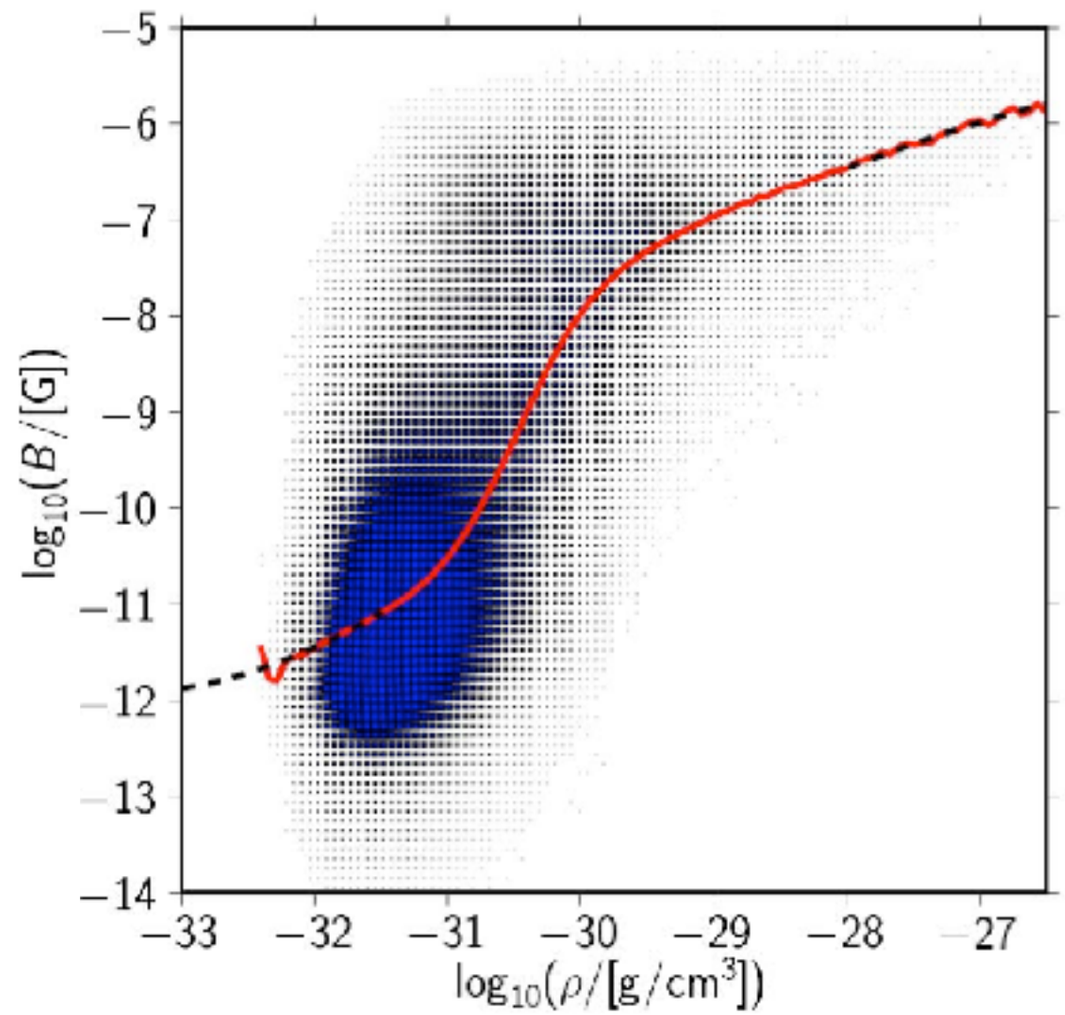

redshift dependence CIB

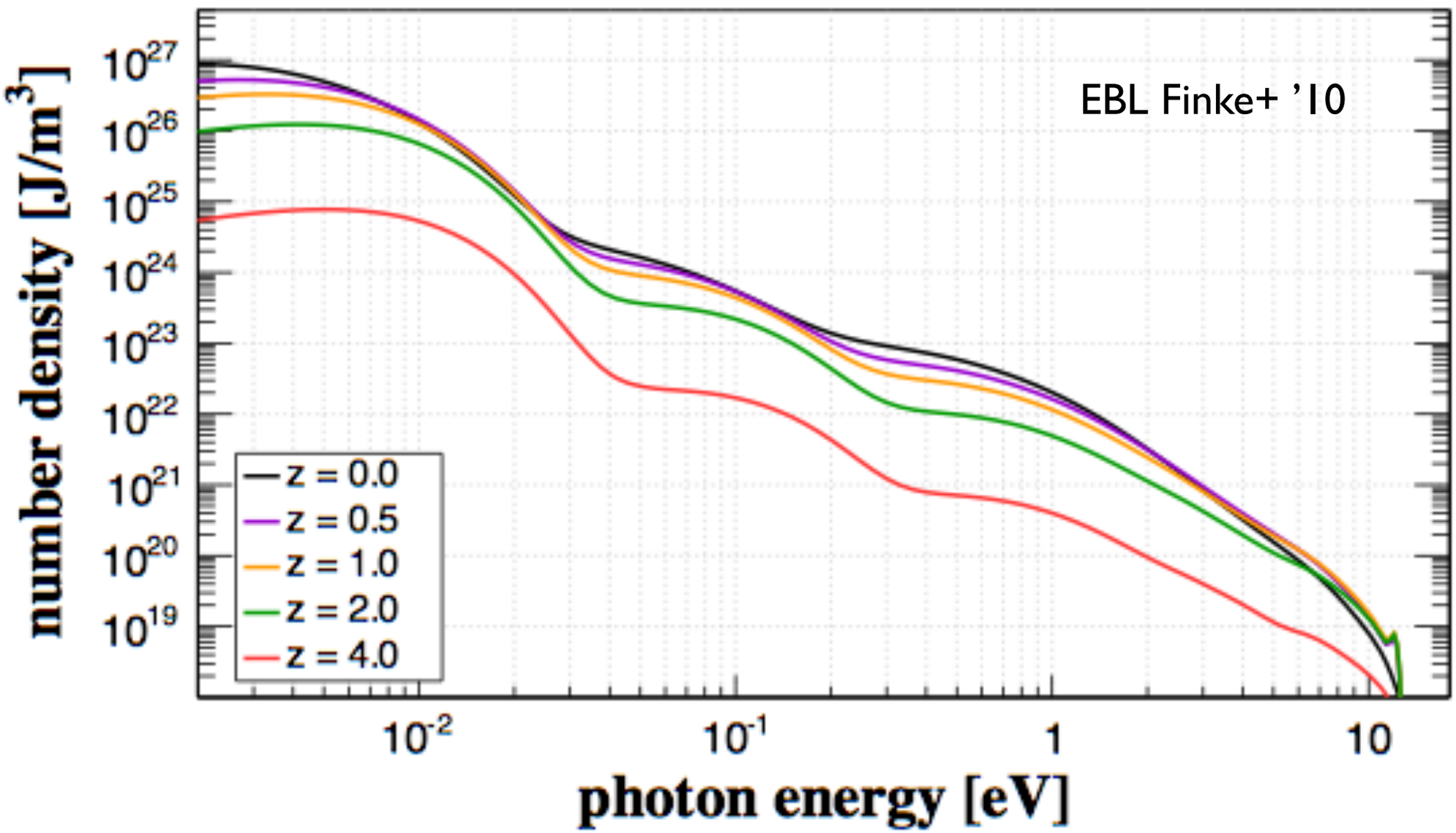

spectrum-composition fits

Aloisio+ '14

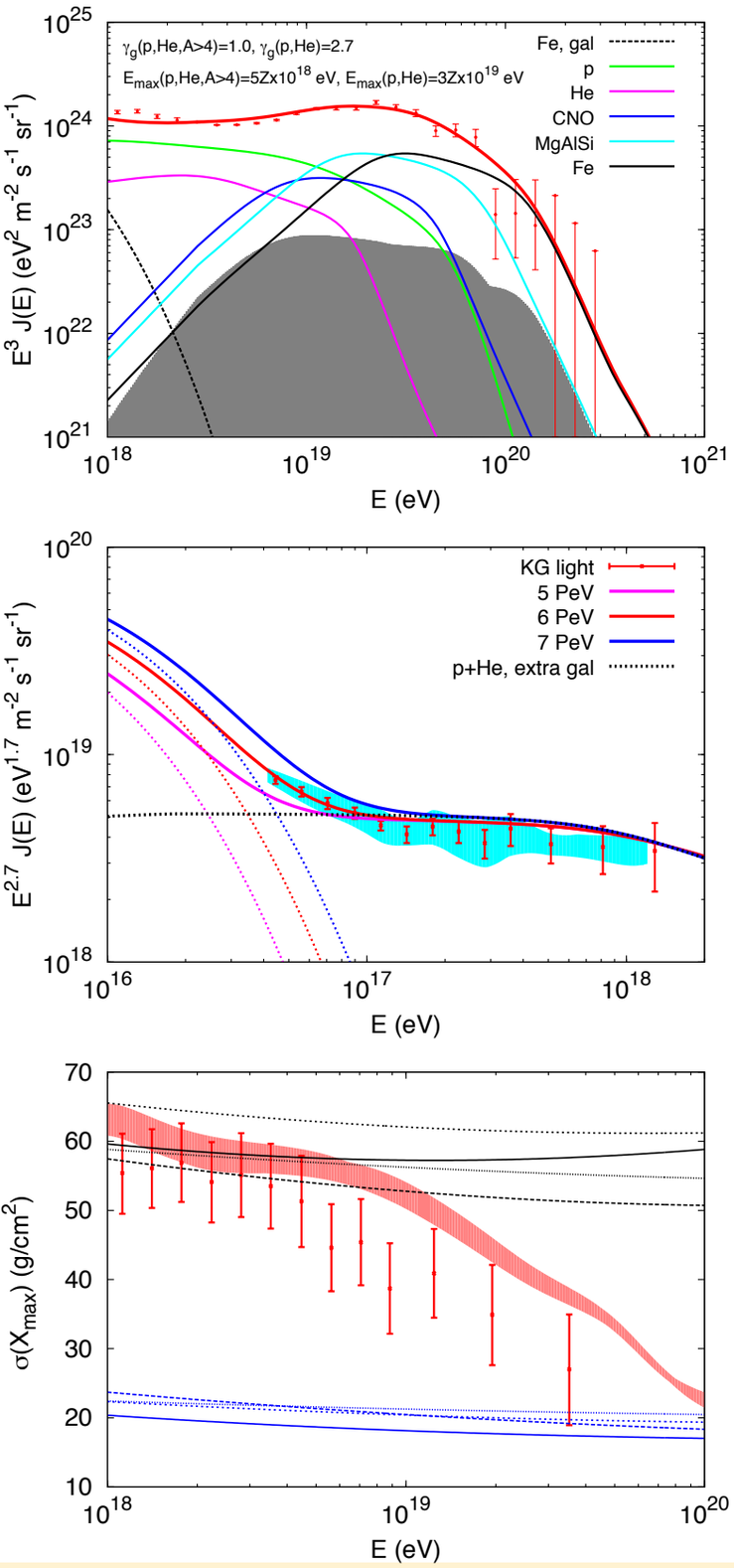

- combined spectrum-composition (1D) fits of the Auger spectrum/ composition *[Aloisio+ '14, Taylor '14]*
- mixed composition; maximum source acceleration cutoff (no GZK)
- results suggest an extra (light) class of sources below the ankle might be needed → Auger + KASCADE-Grande data
- hard spectra "problem" *[Taylor '14]*: these fits seem to suggest that the sources have spectral indexes harder than expected ($\gamma \approx 1.0$-1.6); expected $\gamma \approx 2.0$-2.2 for Fermi acceleration
- magnetic horizon effects might soften the hard spectra, making it again compatible with Fermi shock acceleration *[Mollerach & Roulet '13]*
- magnetic horizon effects do not play a role at EeV energies in realistic extragalactic magnetic field models *[RAB & Sigl '14]*
- caveat I: hadronic interaction models can fail to describe interactions at the highest energies (e.g. muon problem *[Auger '14]*)
- caveat II: source distribution, magnetic field model, nearby sources, etc → shape of the spectrum is sensitive to these parameters

Syrovatskii variable

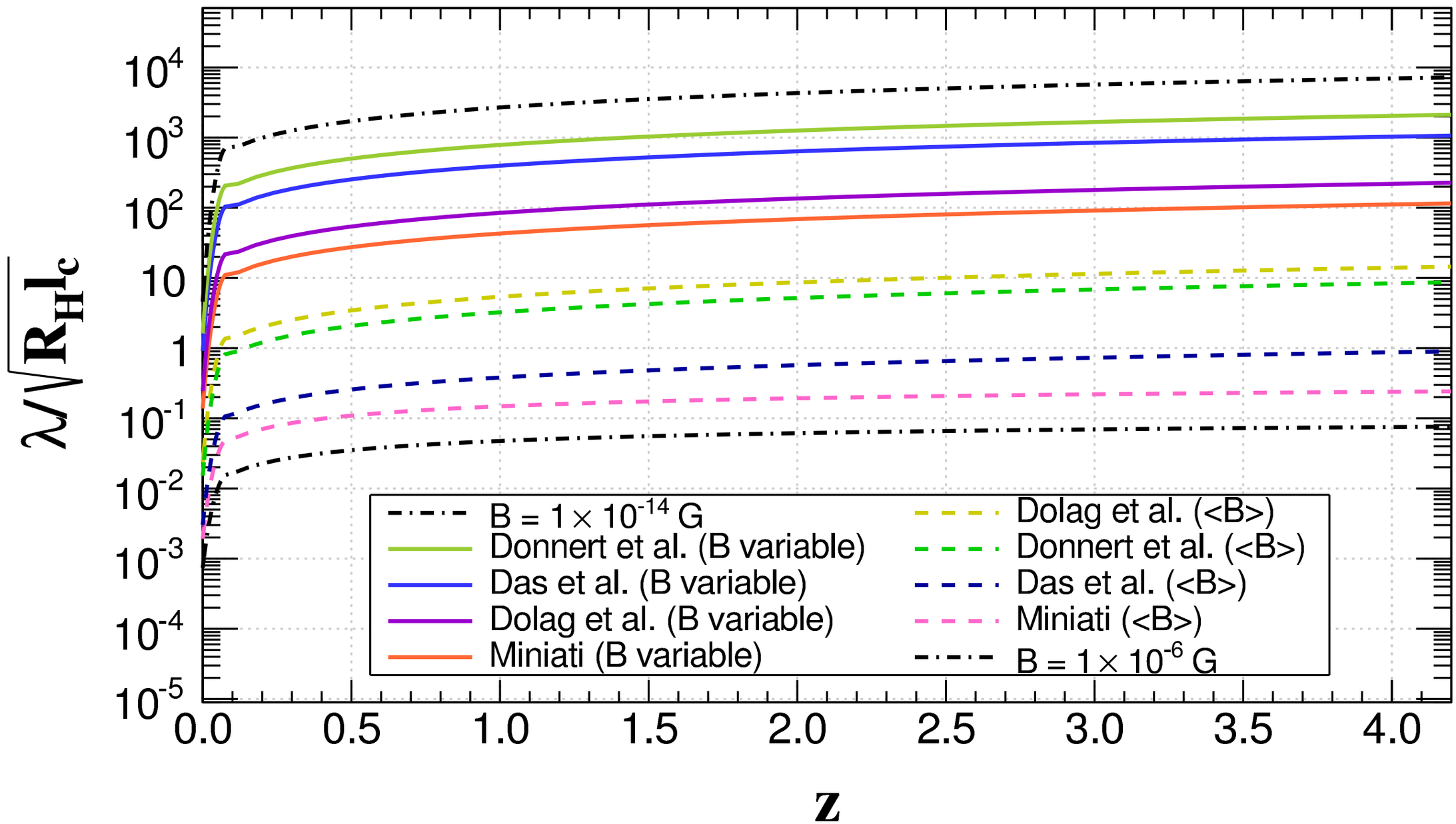

magnetic suppression: best fit parameters

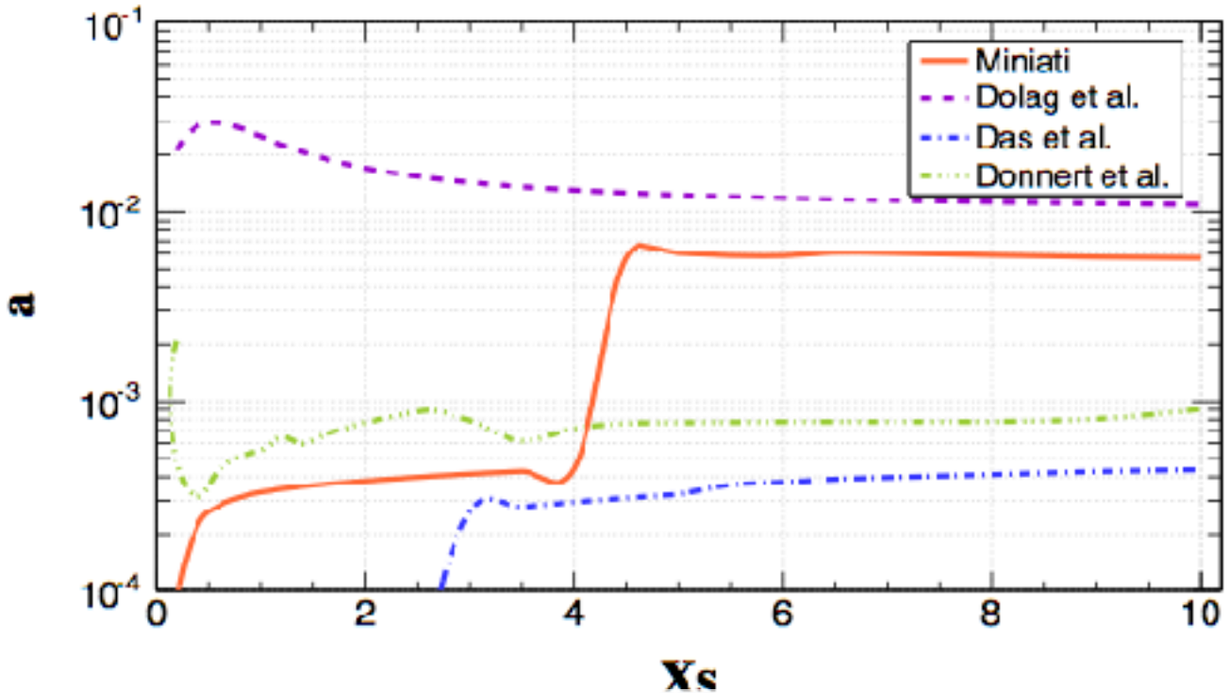

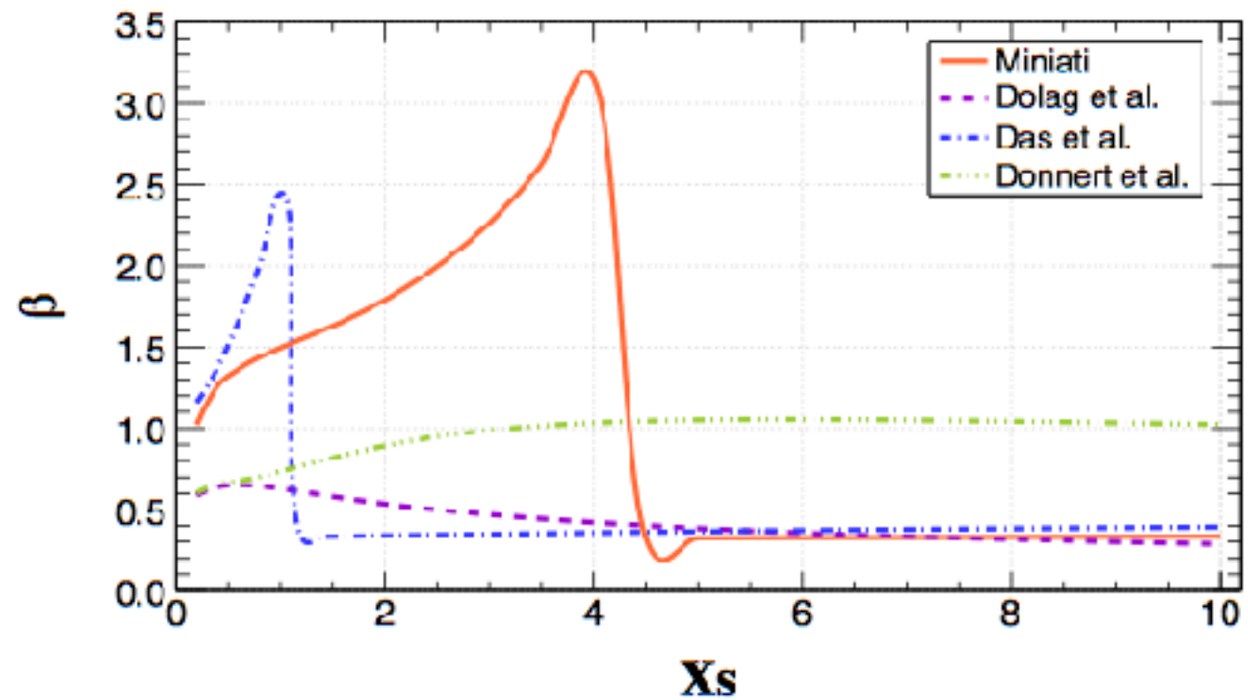

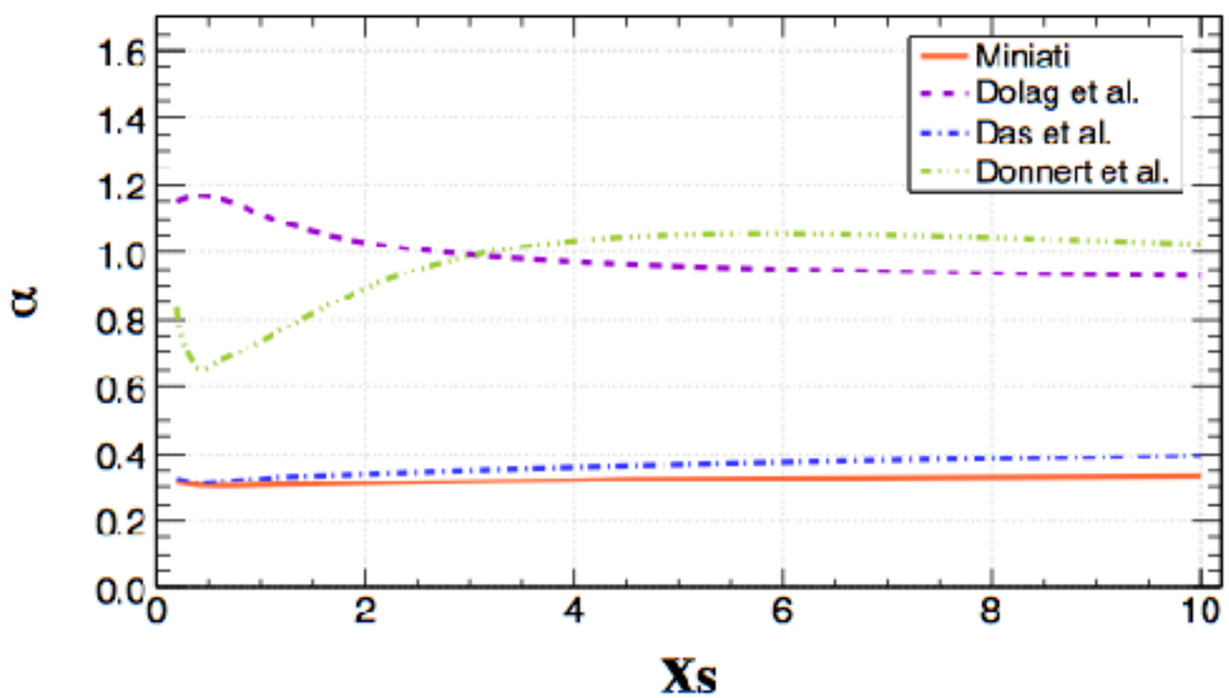

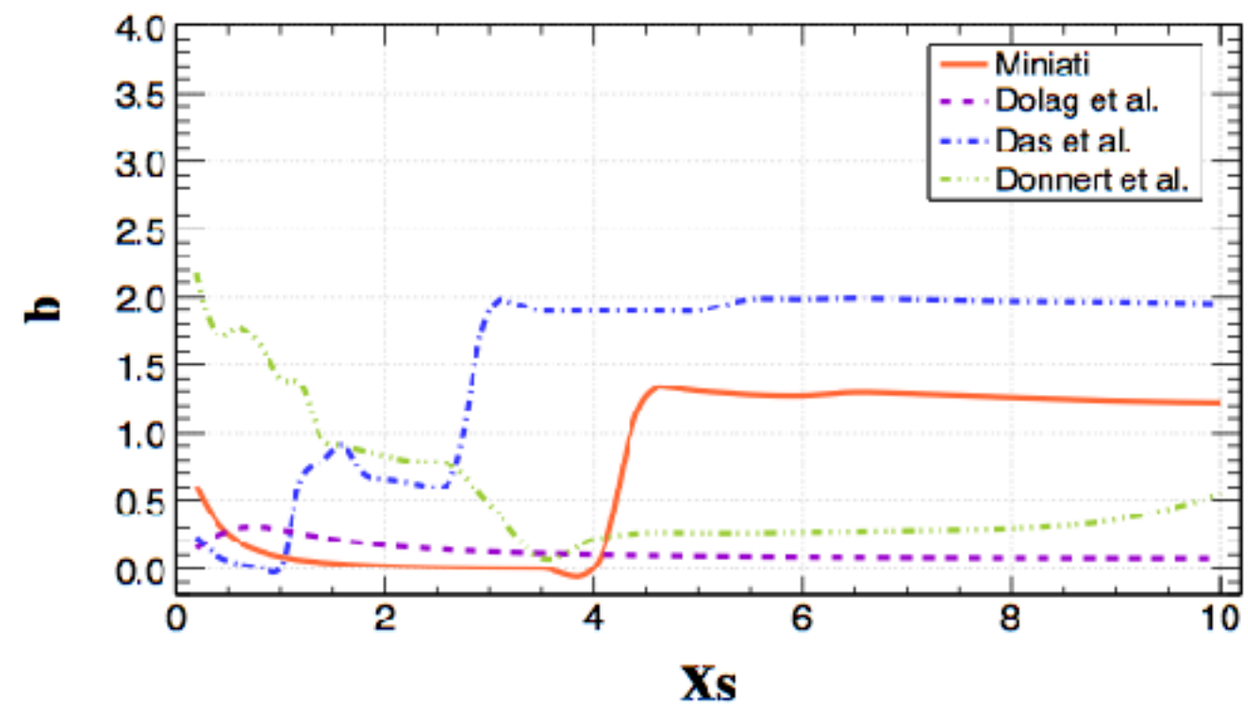

magnetic horizons

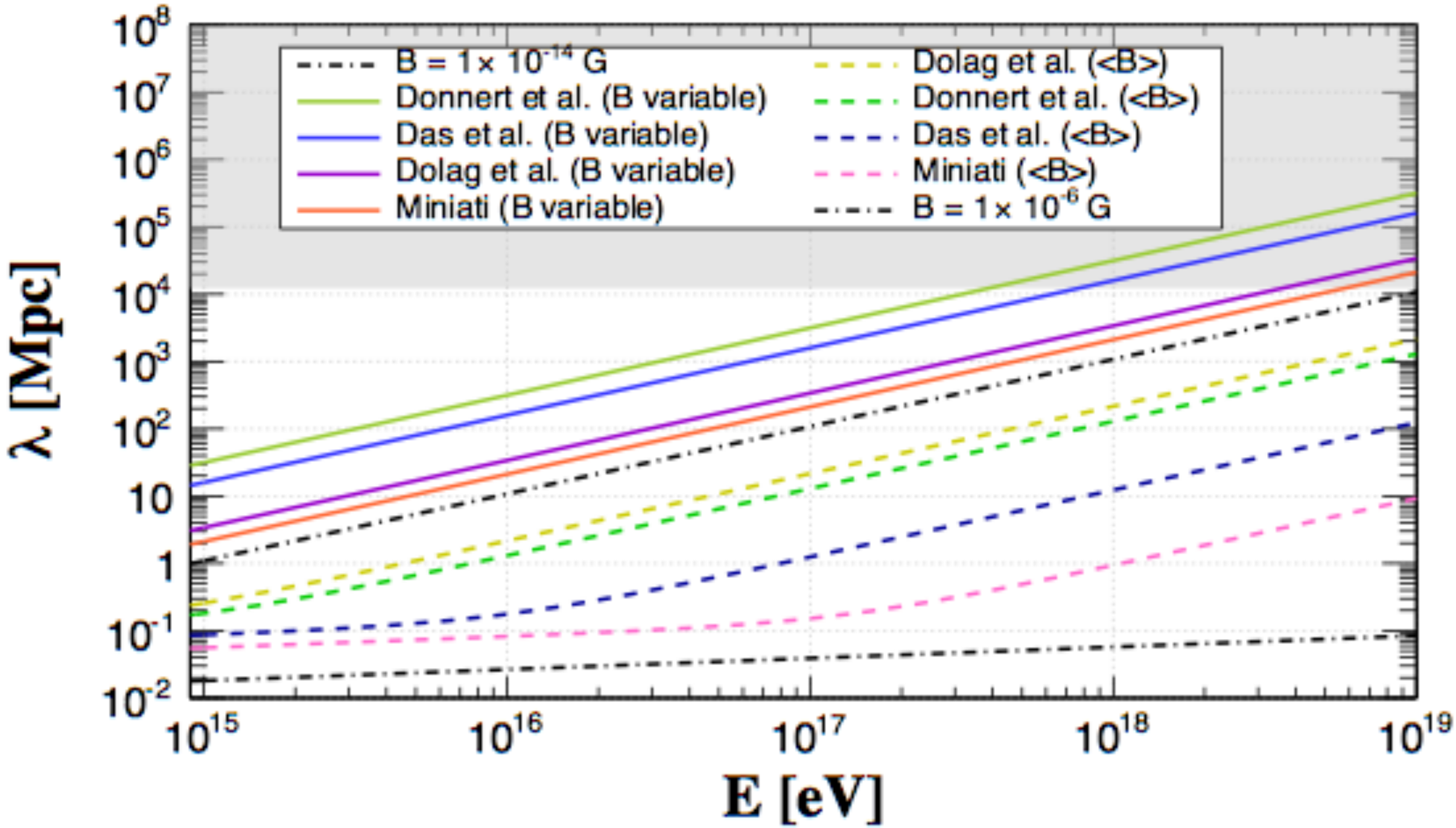

diffusion in extragalactic magnetic fields

diffusive spectrum

$$j_t(E,B) = \sum_{i=1}^{N_s} j_s(E) = \frac{c}{4\pi} \int_0^{z_{max}} dz \left|\frac{dt}{dz}\right| Q(E_g(E,z),z) \frac{dE_g}{dE} \sum_{i=1}^{N_s} \frac{\exp\left(-\frac{r_i^2}{4\lambda^2}\right)}{(4\pi\lambda^2)^{\frac{3}{2}}}$$

redshift evolution | source term | energy losses | F factor: magnetic field and source distributions

Syrovatskii variable

$$\lambda(E,z,B) = \sqrt{\int_0^z dz' \left|\frac{dt}{dz'}\right| \frac{D(E_g,z',B)}{a^2(z')}}$$

diffusion coefficient

$$D(E,z,B) = \frac{cl_c}{3}\left[a_L\left(\frac{E}{E_c}\right)^{\frac{1}{3}} + a_H\left(\frac{E}{E_c}\right)^2\right]$$

- turbulent magnetic field
- coherence length = l_c
- critical energy (Ec): $R_L = l_c$
- uniform source distribution

diffusion in extragalactic magnetic fields

RAB & G. Sigl. JCAP 1411 (2014) 031

- **idea:** weight spectrum by the magnetic field distribution from MHD simulations
- if F=1 spectrum is universal
- else a suppression with respect to the universal case is expected
- λ can be directly translated into the magnetic horizon
- fit suppression factors for different models of EGMF

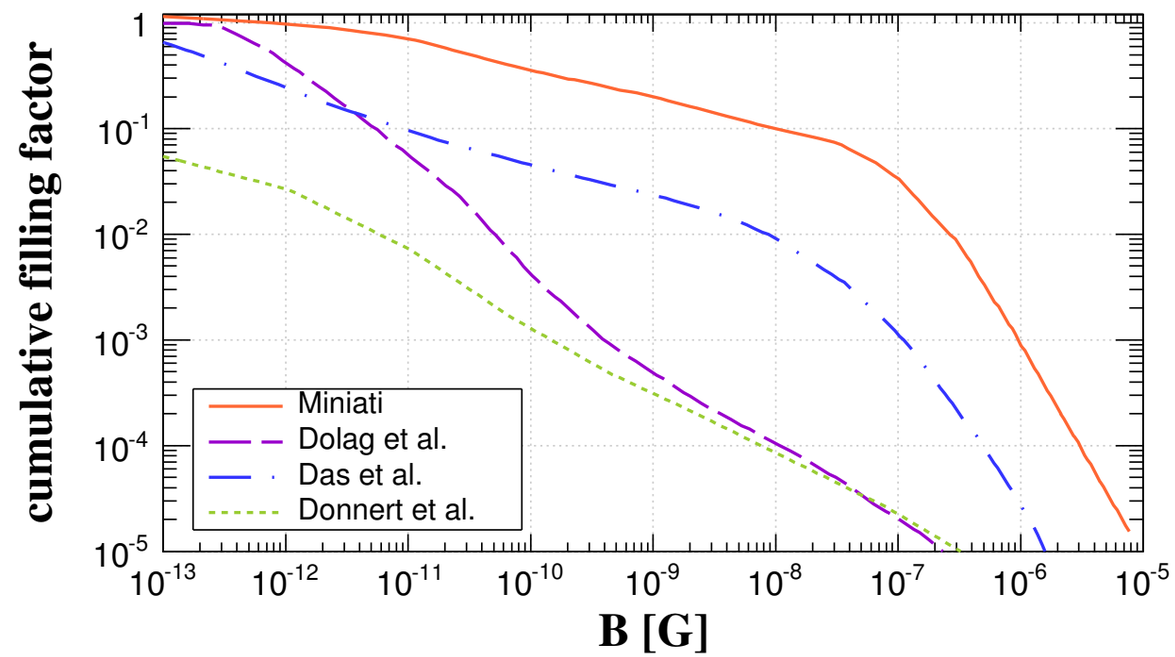

suppression factor

$$G(x) = \frac{j(E)}{j_0(E)} = \exp\left[-\frac{(aX_s)^\alpha}{x^\alpha + bx^\beta}\right]$$

$$x \equiv \frac{E}{\langle E_c \rangle} \qquad X_s = \frac{d_s}{\sqrt{R_H l_c}}$$

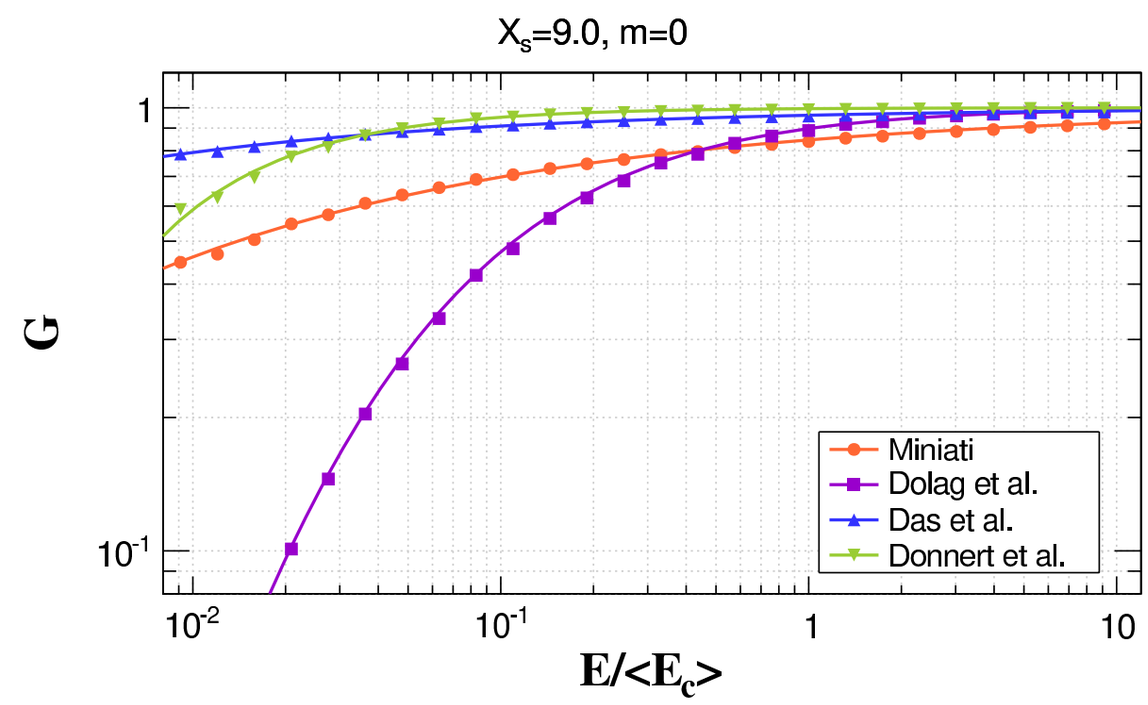

limitations of the diffusive approach

- energy losses can be neglected (see energy loss length plot)
- a spatially constant diffusion coefficient is assumed

$$\vec{\nabla}.\left[D(\vec{x},t)\vec{\nabla}n(\vec{x},t)\right] = D(\vec{x},t)\nabla^2 n(\vec{x},t) + \vec{\nabla}D(\vec{x},t).\vec{\nabla}n(\vec{x},t)$$

- the "convective" term can be neglected for $D/l_D << c$, where l_D is the scale on which D varies
- average source distance for uniform distribution is a sizable fraction of Hubble radius
- the contribution of the neglected convective term can be neglected for sources farther than $(D/l_D\, c)\, R_H << R_H$, which are responsible for most of the flux at E~EeV
- condition satisfied at clusters
- this condition is not satisfied at voids for B<0.01 nG, but then the diffusive approximation is no longer valid (superluminal velocities)

MHD details

- code has to conserve energy, momentum
- div(B) = 0
- no viscosity
- colisionless MHD
- cooling, heat and other energy terms
- grid-scale processes: chemical reaction, convection, ...
- subgrid-scale processes: formation/death of objects, stellar dynamo, feedback, ...

momentum density $\vec{\pi} \equiv \rho \vec{v}$

stress tensor $\overleftrightarrow{T} \equiv \rho \vec{v} \otimes \vec{v} + \left(p + \frac{1}{2}B^2\right) \overleftrightarrow{I} - \vec{B} \otimes \vec{B}$

total energy density $\mathcal{H} \equiv \frac{1}{2}\rho v^2 + \frac{1}{\gamma - 1}p + \frac{1}{2}B^2$

energy flow $\vec{U} \equiv \left(\frac{1}{2}\rho v^2 + \frac{\gamma}{\gamma - 1}p\right)\vec{v} + B^2\vec{v} - \vec{v}.\vec{B}\vec{B}$

Y $\overleftrightarrow{Y} \equiv \vec{v} \otimes \vec{B} - \vec{B} \otimes \vec{v}$

$$\frac{\partial \rho}{\partial t} + \vec{\nabla}.\vec{\pi} = 0$$ conservation of mass

$$\frac{\partial \vec{\pi}}{\partial t} + \vec{\nabla}.\overleftrightarrow{T} = 0$$ conservation of momentum

$$\frac{\partial \mathcal{H}}{\partial t} + \vec{\nabla}.\vec{U} = 0$$ conservation of energy

$$\frac{\partial B}{\partial t} + \vec{\nabla}.\vec{Y} = 0$$ conservation of magnetic flux

Oxford MHD simulations

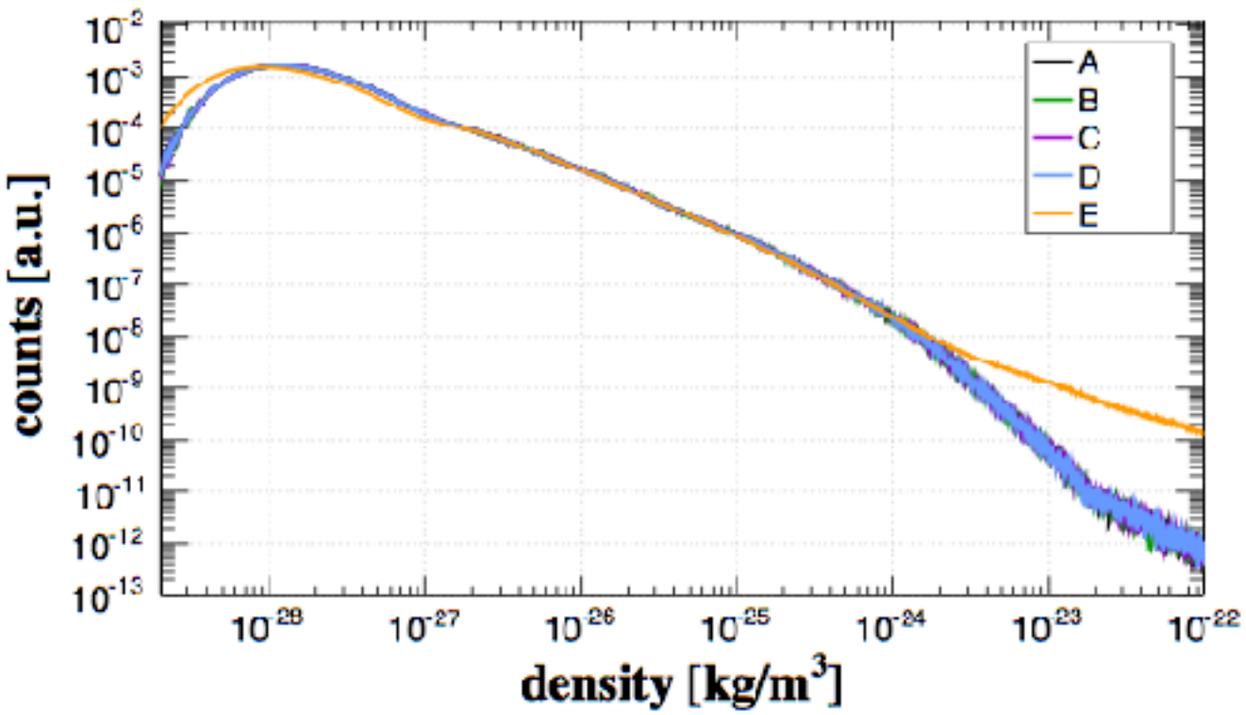

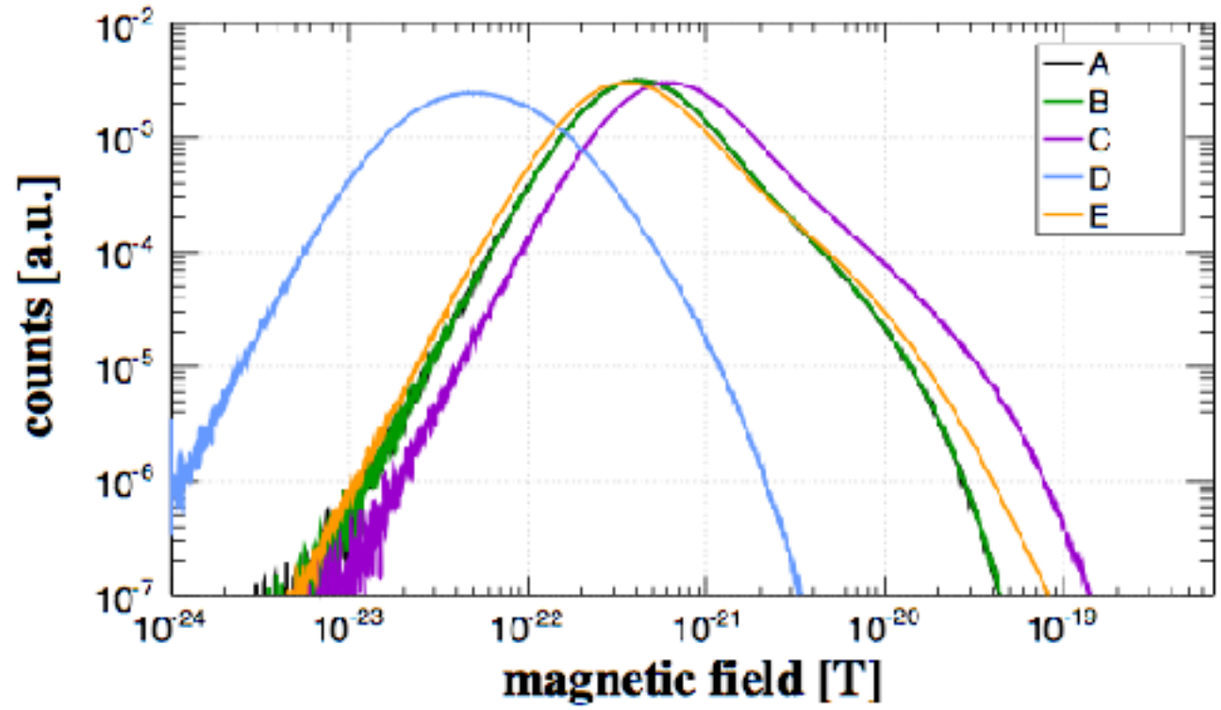

Oxford MHD simulations: convergence and scaling

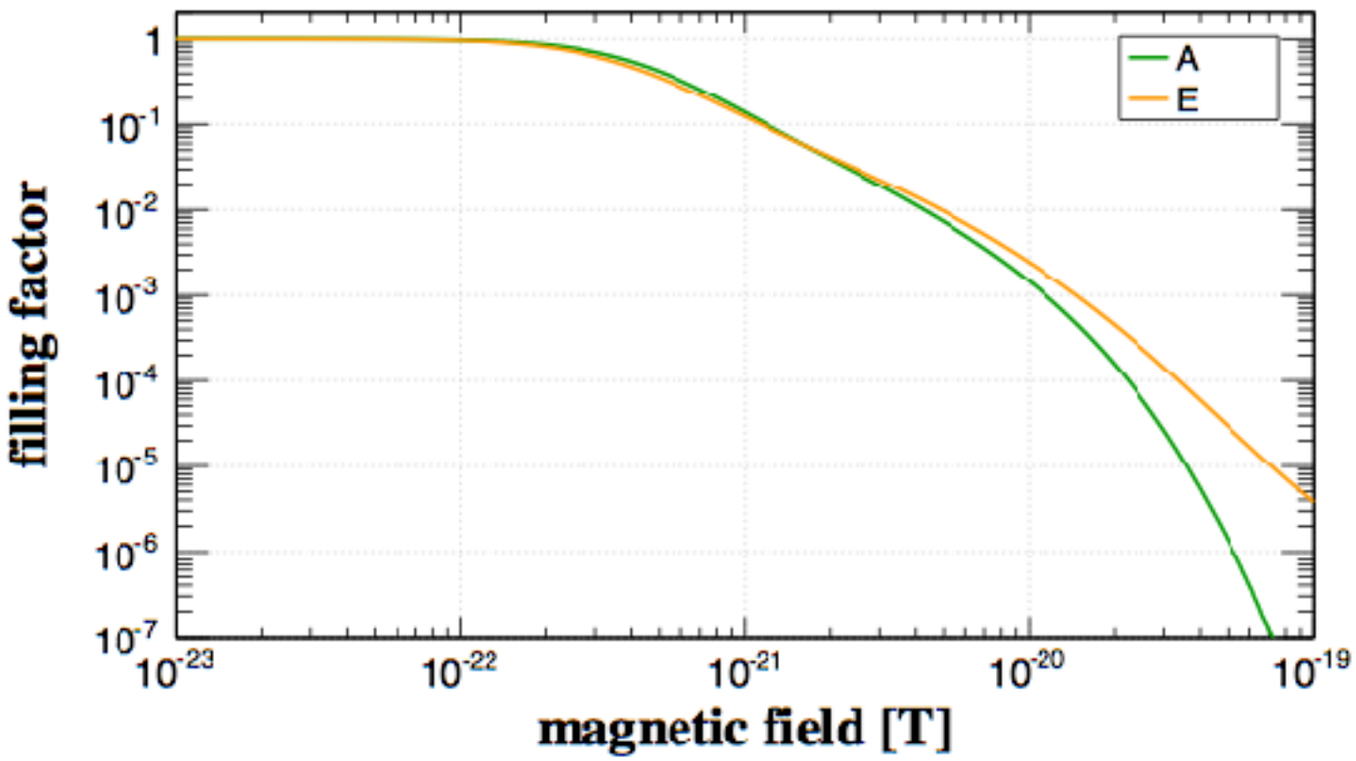

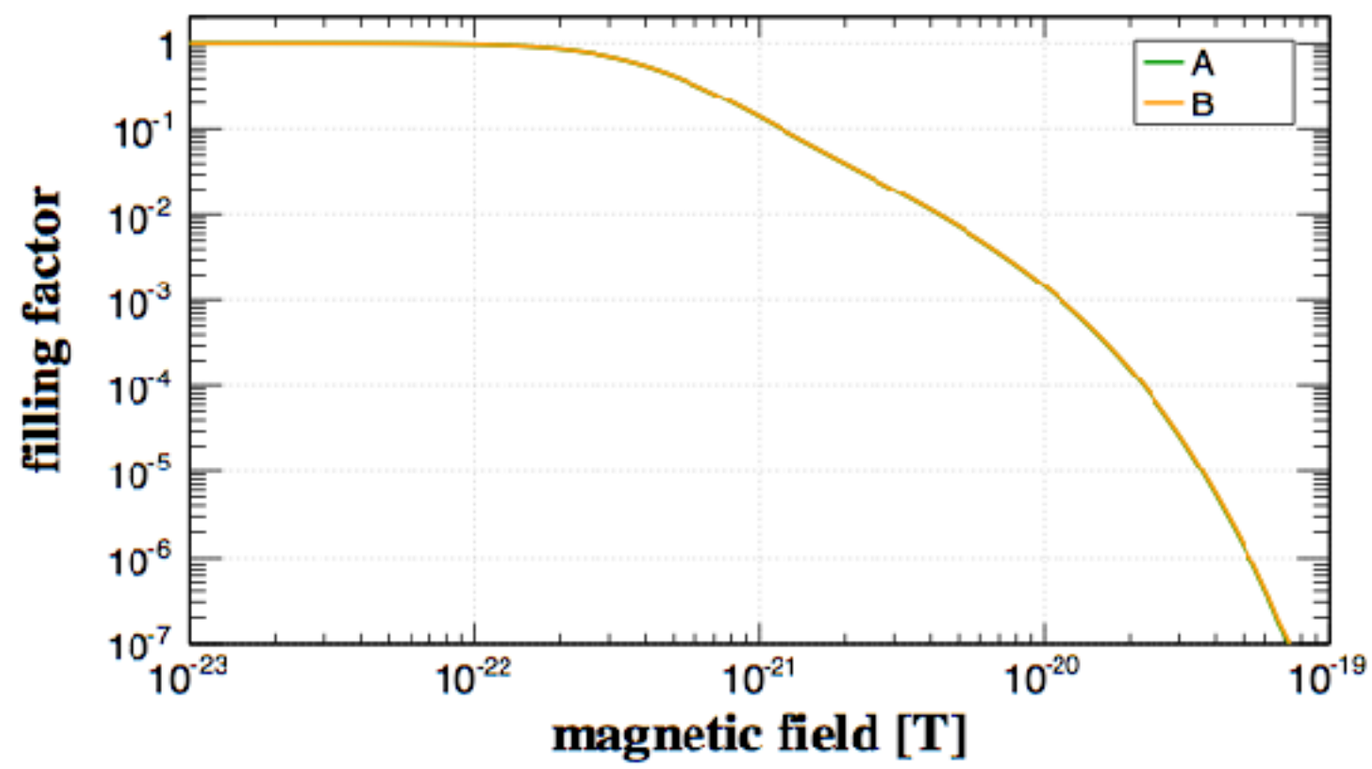

UHECR "tomography" of the cosmic web

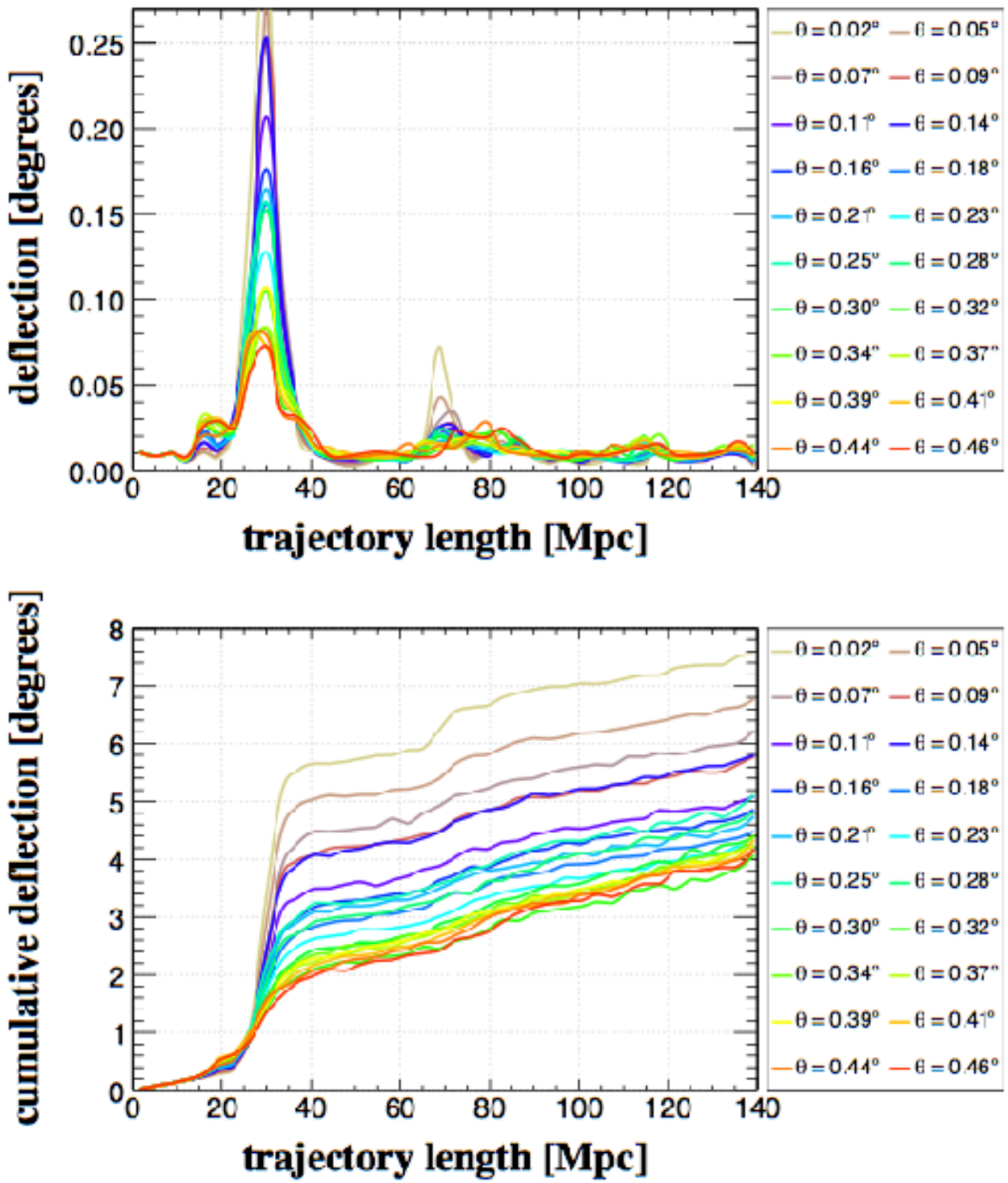

- UHECR "tomography"
- fast readout of AMR grids is rather difficult due to the size of files and number of cells → SQLite-based approach was devised and interface with CRPropa was developed
- simulation of events recording its full trajectory, changing its initial angle within a cone of θ
- the average over 100 realization for each angle is plotted
- high deflections observed when particles cross structures
- useful for cross checks
- size of the structure is given by the angle of the cone in which the deflections start to become small, and the size (trajectory length) around peaks